Technische Universität München

TUM School of Life Sciences

Activation of the susceptibility factor *Hv*RACB in the interaction between *Hordeum vulgare* and *Blumeria graminis* f.sp. *hordei*

Adriana Trutzenberg

Vollständiger Abdruck der von der Fakultät TUM School of Life Sciences der Technischen Universität München zur Erlangung des akademischen Grades einer

Doktorin der Naturwissenschaften
(Dr. rer. nat.)

genehmigten Dissertation.

Vorsitzender:	Prof. Dr. Erwin Grill
Prüfer der Dissertation:	1. Prof. Dr. Ralph Hückelhoven
	2. Prof. Dr. Caroline Gutjahr

Die Dissertation wurde am 24.06.2022 bei der Technischen Universität München eingereicht und durch die TUM School of Life Sciences am 14.11.2022 angenommen.

In Gedenken an Wilhelm Kohnen

Publication

Parts of this Dissertation have been published in:

Adriana Trutzenberg, Stefan Engelhardt, Lukas Weiss, Ralph Hückelhoven.
'Barley guanine nucleotide exchange factor *Hv*GEF14 is an activator of the susceptibility factor *Hv*RACB and supports host cell entry by *Blumeria graminis* f.sp.*hordei*'.
Molecular Plant Pathology 23.10 (2022): 1524-1537.

Abbreviations

aa	amino acids
ABA	absisic acid
At	*Arabidopsis thaliana*
Bgh	*Blumeria graminis* f.sp. *hordei*
BiFC	Bimolecular Fluorescence Complementation
CA	constitutively activated
cDNA	complementary DNA
CFP	Cyan Fluorescent Protein
CPK	calcium-dependent protein kinase
CRIB	CDC42/RAC Interactive Binding
CSEP	candidate secreted effector proteins
cv.	cultivar
CWA	cell wall appositions
Dbl	oncogene for diffuse B-cell lymphoma
DH	Dbl homology
dpi	days post inoculation
DMSO	Dimethyl sulfoxide
DNA	Deoxyribonucleic acid
DN	dominant negative
EDTA	Ethylenediaminetetraacetic acid
EtBr	Ethidium Bromide
ETI	Effector-Triggered Immunity
ETS	Effector-Triggered Susceptibility
EtOH	Ethanol
EV	empty vector
f.sp.	formae speciales
FL	Full Length

FLIM	Fluorescence Lifetime Imaging
FPMK	fragments per million kilobase
FRET	Foerster Resonance Energy Transfer
f.sp.	forma specialis
GAP	GTPase Activating Protein
Gbp	Giga base pairs
GDI	ROP-GDP dissociation inhibitor
GDP	guanosine diphosphate
GEF	Guanine Nucleotide Exchange Factor
GFP	Green fluorescent protein
Gm	*Glycine max*, soy bean
GOI	Gene of interest
GP	Barley cultivar Golden Promise
GTP	guanosine triphosphate
HIGS	host induced gene silencing
Hs	*Homo sapiens*
hpi	hours post inoculation
Hv	*Hordeum vulgare*
IP	immunoprecipitation
KD	knock down
KO	knock out
LB	lysogeny broth
Le	*Lycopersicon esculentum*
LED	Light Emitting Diode
Lj	*Lotus japonicus*
Mg	*Magnaporthe grisea*
MES	2-(N-morpholino)ethanesulfonic acid
ML	Maximum likelihood phylogenic analysis
Nb	*Nicotiana benthamiana*

NCBI	National Center for Biotechnology Information
NLR	Nucleotide-binding Leucine-rich Repeat containing Receptor
Nt	*Nicotiana tabacum*
NTC	No template control (in qRT-PCR)
Os	*Oryza sativa*
OE	over expression
PA	phosphatidic acid
PAMP	Pathogen-Associated Molecular Pattern
PCR	Polymerase chain reaction
PE	*Bgh* Penetration Efficiency
PEG	Polyethylene glycol
PRR	Pattern Recognition Receptor
PRONE	Plant-specific ROP Nucleotide Exchanger
PTI	pattern-triggered immunity
PVDF	Polyvinylidene Difluoride
qRT-PCR	quantitative reverse transcription PCR
Rac	Ras-related C3 botulinum toxin substrate
RHID	root hair initiation domain
RIC	ROP-interactive CRIB motif-containing protein
RIP	ROP Interactive Partner
RLK	receptor-like kinase
RLP	receptor-like protein
RNA	Ribonucleic acid
RNAi	RNA interference
ROP	Rho of Plants
ROS	reactive oxygen species
RT	Room temperature
ROI	region of interest
SD	Synthetic Defined

SDS-PAGE	Sodium Dodecyl Sulfate- Polyacrylamide Gel Electrophoresis
St	*Solanum tuberosum*
TE	transposable elements
TIGS	transient induced gene silencing
UV	Ultra Violet
WT	wild type
Xoo	*Xanthomonas oryzae*
Y2H	Yeast-two-Hybrid
YPDA	yeast peptone dextrose adenine
Zm	*Zea mays*

Zusammenfassung

Die einkeimblättrige Kulturpflanze *Hordeum vulgare* (*Hv*) wird auf dem Feld von mehreren Krankheitserregern befallen. Zu ihnen gehört der biotrophe Gerstenmehltaupilz *Blumeria graminis* forma specialis *hordei* (*Bgh*). Die Interaktion von *H. vulgare* mit *Bgh* dient in der Molekularbiologie als Modellpathosystem zur Studie von Pflanze-Pilz Interaktionen.
Kleine GTPasen der RAC/ROP-Proteinfamilie sind an der Pflanzenentwicklung und -immunität beteiligt und wichtige molekulare Schalter, die in verschiedenen Signalwegen fungieren. Das *H. vulgare* ROP Protein *Hv*RACB ist in der Interaktion mit *Bgh* ein Anfälligkeitsfaktor. Aktiviertes *Hv*RACB unterstützt die Besiedlung von epidermalen Zellen von *H. vulgare* durch *Bgh* und Knock-down des *HvRACB*-Transkripts macht die Pflanze resistenter gegen das Eindringen des Pilzes. Die endogene Aktivierung kleiner GTPasen wird in der Regel durch ihre Interaktion mit Guanin-Nukleotid-Austauschfaktoren (GEFs) katalysiert, indem sie den Austausch von GDP mit GTP erleichtern und dadurch ROPs in einen aktiven Signalzustand versetzen. Pflanzen besitzen eine unabhängige Klasse von GEFs mit einer pflanzenspezifischen RAC/ROP-Nukleotid-Austauschdomäne (engl. plant-specific RAC/ROP nucleotide exchanger domain, PRONE).
In dieser Dissertation wird ein Überblick über *H. vulgare* PRONE GEFs gegeben und ein besonderes Augenmerk auf *Hv*GEF14 gelegt. Dieses PRONE GEF gehört zu einer phylogenetisch eigenständigen Abzweigung von Pflanzen-PRONE-GEFs und wird in *H. vulgare* ubiquitär exprimiert. Darüber hinaus führt die Inokulation mit *Bgh* zu einer Herunterregulierung des *HvGEF14*-Transkripts. Außerdem zeigt sich, dass das PRONE-GEF mit *Hv*ROPs wie *Hv*RAC1 und *Hv*RACB interagiert. Es wurden zudem neue Methoden zur Beobachtung des Aktivitätsstatus von *Hv*RACB in Pflanzen entwickelt, um die GDP/GTP-Austauschfunktion von *Hv*GEF14 *in planta* aufzuzeigen. Darüber hinaus erhöht die Überexpression von *Hv*GEF14 die Anfälligkeit von *H. vulgare* gegenüber *Bgh*, während die vorübergehende Herabregulierung des *HvGEF14* Gens über RNA-Interferenz *H. vulgare* Epidermiszellen tendenziell resistenter gegen den Pilz macht. Zusammen unterstützen diese Daten die Hypothese, dass *Hv*GEF14 über die Aktivierung von *Hv*RACB zur Anfälligkeit der Gerste gegen *Bgh* beiträgt und somit einen neuen Anfälligkeitsfaktor in *Hv*RACB Signalweg darstellt.

Summary

The monocotyledenous crop plant *Hordeum vulgare* (*Hv*) is challenged by several pathogens in the field. Amongst them is the biotrophic powdery mildew fungus *Blumeria graminis* forma specialis *hordei* (*Bgh*). The interaction of *H. vulgare* with *Bgh* has served as a model pathosystem in molecular biology to study plant-fungus interactions.
Small GTPases of the RAC/ROP family are important molecular switches that function in a number of different signalling pathways and have been shown to be involved in plant development and immunity. The *H. vulgare* ROP *Hv*RACB functions as a susceptibility factor in the interaction with *Bgh*. Activated *Hv*RACB supports fungal establishment in epidermal cells of *H. vulgare* and knock-down of the *HvRACB* transcript renders the plant more resistant to fungal penetration. Endogenous activation of small GTPases is typically catalysed by their interaction with guanine nucleotide exchange factors (GEFs) which facilitate the exchange of GDP with GTP, thereby turning ROPs into an active signalling state. Plants possess an independent class of GEFs with a plant-specific RAC/ROP nucleotide exchanger domain (PRONE).
In this dissertation, an overview of *H. vulgare* PRONE GEFs is presented with a special focus on *Hv*GEF14. This PRONE GEF is placed in a phylogenetically distinct branch of plant GEFs and is ubiquitously expressed in *H. vulgare*. In addition, inoculation with *Bgh* leads to a downregulation of the *HvGEF14* transcript. *Hv*GEF14 is shown to interact with *Hv*ROPs, such as *Hv*RAC1 and *Hv*RACB. New methods for observation of the *Hv*RACB activity status were developed to show the guanine nucleotide exchanger function of *Hv*GEF14 *in planta*. Additionally, the over expression of *Hv*GEF14 increases *H. vulgare's* susceptibility towards *Bgh* whereas transient knock-down of *HvGEF14* via RNA interference makes *H. vulgare* epidermal cells by trend more resistant to the fungus. Together, the data support the hypothesis that *Hv*GEF14 is involved in *H. vulgare* susceptibility towards *Bgh* by activating *Hv*RACB.

Contents

1. Introduction

1.1. Plant Immunity and Susceptibility

Plants face multiple environmental challenges in their natural habitats, including pathogenic microbes. During the course of evolution, however, plants with successful strategies to fend off foreign invaders have been selected for. Therefore plants are largely resistant to most potential pathogens in the wild. Susceptibility against pathogens is less common but an important field of investigation to understand the underlying mechanisms of vulnerable plants. Depending on the molecular repertoire of host and pathogen, the outcome of a plant-microbe interaction can lead to plant susceptibility or immunity. During plant defense, three main steps are distinguished. Firstly, the detection of pathogens, subsequently, intracellular signal transduction and finally, the initiation of defense responses.
In terms of detection, two major distinct mechanisms have been observed. On the one hand, **P**attern **R**ecognition **R**eceptors (PRRs) are located at the cell surface (Boller and Felix, 2009) and detect conserved microbial molecules, also known as **M**icrobe-**A**ssociated **M**olecular **P**atterns, or MAMPs (Ausubel, 2005). Cell surface receptors also detect **D**amage **A**ssociated **M**olecular **P**atterns (DAMPs), that are plant derived molecules which can be produced by pathogen attack (Lotze et al., 2007). On the other hand, resistance (R) proteins have evolved to detect pathogenic effectors directly or indirectly (Jones et al., 2016). Based on these two modes of pathogen detection by the plant, the two following immunity pathways have been characterised.

PRR-mediated defense responses are collectively described as so called **P**athogen associated molecular pattern **T**riggered **I**mmunity (PTI). In PTI, the plant detects MAMPs, that are conserved pathogenic molecules which do not primarily function in virulence. These MAMPs are often structural components, such as the fungal cell wall unit chitin. The interaction between a MAMP and a plant receptor leads to intracellular signalling that results in the activation of plant defense responses (Dodds and Rathjen, 2010).
Due to evolutionary pressure, however, pathogens which were able to circumvent PTI had a fitness advantage. This strategy involves the evolution of a variety of so called effector molecules, which target immunity-related plant proteins in order to increase pathogenic virulence. Pathogenic effectors work in many different modes of action that all lead to plant susceptibility. This is why this process is called **E**ffector **T**riggered **S**usceptibility (ETS) (Jones and Dangl, 2006).

With the help of the aforementioned R proteins, plants can resist invading microbes by detection of the introduced effectors. After recognition of a pathogenic effector, a defense program on the plant's side can lead to **E**ffector **T**riggered **I**mmunity, in short ETI (Wang et al., 2018). Even though PTI and ETI have been studied as individual immunity path-

ways in the past, more recent publications highlight how the two perception modes are integrated in the plant's response to pathogens (Yuan et al., 2021; Ngou et al., 2021). For example, Yuan et al. (2021) have shown how mutated *Arabidopsis thaliana* plants lacking PRR receptors (responsible for PTI) have lower ETI-type immune responses. Furthermore, the authors have shown that after perception, central components of surface-receptor-mediated immunity are enhanced (Yuan et al., 2021). In a similar approach, Ngou et al. (2021) showed how each, surface and intracellular perception of pathogenic molecules, potentiate the immune response of the other.
Interestingly, it has recently been shown that the link between pathogen detection and defense gene expression also provides evidence for converging ETI and PTI signalling. This became evident when Pruitt et al. (2021) reported that both cell surface PRRs as well as intercellular NLRs associate with the same intracellular immunity signalling components in order to trigger either an ETI or PTI response. These reports on results obtained in *A. thaliana* pave the way to investigate similar integrated pathways of plant immunity in economically important plants, such as crops.

1.2. Pathosystem *Hordeum vulgare* & *Blumeria graminis* f. sp. *hordei*

Research on the crop plant *Hordeum vulgare* (*Hv*) during its interaction with the powdery mildew fungus *Blumeria graminis* f.sp. *hordei* (*Bgh*) has served as a model in cell-autonomous plant defence and fungal biotrophic pathogenesis for many years (Schulze-Lefert and Vogel (2000); Hückelhoven (2005); Zhang et al. (2005); Hückelhoven and Panstruga (2011), Figure 1A-B). The disease severity of this plant-pathogen interaction, during which a conidiospore of the obligate biotroph ascomycete *Bgh* interacts with an epidermis cell of *H. vulgare*, is governed on a cell-to-cell basis (Aist and Bushnell (1991); Shirasu et al. (1999); Zhang et al. (2005), Figure 1C-D). The biotrophic fungus only propagates on living leaf tissue which makes transformation of *Bgh* challenging but also gives the opportunity to study plant-fungal interactions on a single cell level. In this system, cell biological advances have proven useful in understanding the mechanisms of plant resistance and susceptibility (Hückelhoven and Panstruga, 2011). In the following sections, a detailed description of *Hordeum vulgare*, *Bgh* and known immunity-underlying molecular mechanisms is provided.

1.2.1. *Hordeum vulgare* (*Hv*) L.

Domesticated barley (*Hordeum vulgare, Hv*, Figure 1A) is a grass in the Poacea family and amongst the most important crop plants in the world ranking 4th most farmed (Singh et al., 2019). Its wild relative *Hordeum vulgare* subsp. *spontaneum* has served in human nutrition even long before the cultivation of other crops (Badr et al., 2000). Today, humans use *H. vulgare* mainly for animal feed but it is still a staple food in many parts of the

world. Additionally, an important economic use of *H. vulgare* is in the brewing industry (Harwood, 2019).
H. vulgare is an annual grass which is classified by its growing season. Different varieties are therefore either considered spring or winter cultivars. Breeding efforts have made it possible to plant smaller and high yielding two-rowed or six-rowed cultivars on the field (Harwood, 2019). For this dissertation, Golden Promise (GP), which was improved by radiation treatment, was used. GP is a semi-dwarfed salt-stress tolerant two-rowed spring barley variety and susceptible to the powdery mildew fungus (Thomas et al., 1984). This makes it an excellent cultivar to study the *H. vulgare* -*Bgh* interaction.

To further increase yield, breeding relies on the understanding of molecular markers and mechanisms. In 2012, the first *H. vulgare* genome annotation of the fully sequenced cultivar Morex was published (Mayer et al., 2012). Two more versions of the genome annotation were made available in 2019 (Morex version 2, Monat et al. (2019)) and in 2021 (Morex version 3, Mascher et al. (2021)). *H. vulgare* is a diploid organism with an estimated haploid genome size of approximately 5.3 Giga base pairs (Gbp) on seven chromosomes. One of the characteristics of the *H. vulgare* genome is its highly repetitive nature including many retrotransposons. However, new sequencing approaches make it easier to untangle differences in *H. vulgare* genomes. One example is the multiplex PCR method published as BarPlex which revealed genetic diversity amongst cultivated and wild *Hordeum* spp. that may aid in breeding efforts (Gao et al., 2021b).
In molecular biology, *H. vulgare* serves as a model organism for Triticeae crop plants due to its diploid nature. Compared to other crops in the Triticeae, it is therefore easier to study (Saisho and Takeda, 2011). Increasing availability of genomic resources make it possible to study *H. vulgare*'s molecular mechanisms of plant development and responses to external stimuli (Harwood, 2019). In terms of disease protection, scientific advances have provided growers with resistant varieties, including against attack by powdery mildew. One famous example is the gene locus *Mla* that harbours a variety of resistance (R) genes which have alredy been used in breeding of *H. vulgare*. Another important genetic tool for resistance breeding is the recessive *mlo* gene, successfully protects the plant against *Bgh* infection (Schulze-Lefert and Vogel, 2000; Kusch and Panstruga, 2017).

1.2.2. *Blumeria graminis* f. sp. *hordei* (*Bgh*)

Powdery mildew fungi are amongst the most devastating phytopathogens infecting a broad range of angiosperms including crop plants like grape, tree fruits and grasses like *H. vulgare* (Glawe, 2008). They are a class of filamentous pathogens that most likely originated in the Northern Hemisphere where they first colonised broad-leaved deciduous trees (Takamatsu, 2018). Fungi of the *Blumeria* genus have a biotrophic lifestyle and have evolved alongside their hosts which resulted in the differentiation of *Blumeria* spp. into formae speciales (ff.spp.). One of these biotrophic ascomycetes is specialised to infect *H. vulgare*: *Blumeria graminis* f.sp. *hordei* (*Bgh*).

Bgh asexually propagates by wind dispersal of its so called conidiospores. These spores can germinate on *H. vulgare* leaves by developing a primary and secondary germ tube. The primary germ tube possibly acts in proper adhesion to the leaf and as a surveillance mechanism for suitable infection surfaces. Only when this primary germ tube stops growing, the secondary germ tube starts elongating (Yamaoka et al., 2007). Subsequently, the secondary germ tube swells and forms an appressorium to penetrate the host's epidermal cell. The plant cell responds to contact with the conidiospore by cytoplasmic aggregation and papilla formation below the germ tube contact points. In case of a defended penetration event, the fungal appressorium is hindered from entry under formation of so called **C**ell **W**all **A**ppositions (CWA). During the successful infection, the fungus degrades the plant's cuticle and epidermal cell wall with the help of secreted enzymes. The appressorium grows into a penetration peg that further expands into a structure called haustorium (Figure 1C-D) that is important for nutrient uptake and effector delivery. At the same time, the plasma membrane expands into the cell to accommodate the fungal structure (Aist and Bushnell, 1991; Hückelhoven, 2005; Hückelhoven and Panstruga, 2011; Spanu, 2017). The resulting fungal organ is surrounded by a plant derived extra haustorial membrane (EHM) which was hypothesized to either be derived from the polar invagination of the plant plasma membrane or by *de novo* synthesis. Accumulating evidence points to the fact that the EHM is indeed distinct from the plasma membrane due to a lack of plasma membrane-specific indicator proteins (Koh et al., 2005) as well as the presence of EHM-specific proteins (Berkey et al., 2017).
After successful colonisation of *H. vulgare* cells, the fungus grows hyphae on the cell surface and develops conidiophores that produce new conidiospores for wind dispersal (Aist and Bushnell, 1991). These are then macroscopically visible as white pustules on the leaf surface (Figure 1B).

The *Bgh* genome contains a high amount of transposable elements (TEs) and is considered "one speed" due to the fact that genetic variation is evenly spread across the whole genome. This is in contrast to the so called "two speed" genome that is characterised by differently fast evolving larger parts of the genome and widely found in filamentous pathogens (Frantzeskakis et al., 2018). Studies of the *Bgh* conidiospore proteome (prior to germination) shows the spores' potential for protein biosynthesis and folding (Noir et al., 2009). Using cDNA microarrays at different stages of the life cycle, (Both et al., 2005) could show a shift towards primary metabolism during pathogenesis. While lipids and glycogen are the main energy storage components in conidia, these get broken down during the initial infection. While the haustorium is formed, genes involved in glycolysis are up-regulated and protein synthesis is enhanced during hyphae growth (Both et al., 2005).

The biotrophic lifestyle of *Bgh* offers many hurdles for standard genetic studies that have been developed in other culturable plant pathogens (Zhang et al., 2005). However, recent advances in substrate development have shown to be promising. On artificial media, such

as resin-based synthetic matrices, it is possible to study germination and appressorium formation (Zhu et al., 2018). Following, in-depth transcriptome and proteome analyses have been possible by the addition of *H. vulgare* cuticle components like n-hexacosanal to the growth medium. This setup made it possible to measure a change in the transcriptional machinery towards protein production and energy metabolism during germination which is in accordance with data from *in planta* investigations (Pham et al., 2019; Bindschedler et al., 2009).
Further, to study gene functionality in the biotrophic phytopathogen, **H**ost **I**nduced **G**ene **S**ilencing (HIGS) has been employed. With this method, *Bgh* genes can be silenced via transformation of the host plant. Due to the intimate interaction of plant and pathogen during infection, fungal genes can directly be targeted this way. Important virulence genes, for example those that code for effectors, have been confirmed as functional via HIGS (Nowara et al., 2010; Pliego et al., 2013; Nottensteiner et al., 2018).

1.2.3. Pathogen Virulence and Plant Susceptibility

Pathogenic effectors are an important class of microbial molecules that aid during the infection of a plant host. Different types of effectors, such as proteins or RNA, have been published in a variety of different pathogenic microbes. In the case of *Bgh*, there have been several examples of effector molecules published which will be introduced in the following. For example, *Bgh* possesses a large group of so called **C**andidate **S**ecreted **E**ffector **P**roteins (CSEP) which comprise at least 7% of *Bgh* genes (Spanu, 2014). Via HIGS, individual CSEPs were studied for their virulence supporting capabilities. Paired with expression data measured at different time points during the infection, possible distinguished roles could be hypothesized. These functions range from the initial steps in the interaction to haustorium formation (Aguilar et al., 2016; Ahmed et al., 2016). The first CSEP crystal structure was published of CSEP0064, a pseudo-enzyme that is supposed to interfere with induction of host cell death, which is an important prerequisite for the biotrophic lifestyle of *Bgh* (Pennington et al., 2019).
More recently, accumulating evidence has been published on the role of small RNAs (sRNA) in gene expression during the *Bgh* infection. Amongst the infection-related small RNAs and possible target genes, a number of already established *Bgh* effectors were identified (Hunt et al., 2019). Further, it was shown that small RNAs not only regulate *Bgh* effectors, but that they might also target *H. vulgare* genes during the infection process. This mechanism has been described as cross-kingdom RNA interference and is evidence that small RNAs provide effector functions by increasing *Bgh* virulence (Kusch et al., 2018).

On the plant's side, susceptibility is not as common as resistance. However, in the last decades, a number of susceptibility-supporting proteins have been identified in plants. They were initially characterised as gene products of genetic markers important for the compatible interaction between plants and biotrophic microbes. Evolutionally these genes

were probably selected for due to their role in plant development or physiology, and are often hijacked by pathogens to aid infection. A number of susceptibility genes have been found to be important in pathogenic establishment at every stage of the infection. Due to their function in plant immunity, these proteins have been termed susceptibility factors (Hückelhoven, 2005; Engelhardt et al., 2018; Garcia-Ruiz et al., 2021). Prominent examples of *H. vulgare* susceptibility factors are members of the earlier introduced gene family ***M**ildew resistance **L**ocus **O*** (*MLO*), a group of transmembrane proteins, which have similarities to G-protein coupled receptors. A naturally occurring mutation in the *HvMLO* gene resulted in a loss-of-function variant that showed resistance towards *Bgh*. Although the molecular mechanisms of the susceptibility factor have not yet been fully elucidated, *mlo*-based resistant *H. vulgare* is already widely used in agriculture (Devoto et al., 1999; Opalski et al., 2005; Engelhardt et al., 2018). The family of *MLO* genes has also been widely studied in other plant species and it was proven that *mlo*-based resistance can successfully be applied to the model plant *Arabidopsis thaliana* and to a variety of mono- and dicotyledonous crops (Kusch and Panstruga, 2017).
In addition, other *H. vulgare* proteins play a role in susceptibility, such as the *H. vulgare* protein *Hv*RACB. After activation, *Hv*RACB has an infection- supporting effect in epidermal cells when the plant is challenged with the biotrophic fungus *Bgh* (for more details see section 1.3.5).
However, susceptibility factors are not only restricted to the *H. vulgare-Bgh* interaction. More examples of host proteins involved in susceptibility were reported in other plant species, such as *A. thaliana*, *Oryza sativa* and *Solanum tuberosum* challenged with different pathogens (Chandran, 2015; Muecke et al., 2019; Yang et al., 2006; He et al., 2018).
In *A. thaliana*, a group of plant sugar transporters termed **S**ugar **W**ill **E**ventually be **E**xported **T**ransporter (SWEET) were shown to be involved in plant susceptibility. In short, the modulation of SWEETs leads to an increased sugar transport from the host to the pathogen. Therefore the SWEET family is another example of host proteins that were found to be susceptibility factors in different plant-pathogen interactions. Genes coding for SWEET proteins were found in most plant genomes and it was shown that these susceptibility factors play a role in the interaction with different classes of pathogens (Chandran, 2015).
It has become clear, that especially for biotrophic pathogens it is beneficial to employ infection strategies involving susceptibility factors. In *O. sativa*, the biotrophic leaf blight bacterium *Xantomonas oryzae* (*Xoo*) infects the plant by targeting the transcription of the host gene ***D**owny **M**ildew **R**esistance 6* (*OsDMR6*) via transcription activator-like effectors (Muecke et al., 2019). However, this is not the only known infection strategy by this pathogen involving host proteins. *Xoo* also targets the *O. sativa* susceptibility factor NODULIN3 family protein *Os*8N3 via a type III effector to facilitate bacterial blight (Yang et al., 2006).
Knowledge about susceptibility of agronomically important crops, such as *O. sativa* are vital for breeding efforts. However, the molecular mechanisms underlying the arms race between plant and pathogen are often complex. An example for a multistep susceptibility

mechanism is the interaction between the oomycete *P. infestans* that targets *Solanum tuberosum* via phytopathogenic effectors. After secretion into the host, the pathogenic molecule enhances the interaction of the susceptibility protein *St*NRL1 with another host protein, *St*SWAP70. This interaction leads to degradation of *St*SWAP70 and subsequently to higher susceptibility (He et al., 2018).

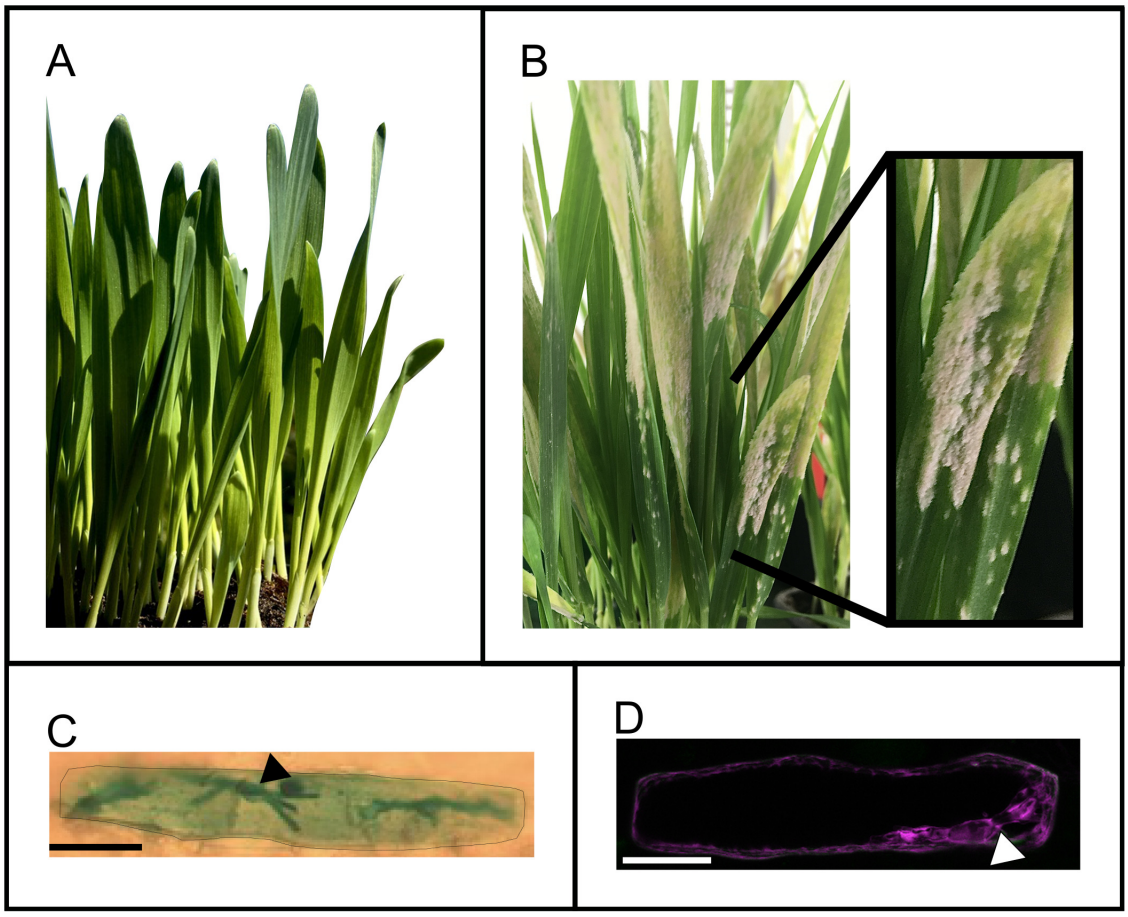

Figure 1: Studying the *H. vulgare*- *B. graminis* f.sp. *hordei* pathosystem. (A) Seven day old *H.vulgare* seedlings grown in soil in a climate chamber under long day conditions. (B) *H. vulgare* infected with *Bgh* spores. White fungal pustules containing conidiospores are visible two weeks after inoculation. (C) Transiently transformed and GUS-stained *H. vulgare* epidermis cell visualised by light microscopy and highlighted by black outline during image editing. Arrow points towards penetration site of *Bgh* from where the haustorium developed (blue). Scale bar: 30 μm. (D) Confocal microscopy image of transiently transformed *H. vulgare* epidermis cell expressing an mCherry fluorescent cytosolic marker to visualise the *Bgh* haustorium within the cell. Image represents stack of horizontal slices, arrow indicates penetration site of *Bgh*. Scale bar: 30 μm.

1.3. Small RHO-GTPases in Plants

Cellular structures such as the extra-haustorial membrane are probably the result of polar growth processes that are at the centre of many developmental and defense mechanisms of plant cells. One of the major players in polar growth of eukaryotic cells are small GTPases of the RAC/Rho family. *Ps*Rho1 was the first plant small GTPase isolated from *Pisum sativum* and shows highest sequence identity to animal Rho proteins within the Ras superfamily (Yang and Watson, 1993). It became evident that these enzymes form a phylogenetically distinct group related to the animal RHO, RAC and CDC42, or in short RHO-type small GTPases. Therefore this plant-specific class of small GTPases has been termed **R**ho **O**f **P**lants, or ROPs (Winge et al., 2000; Zheng and Yang, 2000).
ROP proteins are small, 21-24 kDa proteins with a larger catalytic G-domain at the N-terminus and a shorter variable region at the C-terminus. The G-domain functions in nucleotide and executer binding as well as GTP hydrolysis, whereas the variable region was shown to be important for subcellular localisation. Within the G-domain, five conserved regions have been identified, the so called G-boxes (G1-5) with a P-loop in G1 for phosphate binding, and the switch I and II regions in G2 and G3, respectively. In addition, between G4 and G5 a so-called insert region can be found that was shown to be important for ROP interaction with regulatory proteins. The insert region as well as the two switch regions (G2 and G3) show different conformations when bound to GDP or GTP (Paduch et al., 2001; Thomas et al., 2007, 2009; Feiguelman et al., 2018).
ROPs are molecular switches that have an active signalling, or "on"-state, to initiate molecular pathways by regulating signalling cascades such as cytoskeleton reorganisation and polar growth. These cellular signals are generated by conformational changes in the switch regions (G2 and G3) that either allow the binding of guanosine tiphosphate (GTP) in the signalling active state, whereas ROPs bind guanosine diphosphate (GDP) in their "inactive" form (Zheng and Yang, 2000; Paduch et al., 2001). In basal plant lineages like *Physcomitrium patens*, ROP-signalling has mainly been studied in relation to polar growth (Eklund et al., 2010). In the same way, much of the work published on ROP mechanisms in the model plant *A. thaliana* highlights the role of these molecular switches and their regulators in cellular reorganisation. Examples include processes such as stomal development, outgrowth of root tips and hairs, polar pollen tube growth as well as shaping of pavement cells (more details in section 1.4.3).

A genetic tool to study the role of ROPs has been adapted from RAC/ROP research in animals. Certain amino acids can be mutagenised to keep ROPs in either **C**onstitutively **A**ctivated (CA) or **D**ominant **N**egative (DN) conformation. This knowledge was used for this dissertation in which three amino acids were exchanged to functionally analyse *H. vulgare* ROPs. First, a specific glycine to valine substitution in the G1-motif results in a constitutively activated ROP. Second, the exchange of a threonine with asparagine that also resides in the G1-motif keeps the ROP in a GDP bound, dominant negative conformation. Lastly, a substitution of an aspartic acid in the G3- motif with asparagine

yields a ROP with low nucleotide affinity (Berken and Wittinghofer, 2008).

1.3.1. Regulation of RAC/ROPs

ROPs were classified into two main types based on differences in their C-terminal variable regions. Certain amino acid sequences at the ROP C-terminus allow for post-translational lipid binding that is vital for localisation and function of the mature small GTPase (Winge et al., 2000; Yalovsky, 2015).
Both, type I and II ROPs can be S-acylated but other lipid modification distinguish the two types from each other (Sorek and Yalovsky, 2010). An example for the importance of S-acylation is the coupling of palmitate to the C-terminus of activated *At*ROP6 that is needed for membrane localisation and proper ROP signalling (Sorek et al., 2017). So called type I RAC/ROPs possess the typical CaaX-box (C= cysteine, a= amino acid with aliphatic residue, X = variable amino acid) motif for post-translational prenylation and can be additionally palmitoylated after ROP activation. In contrast, type II RAC/ROPs do not contain a CaaX-box motif in their C-terminal region and are often constitutively S-acylated (Yalovsky, 2015).

Furthermore, ROP signalling is tightly regulated by different classes of proteins due to their function in central signal cascades (Figure 2). In addition, the intrinsic GTP-hydrolysing activity and thereby switching capability of ROPs is inefficient and therefore has to be regulated by ROP activating and inactivating proteins (Vetter and Wittinghofer, 2001).
In metazoans, the signalling inactive, GDP-bound, small GTPase can be kept in this configuration by **G**uanine **D**issociation **I**nhibitors (GDIs) which also mask prenyl residues. On the one hand, GDIs are therefore chaperones of the inactive and cytosolic RHO proteins, on the other hand, they are negative regulators that actively inhibit signalling (Garcia-Mata et al., 2011). The role of plant GDIs was studied in *Nicotiana tabacum* during pollen tube growth (Klahre et al., 2006) and *A. thaliana* where their function in plant development was highlighted (Feng et al., 2016; Ge et al., 2020). *At*GDIs are also important in normal growth and function of pollen tubes and play a role in focussing of activated ROPs at the plasma membrane (Feng et al., 2016). In addition, Ge et al. (2020) revealed that the ROP regulatory function of *At*GDIs is connected to vesicle trafficking to and from the plasma membrane. These examples also highlight the fact that GDIs primarily are ROP inhibitors but are also important in ROP activity.

ROPs are signalling active when bound to GTP. Therefore, the activation requires dissociation of GDP and subsequent binding of GTP in the G-box motif of the protein. The structural change of the ROP protein that is required for this nucleotide exchange is enhanced by the association with **G**uanine nucleotide **E**xchange **F**actors (GEFs). Upon GEF- binding, a conformational change takes place which leads to dissociation of the GDP nucleotide. The empty pocket can then be filled by a new nucleotide (Vetter and Wittinghofer, 2001). The structurally similar Ras proteins have been shown to have increased

affinity to GTP compared to GDP (Feuerstein et al., 1987). Since the cellular concentration of GTP is high, it is the preferred nucleotide for binding. Therefore, after nucleotide loading of a ROP, a GTP-bound conformation is assumed (Berken et al., 2005).

Activated ROPs interact with downstream so-called effectors or executors such as **I**nteractor of **C**onstitutive active **R**OP (ICR) also known as **R**OP **I**nteractive **P**artners (RIPs) as well as **R**OP **I**nterative and **C**RIB-domain containing proteins (RICs) (Lavy et al., 2007; Li et al., 2008; Wu et al., 2001). *At*ICR1/RIP1 overexpression leads to changes in polar growth processes just as the activation of the corresponding *At*ROP does. It was also discovered that ICRs/RIPs fulfil a scaffold protein function, linking activated ROPs with downstream interactors of cellular organisation (Lavy et al., 2007; Li et al., 2008). RICs are another class of scaffold proteins that contain only one conserved domain, called **C**DC42/**R**AC **I**nteractive **B**inding (CRIB). This domain is responsible for ROP-GTP interaction which leads to specific subcellular localisation of RICs during the interaction with activated ROPs. However, it has been shown that RICs perform specified functions in *A. thaliana*. *At*RIC3 and *At*RIC4, for example, co-localise with activated *At*ROP1 but function antagonistically in F-actin dynamics in pollen tubes (Gu et al., 2005). Pollen tube elongation, on the other hand, is regulated by *At*RIC10 which interacts with yet unknown ROPs (Wu et al., 2001).

Once ROPs are GTP- bound, the enzyme can hydrolyse the nucleotide in order to return to an inactive signalling state. However, the intrinsically slow GTPase function of ROPs is supported by the action of GAPs, **G**TPase **A**ctivating **P**roteins (Wu et al., 2000). This function is vital to coordinate polar growth. For example, it was shown that *N. tabacum* polar growth in pollen tubes requires the activity of *Nt*GAP1 which inactivates *Nt*RAC5 at the tube flanks but not at the apex (Klahre and Kost, 2006). Several reports show that *At*GAPs interact with activated *At*ROPs to regulate their activity and thereby control ROP-signalling (Huesmann et al., 2011). Interestingly, a large number of plant GAPs also contain the ROP-executer domain CRIB which is important for GAP activity and has been shown to provide binding affinity to the ROP (Schaefer et al., 2011).

ROPs are cytosolic or plasma membrane bound proteins that are targeted by upstream signal components, like cell surface receptors. One prominent example is the cell-wall sensing **R**eceptor **L**ike **K**inase (RLK) FERONIA (*At*FER) which has been shown to interact with different *At*ROPs via *At*GEFs to transduce signals important for root hair and pavement cell development (Duan et al., 2010; Lin et al., 2021). In addition, *At*FER was found to support pollen tube reception and also plays a role in *A. thaliana* susceptibility towards powdery mildew (Kessler et al., 2010)). Other ROP-related *At*RLKs are important in plasma membrane symmetry breaking to form pavement cells (*At*TMK) and polar pollen tube growth (*At*PRK2a). *Sl*PRK1/2 fulfil the same function in *Solanum lycopersicum* and *Zm*PAN1 works in concert with ROPs to facilitate stomatal development in *Zea mays* (Miyawaki and Yang, 2014). Interestingly, the cytoplasmic kinase *At*AGC1.5 was shown

to also associate with *At*ROP2-downstream interactors *At*RIP3 and *At*RIP4 (Li et al., 2020). The RLK-ROP connection is not only important in growth and development but plays a crucial role in the response to biotrophic and hemibiotrophic stressors. In *O. sativa*, for example, the chitin receptor complex *Os*CERK1/*Os*CEBiP has been shown to interact with *Os*GEFs to activate *Os*RAC1, a regulator of rice immunity and symbiosis (Akamatsu et al., 2016).

Accumulating evidence has been put forward that ROP-signalling in these developmental pathways in parallel also functions in susceptibility towards pathogens (Poraty-Gavra et al., 2013; Molendijk et al., 2004). The hypothesis is that the molecular mechanisms underlying polar outgrowth of organs, such as root hairs or pollen tubes, are similar to those of plasma membrane ingrowth during the accommodation of the fungal haustorium (Schultheiss et al., 2003; Opalski et al., 2005). Within the cell, these processes rely on cytoskeleton (re-) organisation in order to supply the cell wall and steer growth direction (Mathur and Huelskamp, 2002).

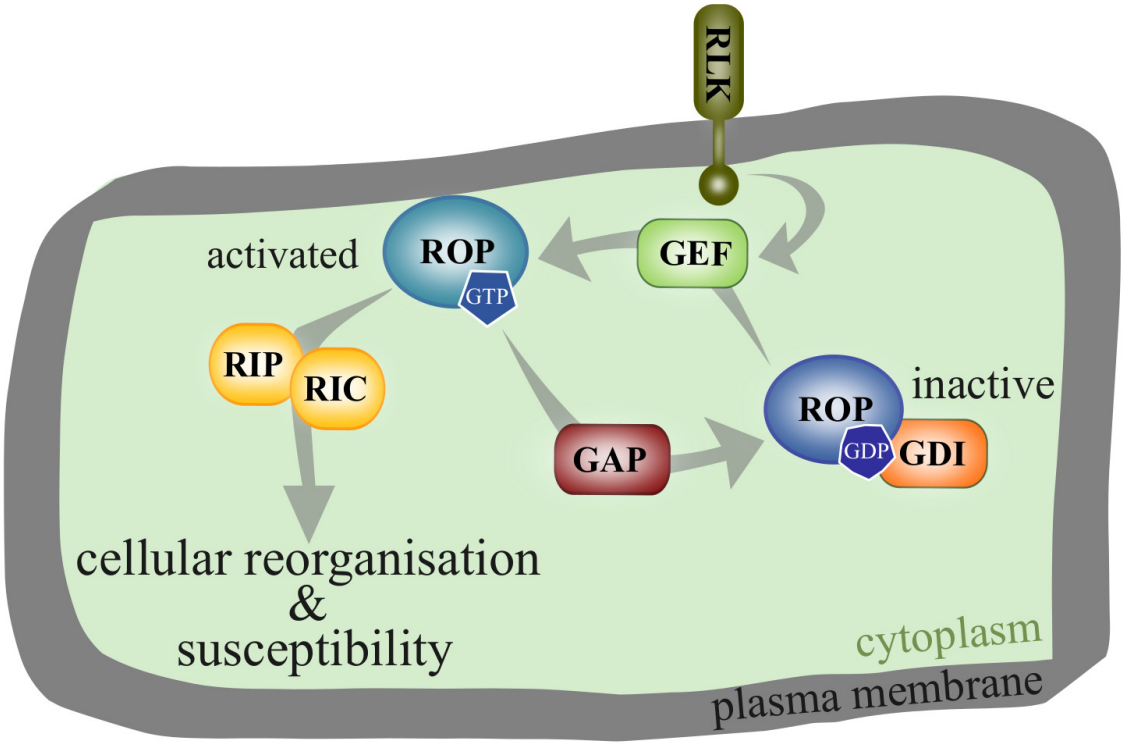

Figure 2: ROP GTPase signalling in plant cells. **R**ho **O**f **P**lants (ROP) GTPases cycle between inactive (GDP bound) and activated (GTP bound) states with the help of regulatory proteins such as inhibiting **G**uanine **D**issociation **I**nhibitors (GDI), activating **G**uanine nucleotide **E**xchange **F**actors (GEF) and inactivating **G**TPase **A**ctivating **P**roteins (GAP). In the activated state, ROPs interact with downstream executers, such as **R**OP **I**nteractive **P**artners (RIP) and **R**OP **I**nterative and **C**RIB-domain containing proteins (RIC) that transfer signals to activate cellular reorganisation and susceptibility. Cell surface receptors such as **R**eceptor **L**ike **K**inases (RLK) perceive environmental cues and interact with GEFs to relay signals intracellularly.

1.3.2. ROP activity sensors

As introduced, ROP activation is important for cellular responses to environmental stimuli. Therefore, the GTP-loading and activation of ROPs has been tested via different means in the past. Several methods have been published on *in vitro* and *in planta* approaches to monitor the ROP activity status. Guanine nucleotide exchange assays that visualise the amount of ROP- bound GDP/GTP have shed light on the GTPase activity of *A. thaliana* and *O. sativa* ROPs (Berken et al., 2005; Gu et al., 2006; Kawasaki et al., 1999).

In animals, GTPase activity has been monitored *in vitro* by immunoprecipitation of Rho proteins bound to interactors of activated GTPases such as CRIB-domain containing protein fragments. This is thought to be a direct measure of the relative amount of activated GTPase (Sander et al., 1998).

Similar approaches have been performed in plants by labelling the guanosines either radioactively or with fluorescent tags. For example, Kawasaki et al. (1999) monitored the amount of radioactively labelled GTP bound to *Os*RAC1 to validate its GTPase function. Later, the ROP activation status was determined via measuring the dissociation of fluorescent GDP from *At*ROP4 in presence of two *At*GEF candidates (Berken et al., 2005). Monitoring the change in fluorescently labelled GTP bound to *At*ROP1 indicates activation of the GTPase in presence of active *At*GEFs (Gu et al., 2006; Wang et al., 2017).

One of the first approaches to visualise ROP activity *in vivo* made use of the fact that animal Rho GTPases are functional when localised to the plasma membrane (Ridley, 2006). The same is true for plant interactors of activated ROPs, such as *At*RIC4 or *At*RIC1. By monitoring the localisation of C-terminally truncated GFP-*At*RIC4ΔC, Hwang et al. (2005) showed *in planta* localisation of activated *At*ROP1. The same method has been employed with the CRIB domain of *At*RIC1 or full length *At*RIC4 fused to GFP to monitor the localisation of activated ROPs (Li et al., 2018a; Zhou et al., 2021).

Inspired by **F**örster **R**esonance **E**nergy **T**ransfer (FRET)-based sensors to measure Ca^{2+}, a Rho GTPase activity sensor called **R**as **A**nd **I**nteracting protein **CH**imeric **U**nit (Raichu) was developed (Nakamura et al., 2005) and adapted for *in planta* measurements of ROP activity (Kawano et al., 2010; Hamers et al., 2014; Wang et al., 2018). These Raichu sensors contain a GTPase C-terminally fused to CFP and the corresponding FRET fluorophore YFP fused to the C-terminus of a **G**TPase **B**inding **D**omain (GBD), an interactor of activated Rho, on one plasmid. In the activated state, the resulting protein will fold in a way that GBD interacts with the activated GTPase, and at the same time bringing the two fluorophore close together. In that confirmation, there will be energy transfer (FRET) from CFP to YFP which can be measured in fluorescence intensity. Therefore, if the YFP/ CFP fluorescence ratio increases, the sensor GTPase is activated (Nakamura et al., 2005). Kawano et al. (2010) designed this Raichu sensor with CFP-*Os*RAC1 interacting with *Hs*CRIB-YFP (*Homo sapiens* CRIB from *Hs*PAK1 as GBD) to measure ROP activity in *O. sativa* protoplasts in presence of the R protein *Os*Pit (Kawano et al., 2010, 2014a). Akamatsu et al. (2013) used the same sensor design to successfully link PTI perception in *O. sativa* to the *Os*RAC1 dependent immunity pathway.

1.3.3. ROP functions in plant-microbe symbiosis

Next to its role in plant immunity, the chitin receptor *Os*CERK1 was also found to be important in the perception of symbiotic fungi in *O. sativa* roots (Akamatsu et al., 2016). Even though, *Os*CERK1 downstream signalling during symbiosis requires other signalling cascades, ROPs have been shown to play important roles in the symbiosis between plants and symbiotic microbes. The two most studied beneficial plant-microbe relationships are between different species of legume plants and symbiotic bacteria or fungi, namely rhizobia and arbuscular mycorrhiza, respectively (Gutjahr and Parniske, 2013; Doermann et al., 2014).

During plant-rhizobia interaction, the plant perceives so called Nod-factors which initiate polarised root hair growth and deformation in order to accommodate the symbiont in the nodule, a newly developed symbiosis organ. A polar growth processes during rhizobia colonisation is the formation of so called infection threads that guide bacteria from the root hair tip towards its base where the nodule is formed. In *Lotus japonicus*, the homeostasis of the molecular switch *Lj*ROP6 is required to facilitate polar growth of infection threads (Liu et al., 2020). For the legume *Glycine max* it was found that the perception of Nod-factor results in activation of the small GTPase *Gm*ROP9 which in turn starts a signalling cascade that activates symbiosis-related genes (Gao et al., 2021b). The corresponding ROP in *Medicago truncatula* is an important regulator of root hair development and rhizobia infection. *Mt*ROP9 has to be activated in order to reprogram root hair growth towards nodule formation (Wang et al., 2021). In a similar manner, the activation of *Mt*ROP10 is important for signalling that leads to root hair deformation during successful symbiosis (Lei et al., 2015). This shows specialised functions of legume ROPs during the symbiosis process.

Interestingly, for *Mt*ROP6 a positive role during rhizobia infection was observed, whereas silencing of the same ROP supports the association with arbuscular mycorrhiza fungi (Kiirika et al., 2012). Other reports in *L. japonicus* have shown similar results for *Lj*ROP3 which is important in nodule formation but does not act during mycorrhiza symbiosis (García-Soto et al., 2021). Apart from these reports, little is known whether ROPs play a role in arbuscular mycorrhiza establishment in plants.

1.3.4. ROP functions during pathogen attack

When challenged with pathogenic fungal spores, a plant cell has to undergo major changes for either defending or hosting the invader. In the case of an interaction between *Bgh* and *H. vulgare* this entails either accommodation of the fungal haustorium or defence against penetration of the appressorial germ tube. As previously introduced, ROP-dependent cytoskeleton reorganisation and polar growth are at the centre of these mechanisms (Berken et al., 2005; Nagawa et al., 2010; Pathuri et al., 2008; Bloch and Yalovsky, 2013). However, accumulating evidence has been put forward that the biotrophic fungus *Bgh* is able to hijack the role of ROPs in development to successfully penetrate *H. vulgare* epidermal

cells (Engelhardt et al., 2020). In other grass species, like *O. sativa*, ROP function has been primarily studied in terms of plant immunity but more recent studies also shine light on the role of these small GTPases in *O. sativa* developmental signalling. The first published *Os*ROP was the type II *Os*RAC1 (Kawasaki et al., 1999). A regulatory function of *Os*RAC1 during cell death and the production of Reactive Oxygen Species (ROS) was described. Transgenic plants overexpressing the dominant negative *Os*RAC1-T24N were compromised in ROS production and showed less cell death as well as fewer lesions after inoculation with the rice blast fungus *Magnaporthe grisea* (Kawasaki et al., 1999). The activated form of *Os*RAC1 is also important in resistance against bacterial blight and regulates transcriptional activation of defense genes (Ono et al., 2001). Further, it was shown that the resistance (R) protein *Os*Pit interacts with the GEF *Os*SPK1 to perform its function in rice blast fungus resistance. *Os*SPK1 in turn activates *Os*RAC1 which regulates ETI in the attacked cells. Interestingly, *Os*RAC1 functions in immunity via the two different pathways, ETI and PTI. During ETI, the *Os*Pit-*Os*SKP1 signal cascade is triggered by pathogenic effectors, while the ROP interacts with *Os*GEF1 after elicitation of the chitin receptors *Os*CERK1 and *Os*CEBiP to induce resistance in PTI (Akamatsu et al., 2021). Further, ROP signalling has been shown to be an essential part of *H. vulgare* susceptibility to powdery mildew.

1.3.5. ROPs in *H.vulgare*

In *H. vulgare*, the role of ROP signalling during the interaction with *Bgh* has been investigated intensively. In total, six ROPs have been identified in the *H. vulgare* genome of which *HvRAC1*, *HvRAC3*, *HvRACB*, *HvRACD* and *HvROP6* are expressed in the epidermis (Schultheiss et al., 2003).

In terms of their biological function, the *H. vulgare* ROP *HvRACB* was knocked-down transiently by RNA interference, which made plant cells more resistant towards *Bgh* (Schultheiss et al., 2003). In addition, *H. vulgare* plants stably transformed with constitutively activated *Hv*RAC1, *Hv*RAC3 or *Hv*RACB are more susceptible when challenged with the fungus (Pathuri et al., 2008). As introduced, during a successful infection fungal structures displace host cell components. In *H. vulgare* it was also shown that this rearrangement and the establishment of the EHM involves the reorganization of the cytoskeleton (Opalski et al., 2005; Hoefle et al., 2011). Especially the role of the *H. vulgare* ROPs *Hv*RAC1 and *Hv*RACB in cytoskeleton organisation seems to make them targets for fungal manipulation. Interestingly, these *Hv*ROPs also each represent the two ROP-types I and II. Therefore, the type II ROP *Hv*RAC1 and type I ROP *Hv*RACB will be introduced in more detail in the following.

*Hv*RAC1

Amongst *H. vulgare* ROPs expressed in the epidermis and functioning in susceptibility, the type II ROP *Hv*RAC1 was reported to also play a role in cell expansion and the devel-

opment of root hairs. Even though the transient transformation of *H. vulgare* epidermal cells with CA-*Hv*RAC1 did not change *H. vulgare* susceptibility, stable transformation of plants over expressing CA-*Hv*RAC1 increased the susceptibility of these plants towards *Bgh* and leaves exhibited elongated epidermal cells. On the contrary, CA-*Hv*RAC1 supported penetration resistance to the rice blast fungus *Magnaporthe oryzae*. (Schultheiss et al., 2003; Pathuri et al., 2008).
The role of *Hv*RAC1 in cellular reorganisation is likely facilitated by its interaction with the **M**icrotubule **A**ssociated **GAP1**, *Hv*MAGAP1 (Hoefle et al., 2011). In order to rely signals, *Hv*RAC1 was tested for its interaction with downstream executers of the RIC and RIP protein families and was not found to interact with scaffold proteins, like *Hv*RIC171 (Schultheiss et al., 2008). However, another downstream interactor of ROPs, *Hv*RIPa, is involved in forming microtubule restricted membrane domains when co-expressed with *Hv*RAC1 and *Hv*MAGAP1. Overall, the function of *Hv*RAC1 in resistance and susceptibility to *Bgh* and other pathogens appears complex and is still under investigation (Hoefle et al., 2020).

*Hv*RACB

The susceptibility factor *HvRACB* is an example of a type I ROP. *Hv*RACB is expressed in *H. vulgare* leaf epidermis but the transcript levels do not change after inoculation with *Bgh* (Schultheiss et al., 2002). Even though, *Hv*RACB has been shown to affect the response of *H. vulgare* epidermal cells towards the powdery mildew fungus *Bgh* in a cell-autonomous manner. Constitutively activated *Hv*RACB supports the penetration of a fungal appressorium into the plant cell (Schultheiss et al., 2002, 2003). Silencing of *Hv*RACB by RNAi, on the other hand, makes the plant less susceptible to *Bgh* penetration (Schultheiss et al., 2002; Hoefle et al., 2011).
As introduced earlier, ROPs can be mutagenised in order to lock them either into an "on" or "off" signalling state. For example, the G15V substitution of *Hv*RACB renders the protein constitutively activated. The mutation occurs in the GTPase domain and disrupts the intrinsic GTPase function so that the ROP stays in a constant GTP-bound state. When this CA-*Hv*RACB is transiently over-expressed in *H. vulgare* epidermis cells, it localises to the plasma membrane where the protein is functional in susceptibility (Schultheiss et al., 2003). CA-*Hv*RACB overexpressing plants have distinct phenotypes in epidermal cell expansion and abolished polar growth in root hairs leading to shorter and bulging appearance. In addition, these plants show increased susceptibility towards *Bgh* (Schultheiss et al., 2005; Pathuri et al., 2008). A dominant negative *Hv*RACB can be created by exchanging threonine 20 with asparagine (T20N). Analogous to previous publications in mammalian Rho and *Os*RAC1, this DN-*Hv*RACB is considered to stay bound to GDP (Hart et al., 1994; Kawasaki et al., 1999).
Next to the role of *Hv*RACB in plant susceptibility, it has been reported to be a regulator of cell polarity. Typical developmental phenotypes that rely on polar growth, such as root hair outgrowth and elongation, are also disturbed in *Hv*RACB RNAi transgenic

plants (Hoefle et al., 2011; Scheler et al., 2016). In addition, *Hv*RACB is involved in abiotic stress as has been shown by investigating transgenic plants stably over expressing CA-*Hv*RACB. These mutants show developmental alterations such as stunted growth of the shoot and roots, increased water loss, decreased CO_2 assimilation and enhanced transpiration (Schultheiss et al., 2005). Increasing evidence has been published that the different roles of *Hv*RACB rely on similar underlying functions (as reviewed by Engelhardt et al. (2020)). One example is the regulation of the cytoskeleton on the one hand, and *Hv*RACB's involvement in susceptibility on the other hand. During *Bgh* infection, polarisation of filamentous F-actin takes place at the site of fungal attack which leads to resistance but the activation of *Hv*RACB triggers a loss of F-actin focusing which is associated with enhanced susceptibility (Opalski et al., 2005).

Like other ROPs, *Hv*RACB should be regulated via post translational modifications as well as via the interaction with regulatory proteins. Indeed, a recent study on post-translational modifications reveals *Hv*RACB phosphorylation *in vitro* and a highly conserved *in vivo* ubiquitination site (Weiss et al., 2022). The interaction of activated *Hv*RACB with downstream signalling proteins (also called ROP effectors or executers) likely induces cellular re-organisation in order to respond to fungal stimuli. Examples of activated *Hv*RACB interactors are executer proteins such as the two RICs *Hv*RIC171 and *Hv*RIC157 as well as the RIP *Hv*RIPb (Schultheiss et al., 2008; Engelhardt et al., 2021; McCollum et al., 2020).

*Hv*RIC171 and *Hv*RIC157 accumulate at fungal penetration sites that are hence probably domains of high *Hv*RACB activity. Moreover, the transient over-expression of either RIC increases penetration efficiency of *Bgh* (Schultheiss et al., 2008; Engelhardt et al., 2021). An other class of ROP-downstream interactors are RIPs, of which *Hv*RIPb is a representative. The scaffold protein probably acts in the susceptibility pathway of *Hv*RACB because it resides at microtubules and is recruited together with activated *Hv*RACB to the fungal penetration site just as the two before mentioned *Hv*RICs (McCollum et al., 2020).

*Hv*RACB activity is also controlled by regulators like *Hv*MAGAP1 which functions antagonistically to *Hv*RACB in susceptibility. More specifically, over-expression of *Hv*MAGAP1 leads to a resistance phenotype towards *Bgh*, whereas over-expression of CA-*Hv*RACB makes *H.vulgare* cells susceptible (Hoefle et al., 2011). As the name suggests, *Hv*MAGAP1 binds to microtubules that polarise at fungal penetration sites when pathogen establishment is hindered. The opposite was reported for sites of successful *Bgh* penetration, where *Hv*MAGAP1 localises with fragmented microtubules and at the haustorial neck. In addition, *Hv*MAGAP1 was shown to be recruited to the cell periphery by activated *Hv*RACB (Hoefle et al., 2011; Hoefle and Hückelhoven, 2014).

Besides the regulation via GAPs, *HvRACB* transcript abundance was suggested to be regulated via a molecular feedback loop. The **R**OP-**B**inding Receptor-Like Cytoplasmic **K**inase 1 (*Hv*RBK1) is an interactor of activated *Hv*RACB and also interacts with the type II S-phase kinase 1-associated (SKP1)-like protein (*Hv*SKP1-like). Both, *Hv*SKP1-like and *Hv*RBK1 were shown to negatively regulate the abundance of *Hv*RACB. In addition,

the expression of *Hv*SKP1-like and *Hv*RBK1 also negatively regulate *Bgh* establishment. Together this points to an other regulatory mechanism during which activated *Hv*RACB is possibly degraded (Reiner et al., 2016).
Besides these regulators networks, other feedback loops have been identified in the *Hv*RACB signalling pathway via a transcriptome analysis of *Hv*RACB RNAi and CA-*Hv*RACB over expressing plants. The results suggested that *Hv*RACB regulates transcripts of other susceptibility genes, such as RLKs. Further studies used **T**ransient **I**nduced **G**ene **S**ilencing (TIGS) to reveal a list of *Hv*RLK candidates that could act in concert with *Hv*RACB. In addition, these *Hv*RLKs are involved in susceptibility (Schnepf et al., 2018).
As introduced earlier, pathogens can make use of host susceptibility factors in order to increase their virulence. An example of a *Bgh* protein that targets *Hv*RACB is the effector ROPIP1. When over-expressed in the plant, ROPIP1 increases *Bgh* penetration success and it was shown to interact with CA-*Hv*RACB. In addition, fungal establishment is partially hindered during HIGS of the effector. This is evidence for a central role of ROPIP1 in *Bgh* virulence. The exact mechanism of how ROPIP1 acts as an effector has not been shown so far. However, the *Bgh* protein is recruited to microtubules by the *Hv*RACB-*Hv*MAGAP1 complex. Transient over-expression of ROPIP1 further points to a possible role in destabilisation of cortical microtubules (Nottensteiner et al., 2018).
Since activated *Hv*RACB supports fungal establishment, the GDP to GTP exchange of *Hv*RACB is a critical step in its function as a susceptibility factor. Until now, however, no *Hv*RACB-activating mechanism has been elucidated.

1.4. Guanine Nucleotide Exchange Factors

As introduced earlier, ROP GTPase signalling was shown to be activated by guanine nucleotide exchange factors which catalyse GDP dissociation from GTPases via a conformational change of the ROP protein (Vetter and Wittinghofer, 2001; Schmidt and Hall, 2002). RHO GEFs are important signalling proteins in all eukaryotes and their roles have been extensively studied in metazoan cells. Research on plant GEFs is more limited but of increasing interest due to their many roles in vital signalling pathways. The following sections provide a brief overview of the current knowledge on metazoan GEFs and a more detailed section on plant GEFs.

1.4.1. Metazoan GEFs

In non-plant eukaryotes, like animals and fungi, GEFs play important roles in host-pathogen interaction. For instance, pathogenic yeast require the activation of small GTPases via GEFs to initiate filamentous growth, an important process in the fungal life cycle (Hope et al., 2008). In mammalian cells, GEFs are targeted by pathogenic bacteria to manipulate actin remodeling of the host cell in order to infect (Patel and Galán,

2006). Other GEFs are important factors of the human immune system. In particular, a mammalian GEF was found to regulate lymphocyte trafficking, which is vital for proper functioning of adaptive immune responses (Kunimura et al., 2020). Knowledge about the molecular mechanisms of GEF function harbour the potential to develop them as drug targets for diseases (Ye, 2020). Metazoan Rho exchange factors are divided into two classes: DH-PH and DOCK GEFs. Both types of GEFs are named after their conserved functional domains and each class contains a motif responsible for exchanger function and one that is important for protein localisation.

The first class contains the earliest found mammalian GEF called Dbl (oncogene for diffuse B-cell lymphoma), which gave the name to the active exchanger domain **D**bl **H**omology, in short DH (Eva and Aaronson, 1985; Hart et al., 1994). The DH domain is subdivided into three **C**onserved **R**egions (CR1-3) which often pose the only similarity amongst DH-GEFs. Structurally, DH-GEFs share the arrangement into 11 α- helices (Worthylake et al., 2000). Another conserved region in these GEFs is the **P**leckstrin **H**omology (PH) domain which has been found in many protein classes and was shown to be important for subcellular localisation via phospholipid binding (Cerione and Zheng, 1996). An overview of other functional but not conserved domains as well as regulation and functions of these DH-PH GEFs is highlighted by Schmidt and Hall (2002). The authors report an additional domain that is not conserved in all DH-PH GEFs, the so called **S**rc-**H**omology 3 (SH3) domain. The second class of metazoan guanine nucleotide exchangers are DOCK GEFs. They do not possess DH-PH domains but the earlier mentioned SH3 can be found in these GEFs. One example of this GEF class is DOCK-180. The exchanger domain of DOCK GEFs is called Dock180-homology-domain-involved-in-exchange-on-Rac (Docker) and contains **D**ock-**H**omology-**R**egion-1 and 2 (DHR1/2) which are conserved amongst eukaryotic cells (Brugnera et al., 2002). As with DH-PH GEFs, the conserved regions DHR1 and DHR2 of DOCK GEFs have different functions: DHR1 binds to phospholipids and is important for localisation, whereas the actual exchanger activity is performed via DHR2 (Kunimura et al., 2020).

1.4.2. DH-PH and DOCK-type GEFs in plants

The only plant DH-PH GEFs published to date are called SWAP70 and were described for the three plant species *O. sativa*, *A. thaliana* and *S. tuberosum*. SWAP70 has the typical DH-PH domain structure and has mainly been studied for its function during plant immunity. In *O. sativa*, *Os*SWAP70A and B activate *Os*RAC1 after chitin elicitation and are therefore involved in plant immunity towards fungi (Yamaguchi et al., 2012). The *A. thaliana* homologue *At*SWAP70 was shown to act in PTI and ETI against the bacterium *P. syringae* (Yamaguchi and Kawasaki, 2012). Lastly, *St*SWAP70 is important in *S. tuberosum* resistance against late blight and is indirectly targeted by a *Phytophthora infestans* effector via the susceptibility factor *St*NRL1 (He et al., 2018).

Analogous to DH-PH GEFs, SPK1 (SPIKE1) is the only published example of DOCK-type plant GEFs. SPK1 was found in several plant species and has been reported to function in immunity and plant development (Qiu et al., 2002; Liu et al., 2020; Wang et al., 2018). *At*SPK1 is named after the mutant phenotype which shows spike-like instead of branched trichome development. The GEF is expressed in most pant tissues and mutant plants lacking *AtSPK1* show severe developmental defects. Most striking are misshaped cells due to aborted polar growth signalling (Qiu et al., 2002). SPK1 is also an important transduction protein during polarised growth of root hairs in the interaction between the legume *L. japonicus* with symbiotic bacteria. *Lj*SPK1 has been shown to activate the earlier introduced *Lj*ROP6, a regulator of root hair development during the interaction with rhizobia (Liu et al., 2020). In *O. sativa*, the corresponding protein has been shown to be involved in resistance against the rice blast fungus. *Os*SPK1 localises to endomembranes where the DHR2 domain of the GEF interacts with the R protein *Os*Pit during ETI (Wang et al., 2018).

1.4.3. PRONE-type GEFs

Next to DH-PH- and DOCK- type GEFs, plants possess a distinct class of ROP activating proteins that can be identified by the **P**lant-specific **R**ac/R**o**p **N**ucleotide **E**xchanger (PRONE) domain. PRONE GEFs are usually around 500-600 amino acids in length, most of which is composed of the PRONE domain itself. With some exceptions, the conserved PRONE is flanked by variable N- and C-terminal regions (Berken et al., 2005; Thomas et al., 2007, 2009; Fricke and Berken, 2009).
PRONE-GEFs have initially been identified in *A. thaliana* in which 14 *AtGEF* genes that code for *At*GEF1-14 can be found in the genome (Berken et al., 2005). Two separate yeast-two-hybrid screens were performed using type I ROP mutants with substitutions for D121 as bait because they were hypothesised to have increased GEF affinity. More specifically, the Y2H assays using *At*ROP4-D121N (Berken et al., 2005) and *At*ROP1-D121A (Gu et al., 2006) identified PRONE-containing proteins as ROP interactors and possible ROP nucleotide exchangers. In addition, *O. sativa* PRONE GEFs were also identified via their interaction with the corresponding *Os*RAC1amino acid substitution, namely *Os*RAC1-D125N (Akamatsu et al., 2013).

Shortly afterwards, crystallisations of the *A. thaliana* ROP-GEF complex were published (Thomas et al., 2007, 2009). The PRONE domain of *At*GEF8 was crystallised in a homodimer, in which the two N-terminally oriented α-helices 1 interact with each other. In addition, *At*ROP4-GDP was shown together with *At*PRONE8 in a complex (Thomas et al., 2007). Later, a heterotetramer consisting of two *At*PRONE8-domains in a dimer formation with two *At*ROP7 proteins attached to both PRONE protomers was published in the same conformation as two years before but without GDP nucleotide (Thomas et al., 2009). These studies also show that *At*ROP4 undergoes structural changes in the switch I and II regions upon *At*GEF binding which leads to GDP release. The GEF-ROP complex seems to be stable after this process, indicating a continued interaction of the nucleotide-

free ROP with the GEF (Thomas et al., 2007; Berken et al., 2005). For *At*GEF8 it was further shown that the interaction between the PRONE domains of two GEFs depends on amino acid L23 since proteins with an L23D mutation seize to interact. In addition, the homo-dimerisation is important for GEF function because the dimerisation mutant *At*GEF8-L23D lacks exchanger function towards the ROP (Thomas et al., 2007). On the ROP side, one amino acid was shown to play particular importance for the interaction. A conserved serine residue (S74) was proven crucial for the GEF-ROP interaction (Fodor-Dunai et al., 2011).

In order to analyse the function of individual GEFs, it is important to first find out where and under which environmental conditions the corresponding genes are transcribed in the plant. *GEFs* are indeed expressed in different plant tissues and respond to various stimuli. A comprehensive analysis by Shin et al. (2009) presents tissue specific as well as stress induced expression pattern of the 14 *AtGEFs*. For example, the transcript levels of *AtGEFs 1*, *4*, *5*, *6*, *10*, *11* and *12* were recorded in root tissue. Leaf expression was observed in an other, partially overlapping, group of *AtGEFs* (*1*, *4*, *5*, *11* and *14*). On the contrary, *AtGEF* expression in reproductive tissues is rather ubiquitous. Transcripts of all 14 *AtGEFs* were observed in flower tissue (Shin et al., 2009) but the expression of only *AtGEFs 8*, *9*, *10*, *12* and *13* were found in samples from pollen tubes (Zhang and McCormick, 2007). In addition, upon several abiotic stresses, certain *AtGEFs* were differentially expressed, hinting towards a possible specialised function in subcellular signalling (Shin et al., 2009).

PRONE GEFs in plant development

As ROP activators, GEFs play important roles in a number of signalling cascades in different plant tissues. Especially their role in polar growth processes such as the development of root hairs and cell shape but also polar growth in reproductive organs and during immunity has been recorded. The following section provides an overview on reports of GEF function in development which has primarily been studied in *A. thaliana*.

Root hair development is regulated by the production of ROS which is triggered by the molecular switch *At*ROP2 (Jones et al., 2007). The GTPase is activated by a signalling cascade that originates with different kinases. In literature, three examples of these kinases interacting with different *At*GEFs are found. Firstly, the RLK *At*FER which interacts with *At*GEF1 that in turn activates *At*ROP2 to regulate ROS-triggered root hair development (Duan et al., 2010). Another class of protein kinases from the family of [**C**a^{2+}]cyt-**A**ssociated **P**rotein kinases (CAP) interact with *At*GEF1 to regulate root hair growth. *At*CAP1 interacts with and possibly activates *At*GEF1 to turn on the *At*ROP2 and *At*ROP6 signalling pathways that are important in development (Huang et al., 2018a). However, the interaction of GEFs with CPKs can also lead to a repression of polar growth. During stress, *At*CPK4 phosphorylates *At*GEF1 at S51, which leads to its degradation and shifts cellular resources towards stress response rather than development (Li et al., 2018b).

Lastly, it was shown that the kinase *At*AGC1.5 interacts with *At*GEF4 and *At*GEF10 to organise root hair growth. A positive feedback loop is created by repeated phosphorylation of the GEFs and hetero-oligomerisation of activated ROP2 and its downstream executers (Li et al., 2020).
It has become more and more visible that the coordinated action of different GEFs is key for complex signalling processes such as asymmetric growth during the development of root hairs. The two GEFs *At*GEF3 and *At*GEF4 are reported to function in different stages of this process. After plasma membrane recruitment of *At*ROP2 via interaction with phospholipids, *At*GEF3 functions as initiator for root hair emergence at the root hair initiation domain (RHID) and creates a nano-domain of activated *At*ROP2. This domain of immobilised and activated *At*ROP2 is then targeted by *At*GEF4 which triggers root hair outgrowth and elongation. (Denninger et al., 2019; Fuchs et al., 2021). The ROP-GEF nano-domains are typically smaller than 1 μm^2 and can aggregate to bigger domains of 10 to 50 μm^2 in size. Initiation of nano-domains happens due to the interaction of ROPs and the PRONE domain of GEFs. GAPs then function to shape the domains (Sternberg et al., 2021).
Not only the outgrowth of root hairs is a polar growth process that requires ROP-signalling but the development of the roots themselves do, too. Root growth is regulated by the phytohormone auxin which induces *At*GEF7 expression and the GEF in turn activates *At*RAC1-dependent signal transduction that leads to the regulation of the auxin efflux carrier *At*PIN (Chen et al., 2011).

The jig saw puzzle-like shape of epidermal pavement cells in plants, as observed in *A. thaliana* require specialised out- and ingrowing lobes of the cell wall and plasma membrane. ROPs have been found to play key roles in the formation of these shapes. Activation of *At*ROP2 and *At*ROP4 was observed to trigger lobe outgrowth whereas *At*ROP6 signals in the lobe indentions (Fu et al., 2005, 2009). Important proteins triggering this signalling are cell surface receptors which interact with GEFs in order to target their downstream ROPs. Recently, a link between the earlier introduced RLK *At*FER, which is a cell wall receptor, and *At*ROP6 have been elucidated. After pectin perception of *At*FER, *At*GEF14 was shown to signal via *At*ROP6 to induce pavement cell shaping (Lin et al., 2021).

Cell surface receptors also play an important role in the development of reproductive organs. Pollen tube growth responds to the attractant peptide *At*LURE1 that can be perceived by *At*PRKs, namely *At*PRK2 and *At*PRK6. Each receptor signals via a different GEF, *At*PRK2 via *At*GEF1 and *At*PRK6 activates *At*GEF12 . Both GEFs, however, were shown to activate *At*ROP1 to foster pollen tube growth. Importantly, *At*PRK2 as well as *At*ROP1 interact with *At*GEF1 via its C-terminal region. After mutation of conserved serine residues S460 and S480 in this part of the GEF protein, the function of *At*GEF1 was abolished. These results again highlight the regulatory role of the PRONE GEF C-terminus in signalling (Gu et al., 2004; Zhang and McCormick, 2007; Chang et al., 2013; Takeuchi and Higashiyama, 2016). A different class of receptor kinases that regulate

pollen tube growth via the ROP- pathway are *At*FER-like *At*BUPS1 and *At*BUPS2 (Zhu et al., 2018; Zhou et al., 2021). *At*BUPS1 interacts with all pollen-expressed *At*GEFs and since *At*GEF1 and *At*GEF12 were previously communicated to interact with *At*ROPs and *At*BUPS (Zhu et al., 2018), these two GEFs were further characterised in their role of pollen tube growth. Specifically, mechanical stress signals lead to activation of *At*GEF12 to preserve cell wall integrity via the activation of *At*ROP1 (Zhou et al., 2021).
The cytoplasmic kinase *At*AGC1.5 restricts localisation of ROP-GTP during pollen tube growth by interacting with the PRONE domain of *At*GEF1. When the kinase is restricted from phosphorylating the GEF (at residue S333), the kinase and GEF complex is mistargeted in pollen tubes and possibly unable to signal to *At*ROPs (Li et al., 2020). These results indicate, that microscopically visible growth processes rely on the coordinated molecular interplay of different signalling components in the ROP-dependent pathways. Just as previously described for RLK-ROP signalling, GEFs are important links between signal perception and ROP activation. It has become apparent that GEFs are also found to be important downstream links of other signalling molecules. This is for example the case during light sensing and gas exchange. In order to transduce light signals, the two *At*GEFs 2 and 4 link signal perception to ROP action. Both GEFs can be targeted by phyB which is a red light sensor. The signal gets transduced via the activation of *At*ROP1 and *At*ROP2 to regulate excessive stomatal opening. That way, gas exchange is regulated during high light periods (Wang et al., 2017). An other response to stress can be relayed via lipid messenger molecules such as phosphatidic acid (PA). A direct connection of *A. thaliana* GEFs to this class of lipids was reported in Cao et al. (2017). *At*GEF8 interacts with PA at specific amino acids (K13 and K18) which induces *At*GEF8 interaction with *At*ROP7 and *At*ROP10. However, only *At*ROP7 was shown to be activated by the GEF *in vitro*. It was further hypothesised that PA facilitates and stabilises the interaction with and activation of *At*ROP7 by *At*GEF8 to relay signals triggered by sensing the stress hormone ABA (Cao et al., 2017).

O. sativa GEFs are also involved in developmental pathways such as the emergence of small cuticular papillae, floral organs, pollen development and root hairs (Yoo et al., 2011; Huang et al., 2018b; Xu et al., 2021; Kim et al., 2021). Upstream of *Os*RAC1, *Os*GEF10 specifically interacts and most probably activates the formation of small cuticular papillae (Yoo et al., 2011). On the other hand, the floral meristem expressed *Os*GEF7B interacts with most *Os*RACs to facilitate proper organ development (Huang et al., 2018b). Recently, the role of *Os*GEFs has also been elucidated in the development of *O. sativa* pollen. Interaction and activation assays showed that several *Os*GEFs can activate *Os*RACB in order to facilitate pollen germination and tube growth. More specifically, *Os*GEF2, *Os*GEF3 and *Os*GEF6 were shown to activate *Os*RACB in order to signal for pollen germination (Xu et al., 2021). Concerning root hair growth in *O. sativa*, *Os*GEFs were also shown to be important. Analogous to the role of *At*GEF3, *Os*GEF3 interacts with *Os*RAC3 which in turn induces production of ROS via the NADPH oxidase *Os*RBOH5 to control root

hair elongation (Kim et al., 2021).

PRONE GEFs in immunity

Just as signal perception during development is transduced by GEFs, there are several examples of how the exchangers function during the interaction of plants with pathogenic microbes. Here, also the only available knowledge was generated by investigating GEFs in *A. thaliana* and *O. sativa*.

In *A. thaliana*, there are only a few reports on the role of GEF-signalling during pathogen attack. However, one example is the connection of *At*GEF14 with the RLK *At*FER, which is a susceptibility factor in the interaction of *A. thaliana* with the powdery mildew fungus (Kessler et al., 2010). Even though the direct link between *At*FER-signalling to *At*GEFs in susceptibility has not been reported, as introduced earlier, the receptor interacts with *At*GEF14 in a molecular pathway that regulates pavement cell shaping (Lin et al., 2021). Another prominent example is the FER-related cell wall sensing RLK THESEUS1 (*At*THE1) which has initially been identified as a sensor involved in growth processes like cell elongation. In addition, it was reported that *At*THE1 plays a role in the plant's immune response against the necrotrophic fungus *B. cinerea*. To relay the immunity triggering signal, *At*THE1 interacts with *At*GEF4 in order to trigger subcellular defense responses within the attacked cells (Qu et al., 2017).

In contrast to ROP-related research in *A. thaliana*, there have been more reports in their role of plant immunity in the monocotyledonous crop *O. sativa*. 11 *O. sativa* PRONE GEFs were identified with similar protein structure as in *A. thaliana* (Kawasaki et al., 2009; Kim et al., 2020). All published *Os*GEFs interact and activate *Os*RAC1 (Kawasaki et al., 2009). This *O. sativa* ROP has been known for its role in immunity which is triggered by chitin perception. Just as in plant developmental processes, a number of immunity pathways are turned on by the hetero-dimerisation of *Os*GEFs with *Os*RLKs. Specifically, the interaction of *Os*GEF1 and *Os*GEF2 with the RLK *Os*CERK1 plays a central role in ROP-related immunity of *O. sativa* (Akamatsu et al., 2015). Further, it has been shown that complex formation of the so called defensome comprised of the chitin receptor/co-receptor *Os*CEBiP/*Os*CERK1, the nucleotide exchanger *Os*GEF1 and the ROP *Os*RAC1 aids in *O. sativa* resistance against the blast fungus *Magnaporthe oryzae*. Mechanistically, this resistance pathway has been elucidated comprehensively. Upon chitin elicitation, *Os*GEF1 is phosphorylated by *Os*CERK1 and subsequently interacts with *Os*RAC1 at the plasma membrane to facilitate the defence response (Akamatsu et al., 2013). This mechanism is reminiscent of earlier introduced signalling cascades from signal perception via cell surface receptors that turn on ROP signalling via their interaction with GEFs (Figure 2).

Recent reports complement our understanding of ROP-immunity-signalling in *O. sativa* by uncovering the interplay of R proteins in effector triggered immunity with the *O. sativa*

GEF *Os*SPK1 (Wang et al., 2018).

1.5. Aim of this Dissertation

Studying *H. vulgare* susceptibility towards *Bgh* on a molecular level provides an insight into the plant's accommodation of the pathogen. In addition, pathogenic strategies of the biotrophic fungus can be observed. To understand the mechanisms underlying *Hv*RACB susceptibility-related signalling, it is crucial to elucidate the activation of this molecular switch. Due to the fact that activated *Hv*RACB facilitates fungal entry into epidermis cells, understanding the GDP to GTP exchange is of high value. Since it has been reported in other plants that PRONE-GEFs can facilitate ROP activation, this protein family became the subject of this dissertation.

Prior to this publication, the activation mechanism of *Hv*RACB has not been identified even though it likely is a crucial step to understand *Hv*RACB-mediated susceptibility on a molecular level. Therefore, the aim of this dissertation was to identify *H.vulgare* PRONE-GEFs that can activate the susceptibility factor *Hv*RACB to facilitate fungal establishment.

To that end, the protein family of *H. vulgare* PRONE-GEFs was annotated as they are possible candidates to activate ROPs. The results of gene expression and phylogenetic studies highlighted a possible role of *Hv*GEF14 in *H. vulgare* susceptibility towards *Bgh*. Further, the activator candidate *Hv*GEF14 was investigated for its possible interaction with *Hv*ROPs in *H. vulgare* epidermis cells. In addition, a novel *in planta* assay was established to observe *Hv*GEF14 activating capability towards the susceptibility factor *Hv*RACB. Finally, the influence of *Hv*GEF14 on *H. vulgare* susceptibility towards *Bgh* was evaluated.

2. Material and Methods

2.1. Plant and Fungal Material

The spring barley (*Hordeum vulgare, Hv*) cultivar Golden Promise (propagated in the greenhouse) was grown in a climate chamber at 20°C, 50 % humidity and long day conditions (16h light, 8h dark) for 7-8 days in standard potting soil (Einheitserde Classic). *Nicotiana benthamiana* was grown in standard potting soil (Einheitserde Classic) mixed with vermiculite in a ratio 9:1 under long day conditions (16h light, 8h dark) at 24 °C and 60 % humidity. *Blumeria graminis* f.sp. *hordei* race A6 (*Bgh*) was maintained on 7-21 day old *H. vulgare* cv. Golden Promise (propagated in the field) in a climate chamber with 18°C and 60 % humidity in long day conditions (16h light, 8h dark).

2.2. Plant Inoculation with *Bgh*

Detached *H. vulgare* leaves were placed at the bottom of an inoculation tower (200cm high, 80cm wide and long). *Bgh* conidiospores were blown off plants 14 days after their inoculation from approximately 130 cm above leaves. A density of 55-100 conidiospores per mm^2 was used for gene expression analysis and susceptibility assays. Conidiospores were allowed to settle onto detached leaves for 10-15 min. Inoculated leaves were further incubated in closed Petri dishes in a climate chamber (18°C, 60 % humidity, 16h/8h light/dark).

2.3. Cloning

Gene Amplification

Hv genes were amplified from whole leaf cDNA (RNA extraction and cDNA synthesis was performed as mentioned in section 2.7) of *Hordeum vulgare* cv. Golden Promise in standard PCR (Table 1) with primers designed on the basis of sequences from the Barley Genome (International Barley Genome Sequencing Consortium, 2012). Phusion polymerase (Thermo Fischer) was used to amplify genes of interest (GOI). The PCR product was purified via gel electrophoresis in 1% agarose gel stained with 0.002% Ethidium Bromide (EtBr). The DNA band was cut from the gel and DNA was isolated with the NucleoSpin Gel- and PCR-clean up kit (Macherey-Nagel) according to the suppliers protocol.

Table 1: Thermocycling Program Standard PCR.

Step	Cycle No.	Temperature in °C	Duration
Hot Start	1	98	3 min
Denaturation	2-30	98	5 sec
Annealing	2-30	depending on primer Tm	depending on primer length
Extension	2-30	72	depending on fragment length (1Kb/min)
Final Elongation	31	72	5 min

Plasmid Construction

Over-expression plasmids were constructed via the Gateway cloning system (Katzen, 2007) by first inserting an amplified gene of interest (GOI) with flanking attB-sites into the pDONR223 entry vectors (BP reaction, Table 2). GOIs were then transferred to the specific destination vectors (pGY1 for over expression in *H. vulgare* epidermis, pGBKT7 and pGADT7 for yeast-two-hybrid) via LR reactions (Table 2).
RNAi plasmids were constructed with a combination of classical and Gateway cloning (Katzen, 2007). RNAi target sequences were amplified from cDNA, flanked with restriction enzymes and transferred into attL-site containing pIPKTA38 via restriction digestion and ligation according to the manufacturer's protocol (Thermo Fisher). The RNAi sequence was transferred to the hairpin-forming expression vector pIPKTA30N via LR reaction (Table 2).
Binary *Agrobacterium* plasmids for FRET-FLIM measurements in *N. benthamiana* were cloned using a combination of GoldenGate (Engler et al., 2008) and Gateway (Katzen, 2007) techniques (for details see Trutzenberg et al. (2022)).

Transformation into *E.coli*

50 μl *E.coli* competent DH5α cells were thawn on ice and mixed with 2.5 μl BP/LR reaction and incubated on ice for 30 min. Heat shock was performed at 42°C for 45 sec. and cells were inverted in 500 μl LB medium (Table S25) at 37 °C for 1 h. Positive colonies were selected on LB-agar plates with respective antibiotics by growth over night at 37 °C.

Table 2: Standard protocol for BP and LR reactions in Gateway cloning.

BP	**LR**	**amount**
attB-PCR product	entry vector with GOI	ca. 150 ng
pDONR223 vector	destination vector	150 ng
BP Clonase II enzyme mix (Invitrogen)	LR Clonase II enzyme mix (Invitrogen)	0.5 μl
TE-buffer pH 8.0	TE-buffer pH 8.0	up to 2.5 μl
25 °C for 1 hr		

Plasmid Preparation

Positive colonies were grown over night at 37 °C in 2 ml LB liquid medium (Table S25) with respective antibiotics and collected by centrifugation (18213 g, 2 min, room temperature (RT)). Mini preparations for use in cloning were performed with the NucleoSpin Plasmid kit (Machery Nagel). For biolistic and *Agrobacterium*-mediated transformations, plasmids were isolated with NucleoBond Xtra Midi kit (Machery Nagel) according to the suppliers protocol. Plasmids used for Yeast-two-Hybrid assays purposes were isolated by alkaline lysis.

To perform the latter, the pellet was re-suspended in 150 μl buffer P1, subsequently 150 μl buffer P2 was added and the tubes were inverted (Table S16). After incubation at room temperature for 5 min, 150 μl buffer P3 was added and tubes were inverted again (see buffers in Table S16). The supernatant was added to 300 μl isopropanol and vortexed. Plasmids were collected by centrifugation (18213 g, 10 min, 4 °C) and washed with 70 % EtOH before reconstitution in milliQ-H_2O.

2.4. Biolistic Transformation of *H. vulgare* Leaves

Three detached 7-day old *H. vulgare* leaves were placed with the adaxial side facing upwards on a 1% H_2O-agar petri dish and fixed in place with a metal ring (Figure 1E). 25 mg/ml gold particles (1 μm, Bio-rad or Nanopartz) resuspended in glycerol were homogenised by sonication for 10 min and vortexing. For each transformation, 11 μl gold particles were mixed with 1 μl of 1 μg/μl diluted midi preparation of the corresponding plasmid. 12 μl of 1M $CaCl_2$ was added drop-wise under vortexing and 3.33 μl of protamine (Sigma, 20 mg/ml dilution) were added. The gold particles were coated for 30 min at RT with frequent mixing (every 5-10 min). Coated gold particles were washed once with 150 μl 70% EtOH and once with 150 μl of 99% EtOH before resuspension in 6 μl 99% EtOH

via ultrasonification. Particle bombardment was performed with the Particle Delivery System PDS-1000/He (Bio-Rad) in vacuum (26mm Hg) with a pressure of 900-1000 psi. Bombarded leaves were incubated in closed petri dishes inside a climate chamber (A1000 Conviron, 22°C, ca 100% humidity, 16h light/ 8h dark).

2.5. *Agrobacterium tumefaciens*-mediated Transformation

Agrobacterium tumefaciens strain GV3101 was transformed with binary expression vectors pGWB containing either meGFP-*Hv*RACB WT, meGFP-*Hv*RACB G15V (CA), GST-mCherry, *Hv*CRIB46-mCherry or 3xHA-*Hv*GEF14 (Tables 8 and 9). 50 μl cells were thawn on ice and mixed with 5 μl plasmid from a Midi prep. After 30 min incubation on ice, the cells were shock frozen in liquid N_2 and incubated at 37°C for 5 min. Subsequently, the cells were stabilised on ice for 5 min and incubated in 1 ml LB medium (Table S25) at 28°C for 3 hours while shaking. Cells were collected by centrifugation at maximum speed for 10 seconds and plated on LB-agar plates (Table S25) including antibiotics for selection of transformed cells.

2.6. Bioinformatic Analyses

Muscle alignment of 11 *O. sativa*, 14 *A. thaliana* and 11 *H. vulgare* PRONE-GEFs (sequences downloaded from NCBI) was performed in Seaview. A PhyML analysis was performed with an LG model, bootstraps with 100 replicates, model-given amino acid equilibrium frequencies, NNI tree searching and 5 random starts. *O. sativa* and *H. vulgare* PRONE-GEFs were annotated based on the *A. thaliana* nomenclature. The resulting tree's design was further coloured in InkScape. *Hv* PRONE domains were annotated from published resources or in silico predictions.
To create the computational model of the *Hv*GEF14-*Hv*RACB hetero-tetramer, the browser-based online tool Swissmodel.expasy.org was used. As target sequence, the *Hv*GEF14 sequence from MOREXv3 was selected and *Hv*RACB was used as hetero-target. After running the predictions, 2wbl.1 was selected as the template and the model was exported to Phymol. The proteins were subsequently coloured and turned for better visibility.

2.7. Gene Expression Analysis

Sample collection, RNA extraction and cDNA synthesis

Seven day old *H. vulgare* cv. Golden Promise plants were either inoculated with *Bgh* or not treated with the fungus. In three biological replicates, whole leaf and epidermal peels were collected from the inoculated and non-inoculated plants at 1 dpi and frozen in liquid N_2. Leaf tissue was ground in a Quiagen TissueLyser II with glass beads in reaction tubes. RNA was extracted with TRIzol according to the protocol published by Chomczynski and Sachhi (1987).

Subsequently, cDNA synthesis was performed with the QuantiTect Reverse Transcription Kit (Quiagen) according to the supplier's protocol. cDNA from 1 μg RNA was diluted 1/10 for further analysis.

Bgh inoculation was verified by standard PCR of "inoculated" samples with *Bgh*- specific primers (Table 7) and subsequent gel-electrophoresis. Amplified *Bgh* DNA was visualised with Ethidium-Bromide staining under UV-excitation.

Primer Efficiency and qRT-PCR

Primers were designed on the published *H. vulgare* coding sequences (cv. MOREX, International Barley Genome Sequencing Consortium (2012)) with the following specificities:

Table 3: Requirements for primer design used in qRT-PCR.

Melting Temperature (Tm)	60°C
Tm difference	< 5°C
Intron spanning	if possible
Length	80-150 bp

Primer efficiency was analysed by determining the threshold values of a three-step dilution series of a pool of cDNA used in the subsequent analysis (Figure 5). A standard curve was calculated and the slope (-3.116) was used to determine primer efficiency and amplification factor (2.09) via the online calculator "qPCR Efficiency Calculator" (Thermo Fischer).

qPCR was performed on 96-well plates with two technical and three biological replicates as well as no template controls. *Hv*Ubiquitin was measured as housekeeping gene on every plate and each primer pair was tested for contamination or unspecific binding with two technical replicates of no template controls (NTC). A 2x SYBR green master mix containing ROX passive reference dye (Thermo Fisher) was used in 10 μl reactions. Forward and reverse primers (Table 7) were used at a 200 nM concentration each, ca 10 ng cDNA (based on 1 μg RNA) was used per reaction. The Aria Mx3000 thermocycler (Agilent) was run with the program in Table 4.

Table 4: Standard qPCR cycler program for primers designed according to Table 3.

Step	**Cycle No.**	**Temperature in °C**	**Duration**
Hot Start	1	95	5 sec
Denaturation	2-41	95	5 sec
Annealing and Extension	2-41	60	15 sec
Denaturation	42	95	10 sec
Melting curve	43	65-95	1 min

The AriaMx software (Agilent) was used to validate NTCs, as well as amplification plots of the amplification cycles and melt curve. Threshold values were exported from the software and foldchanges were calculated via the $2^{-\Delta\Delta Ct}$ method by Livak and Schmittgen (2001). Figures were made with RStudio's ggplot (R Core Team, 2020).

2.8. *H. vulgare* Susceptibility Assay

Susceptibility towards *Bgh* was tested on detached *H. vulgare* leaves. 7-day old leaves were transformed (section 2.4) with 1 μg/transformation pGY1 over-expression vectors or pIPKTA RNAi vectors and 0.5 μg pUbi_GUSplus (Addgene, encoding β-Glucuronidase) transformation marker. An empty vector control was transformed with every repetition. Transformed leaves were inoculated with *Bgh* as described in section 2.2 and incubated for 1-2 days in the climate chamber. Cell autonomous susceptibility of *H. vulgare* towards *Bgh* was assessed by microscopy with a Leica DM2000 LED- fluorescence microscope. Transformed and inoculated leaves were stained with X-Gluc (5-Bromo-4-chloro-3-indolyl β-D-glucuronic acid) solution 48 hours after inoculation and fixed in 80% EtOH. GUS stained cells were analysed for their response to *Bgh* penetrating appressoria. Three categories were determined: no interaction, incompatible interaction (penetration attempt defended, often with papilla formation) and compatible interaction (formation of haustorium in analysed cell). For every construct, at least three technical replicates (from three different transformations) were analysed. A minimum of 50 interactions per construct (defended or successful) were counted in each experiment and at least five experiments were conducted. The absolute *Bgh* Penetration Efficiency (absolute PE) was calculated with equation Equation 1 and normalised to the empty vector penetration efficiency (equation Equation 2) to obtain relative Penetration Efficiency (relative PE). Figures were created

with the ggplot package and statistical analysis was performed with RStudio.

$$\text{absolute PE} = \frac{\text{number of successful interactions}}{\text{sum of all interactions}} * 100\% \qquad \text{(Equation 1)}$$

$$\text{relative PE} = \frac{\text{absolute PE GOI}}{\text{absolute PE empty vector}} \qquad \text{(Equation 2)}$$

2.9. Transient Transformation of *N. benthamiana* with *A. tumefaciens*

Transformed *A. tumefaciens* strain GV3101 was picked from LB-agar plates and incubated in liquid LB medium (Table S25) containing respective antibiotics (without rifampicin) over night at 28°C while shaking in 2.5 ml Induction Medium (Table S26). Bacterial liquid cultures were grown to OD600 0.5 and mixed in equal amounts including P19 silencing suppressor and subsequently infiltrated into five-week-old *N. benthamiana* leaves according to Yang et al. (2000). FRET-FLIM analysis was performed on several leaf discs taken from two different plants 48 hours after infiltration. From the same leaves, proteins were extracted for Western Blotting.

2.10. Protein-Protein Interactions and Activity Assay

Yeast-2-Hybrid

Protein-protein interactions were screened via yeast-two-hybrid (Y2H) assays as described by Fields and Song (1989). *Saccharomyces cerevisiae* strain AH109 was propagated on YPDA agar plates and grown in 5 ml pre-culture over night and 100 ml main culture YPDA liquid medium for 4-5 h (Table S23) at 30 °C with 260 rpm rotation.
Yeast cells were collected at 4000 rpm for 15 min (4°C) and washed once with H_2O before resuspension in 2 ml LiAc buffer (Table S17). 200 ng of each, bait (pGBKT7) and prey (pGADT7) plasmids were mixed with 10 μl of 10μg/μl herring sperm DNA (previously sonicated for 10 min and heated to 95 °C for 5 min). 100 μl yeast cells were combined with the DNA and 600 μl PEG/LiAc buffer (Table S18) was added. Tubes were inverted frequently while incubated at 30 °C for 30 min. 70 μl DMSO (Sigma-Aldrich) was added to each reaction and tubes were inverted while incubating at 42 °C for 15 min. Cells were cooled on ice for 2 min and centrifuged at 6000 rpm for 1 min. The pellet was resuspended in 1xTE buffer (Table S19) before plating on SD-L-W agar plates (Table S24). Transfor-

mation plates were incubated for 3-6 days at 30 °C.
Transformed colonies were cultured in 4 ml liquid SD-L-W medium (Table S24) over night. A dilution series (pure, 1:10, 1:100, 1:1000) was dropped onto selective media lacking different amino acids/nucleotides. Interaction plates were incubated at 30°C for 3-7 days until growth could be observed.

Foerster Resonance Energy Transfer (FRET) and Fluorescence Lifetime Imaging (FLIM)

In planta interactions

H. vulgare leaves were transformed by biolistic bombardment (section 2.4) with 2 μg/ transformation of each monomeric enhanced GFP-fused donor plasmids and mCherry-fused acceptor plasmids. Microscopy of transformed *H. vulgare* epidermis cells was performed with Olympus FV 3000 microscope with 488 nm (20 mW) and 561 nm (50 mW) diode lasers. Confocal images of analysed cell plane were taken to analyse localisation and confirm co-transformation.

In-planta ROP-activity Assay

The ROP activation status of *Hv*RACB was measured via a FRET-FLIM -based sensor consisting of an N-terminally mCherry-fused interactor of the activated ROP (*Hv*CRIB46) and wild type *Hv*RACB, which was N-terminally fused to meGFP. The two sensor parts were co-transformed into *N. benthamiana* via agrobacterium transformation together with the silencing inhibitor P19. Potential *Hv*RACB activators proteins were additionally co-transformed without flurophores.

Life Time Analysis

GFP fluorophores were excited with a 485 nm (LDH-D-C-485) pulsed diode laser. and time-correlated single photon counting (TCSPC) was performed with 2x PMA Hybrid 40 photon counting detectors. A minimum of 900 photon counts were collected and subsequently analysed with the PicoQuant SymPhoTime 64 software. Figure preparation and statistical analysis was performed with RStudio.

2.11. Protein Extraction and Visualisation

Protein Extraction from Yeast

Yeast was cultured in 4 ml SD-L-W liquid medium (Table S24) over night and centrifuged at 4000g for 5 min at 4°C. Cells were kept on ice during the whole procedure and resuspended in 100 μl of 2M lithium acetate (LiAc) by invertion and centrifuged for 3 min at

4000 g and 4°C. The supernatant was exchanged with 100 μl of 0.4 M sodium hydroxide (NaOH) and after invertion incubated on ice for 5 min. The pellet was collected by centrifugation (4000g for 3 min at 4°C) and resuspended in 50 μl 4x-SDS-sample buffer (Table S21). After vortexing, the proteins were denatured at 100 °C for 3 min and centrifuged (13000rpm for 1min) before loading on a gel.

Protein Extraction from *N. benthamiana*

N. benthamiana proteins were extracted by harvesting five leaf discs with a 1.2mm biopsy punch and direct freezing in liquid N_2 with two glass beads per 2ml-reaction tube. Leaf tissue was homogenised two times in a Quiagen TissueLyser II for 1 min at 30 Hz. Subsequently, samples were heated for 20 min at 95°C in 500 μl of 4x-SDS-sample buffer (Table S21).

SDS-PAGE and Western Blot

Proteins were separated by electrophoresis in a 12% acrylamide gel (Table 5) and in 1x Running Buffer (Table S22). Subsequently, proteins were blotted onto PVDF membrane (Roth) via semi-dry or wet Western Blotting. Semi-dry blotting was performed with a Bio-RAD blotting device at 1 mA/ cm^2 membrane for 70 min. Wet blotting was performed with a Bio-RAD blotting device at 80 V, 400 mA for 60 min. Transfer efficiency was tested with Ponceau (Sigma) staining of the membrane. Unspecific binding of antibodies was prevented by blocking with 5% milk in PBS-T (Table S20). The membrane was incubated over night at 4 °C with primary antibodies, diluted 1:2000 in 5% milk-PBS-T. For detection of proteins see list of antiboidies used (Table 6). Three washing steps of 10 min each were performed with PBS-T and the membrane was subsequently incubated in 1:5000 dilution of secondary antibody in 5% milk-PBS-T for 2 h. Proteins were detected by chemiluminescence with SuperSignal West DURA or FEMTO Chemiluminescence-Substrate (Thermo Scientific) and a Fusion SL Vilber Lourmat camera.

Table 5: Recipe for one 12 % Acrylamide Gel.
Amounts for 2 ml stacking gel and 5 ml resolving gel.

	5% Stacking Gel [ml]	**12 % Resolving Gel [ml]**
H_2O	1.4	1.6
30 % Acrylamide	0.33	2.0
1.5M Tris-HCl pH 6.8	0.25	-
1.5M Tris-HCl pH 8.8	-	1.3
10% SDS	0.02	0.05
10 % ammonium persulfate (APS)	0.02	0.05
TEMED	0.002	0.002

Table 6: List of Antibodies

Protein tag	**Primary Antibody**	**Secondary Antibody**	**Company**
HA	anti-HA-HRP (3F10)	-	Roche
myc	c-myc (9E10)	m-IgGκ BP-HRP (sc-516102)	Santa Cruz Biotechnology
RFP (mCherry)	anti-RFP-rat mAb (5F8)	anti-rat (A9542)	ChromoTek
GFP	anti-GFP (B-2) (sc-9996)	m-IgGκ BP-HRP (sc-516102)	Santa Cruz Biotechnology

2.12. List of Primers

Table 7: List of Primers used in this Dissertation.

Name	**Primer No.**	**Sequence**	**Description**
qPCR GEF14 Fwd	5036	CGCCCATGGCCACCCTCAA	forward primer *Hv*GEF14
qPCR GEF14 Rvs	5037	CCACCACACCCGCATCAC	reverse primer *Hv*GEF14
qPCR *Hv*Ubiquitin Fwd	1255	TCTCGTCCCTGAGATTGCCC ACAT	forward primer house-keeping gene
qPCR *Hv*Ubiquitin Fwd	1256	TTTCTCGGGACAGCAACACAA TCTTCT	reverse primer house-keeping gene
attB1 + FERlike1 (433-885) Fw	6052	CAAGTTTGTACAAAAAAGCA GGCTATCCGTCTGCCGGAGG GAAATC	forward primer *Hv*FERlike1 cytoplasmic (433-885) with attB1 sites for cloning into pDONR223
FERlike1 + attB2 Rv	6051	GGGGACCACTTTGTACAAGA AGCTGGGTTTCATCTGCCAC CCGGAC	reverse primer *Hv*FERlike1 cytoplasmic (433-885) with attB2 sites for cloning into pDONR223
SDM GEF14 at insert Fwd	6048	CCAACTTTGTACAAAAAAGC AGGCTATATGAGGATGAAG ACGCTGG	forward primer for in frame cloning of *Hv*GEF14 S394 mutants
SDM GEF14 at insert Rv	6049	CCAGCGTCTTCATCCTCATAT AGCCTGCTTTTTTGTACAAA GTTGG	reverse primer for in frame cloning of *Hv*GEF14 S394 mutants

Table 7: List of Primers used in this Dissertation.

Name	Primer No.	Sequence	Description
AK371648 PRONE 124-485 F	5481	ATGGCTGATATTGAAACCAT GAAGGAG	forward primer for amplification of *Hv*GEF14 PRONE domain (124-485)
AK371648 PRONE 124-485 Rv	5482	CTACTTCTTGATCAGGTCGTC CTCC	reverse primer for amplification of *Hv*GEF14 PRONE domain (124-485)
AK371648 P124-485 F attB	5483	CAAAAAAGCAGGCTTAATGG CTGATATTGAA	forward primer for cloning of *Hv*GEF14 PRONE domain (124-485)
AK371648 P124-485 R attB	5484	CAAGAAAGCTGGGTTCTACTT CTTGATCAGG	reverse primer for cloning of *Hv*GEF14 PRONE domain (124-485)
AK371648 +attB F	5485	GGGGACAAGTTTGTACAAAAA AGCAGGCTTAATGAGGATGAA GACGCTGG	forward primer for cloning of *Hv*GEF14 full length
AK371648 w/o STOP +attB R	5486	GGGGACCACTTTGTACAAGAA AGCTGGGTTCCACATGAGCT GCTTGGCC	reverse primer for cloning of *Hv*GEF14 full length without STOPcodon

2.13. List of Plasmids

Table 8: List of bacterial glycerol stocks with plasmids newly cloned for this dissertation.

Glycerol ID	Plasmid name	Description	Host strain	Lab book
R972	pGY1 *Hv*GEF-AK376075Prone	overexpression GEF Prone domain (AK376075)	DH5α	No. I, p. 146
R973	pGY1 (GW)-*Hv*GEF-AK371648Prone	overexpression GEF Prone domain (AK371648)	DH5α	No. I, p. 146
R974	pGY1 (GW)-*Hv*GEF-AK371648 FL	overexpression GEF AK371648 FL	DH5α	No. I, p. 146
R975	pGY1 (GW)-*Hv*GEF-AK371648Prone	overexpression GEF Prone domain (AK371648)	DH5α	No. I, p. 146
R976	pGADT7 (GW)-*Hv*GEF-AK371648 FL	Y2H prey construct with myc tag	DH5α	No. I, p. 146
R977	pGBKT7 (GW)-*Hv*GEF-AK371648 FL	Y2H bait construct with HA tag	DH5α	No. I, p. 146
R978	pGADT7 (GW)-*Hv*GEF-AK371648Prone	Y2H prey construct with myc tag	DH5α	No. I, p. 146
R979	pGBKT7 (GW)-*Hv*GEF-AK371648Prone	Y2H bait construct with HA tag	DH5α	No. I, p. 146
R980	pDONR223-*Hv*GEF-AK371648-RNAisequence	entry vector for RNAi vector	DH5α	No. I, p. 147

Table 8: List of bacterial glycerol stocks with plasmids newly cloned for this dissertation.

Glycerol ID	Plasmid name	Description	Host strain	Lab book
O052	pGY1 GW GFP-GEF14 (AK371648) FL	*Hv*GEF14 AK371648 N-terminally tagged with GFP	DH5α	No. II, p.36
O143	pGBKT7 GW with AK252312 cytoplasmic domain (aka WAK3)	Y2H prey construct with myc tag	DH5α	No. II, p. 30
O144	pGBKT7 GW with AK361450 cytoplasmic domain (aka LRR)	Y2H prey construct with myc tag	DH5α	No. II, p. 30
O145	pGBKT7 GW with AK357077 cytoplasmic domain (aka CERK1)	Y2H prey construct with myc tag	DH5α	No. II, p. 30
O146	pGADT7 GW with AK252312 cytoplasmic domain (aka WAK3)	Y2H bait construct with HA tag	DH5α	No. II, p. 30
O147	pGADT7 GW with AK361450 cytoplasmic domain (aka LRR)	Y2H bait construct with HA tag	DH5α	No. II, p. 30
O148	pGADT7 GW with AK357077 cytoplasmic domain (aka CERK1)	Y2H bait construct with HA tag	DH5α	No. II, p. 30
O164	pIPKTA30N with AK371648 (*Hv*GEF14) RNAi	silencing construct targeting *Hv*GEF14 (AK371648)	DH5α	No. II, p.41
O207	pUC SPYNE AK371648 Prone (N-term tagged)	nYFP for BiFC analysis, AK371648 *Hv*GEF14 PRONE domain	DH5α	No.II, p. 82

Table 8: List of bacterial glycerol stocks with plasmids newly cloned for this dissertation.

Glycerol ID	Plasmid name	Description	Host strain	Lab book
O208	pUC SPYNE AK371648 FL (N-term tagged)	nYFP for BiFC analysis, AK371648 *Hv*GEF14 full length	DH5α	No. II, p. 82
O448	pGY1 GUS	GUS over expression as control for biolistic transformation of RNAi constructs	DH5α	No. II, p. 121
O482	pDONR223 AK371648 Prone 124-485 +Start+Stop	long PRONE domain (aa 124-485) of *Hv*GEF14 (AK371648)	DH5α	No. II, p.133
O483	pGY1 AK371648 Prone 124-485 +Start+Stop	Over expression of long PRONE domain (aa 124-485) of *Hv*GEF14 (AK371648)	DH5α	No. II, p.133
O530	pGY1 mCherry-*Hv*GEF14 (AK371648) FL	*in planta* over expression of N-terminal mCherry tag to *Hv*GEF14	DH5α	No. II, p.153
O531	pGBKT7 *Hv*GEF14 124-485 (AK371648 PRONE)	Y2H bait vector with N-terminal myc-tag of *Hv*GEF14 PRONE (amino acids 124-485)	DH5α	No. II, p.153
O532	pUC SPYCE *Hv*GEF14 (AK371648) FL	BiFC YFPc fused to *Hv*GEF14 full length	DH5α	No. II, p.153
O759	pGADT7 GW *Hv*Rac1 delta C (1-211) WT	Yeast two Hybrid activation domain with *Hordeum vulgare* Rac1 aa 1-211 (delta C-terminus) wild type	DH5α	No. III, p. 66

Table 8: List of bacterial glycerol stocks with plasmids newly cloned for this dissertation.

Glycerol ID	Plasmid name	Description	Host strain	Lab book
O760	pGADT7 GW *Hv*Rac1 delta C (1-211) CA	Yeast two Hybrid activation domain with *Hordeum vulgare* Rac1 aa 1-211 (delta C-terminus) constitutively activated (G23V)	DH5α	No. III, p. 66
O761	pGADT7 GW *Hv*Rac1 delta C (1-211) DN	Yeast two Hybrid activation domain with *Hordeum vulgare* Rac1 aa 1-211 (delta C-terminus) dominant negative (T28N)	DH5α	No. III, p. 66
Y126	pGY1-PIP2a-mCherry	PIP2a plasma membrane marker for over expression in barley epidermal cells, high copy, golden gate cloned	DH5α	No. III, p. 149
Y310	pGY1 mCherry-*Hv*RAC1 FL WT	in planta over expression vector *Hv*RAC1 N-terminally tagged with mCherry	DH5α	No. III, p. 81
Y311	pGY1 mCherry-*Hv*RAC1 FL CA (G23V)	in planta over expression vector *Hv*RAC1 constitutively activated N-terminally tagged with mCherry	DH5α	No. III, p. 81
Y312	pGY1 GFP-*Hv*RAC1 FL WT	in planta over expression vector *Hv*RAC1 N-terminally tagged with GFP	DH5α	No. III, p. 81

Table 8: List of bacterial glycerol stocks with plasmids newly cloned for this dissertation.

Glycerol ID	Plasmid name	Description	Host strain	Lab book
Y313	pGBKT7 *Hv*RAC1 deltaC WT	Y2H bait vector with N-terminal myc-tag of *Hv*RAC1 (1-211) WT	DH5α	No. III, p. 81
Y314	pGBKT7 *Hv*RAC1 deltaC DN (T28N)	Y2H bait vector with N-terminal myc-tag of *Hv*RAC1 (1-211) dominant negative	DH5α	No. III, p. 81
Y315	pGY1 *Hv*GEF14 S394A	in planta over expression vector *Hv*GEF14 (AK371648) S394A phosphoablation	DH5α	No. III, p. 186
Y316	pGY1 *Hv*GEF14 S394D	*in planta* over expression vector *Hv*GEF14 (AK371648) S394D phosphomimic	DH5α	No. III, p. 186
Y416	pGADT7-*Hv*GEF14-PRONE	AK371648 Prone domain (124-485) in Y2H prey vector with HA-tag	DH5α	No. IV p.24
Y460	pGWB15-3HA-*Hv*GEF14	N-terminally HA-tagged FL *Hv*GEF14 (AK371648) in binary pGWB15	DH5α	No. IV, p.43
Y461	pGWB2-*Hv*GEF14	FL *Hv*GEF14 (AK371648) in binary pGWB2	DH5α	No. IV, p.43
Y462	pGWB15-3HA-*Hv*GEF14	N-terminally HA-tagged FL *Hv*GEF14 (AK371648) in binary pGWB15 in *A.tumefaciens*	GV3101	No. IV, p.47

Table 8: List of bacterial glycerol stocks with plasmids newly cloned for this dissertation.

Glycerol ID	Plasmid name	Description	Host strain	Lab book
Y463	pGWB2-*Hv*GEF14	FL *Hv*GEF14 (AK371648) in binary pGWB2 in *A.tumefaciens*	GV3101	No. IV, p.47
Y615	pGBK *Hv*FERlike1 cytoplasmic	Y2H bait vector of barley FERONIA-like 1 cytoplasmic domain with N-terminal myc-tag	DH5α	No. IV, p.70
Y616	pGAD *Hv*FERlike1 cytoplasmic	Y2H prey vector of barley FERONIA-like 1 cytoplasmic domain with N-terminal HA-tag	DH5α	No. IV, p.70
Y617	pDONR223 *Hv*FERlike1 cytoplasmic	Gateway donor vector of barley FERONIA like 1 cytoplasmic domain	DH5α	No. IV, p.70
Y618	pGBKT7 *Hv*CRK8 cytoplasmic	Y2H bait vector of barley CRK8 (cystein rich receptor like kinase) cytoplasmic domain with N-terminal myc-tag	DH5α	No. IV, p.70
Y619	pGADT7 *Hv*CRK8 cytoplasmic	Y2H prey vector of barley CRK8 (cystein rich receptor like kinase) cytoplasmic domain with N-terminal HA-tag	DH5α	No. IV, p.70

Table 9: List of additional Plasmids used in this Dissertation.

Glycerol ID	Plasmid name	Description	Host Strain
L718	pDONR223-AK371648-(*Hv*GEF14)-FL	Gateway entry vector	DH5α
S219	pGY1 EV	non-Gateway compatible empty vector for over-expression in *H. vulgare* epidermis cells	DH5α
O124	pIPKTA30N EV	Gateway-compatible RNAi destination vector for transient RNAi in *H. vulgare* epidermis cells	DH5α
R964	pUbi GUSplus	GUSplus reporter gene under control of the maize ubiquitin promoter; vector obtained from Addgene (ID: 64402) used in transient transformation of *H. vulgare* epidermis cells	DH5α
O195	pGY1 mCherry-*Hv*RACB WT	Over-expression in *H. vulgare* epidermis cells	DH5α
O193	pGY1 mCherry-*Hv*RACB G15V	Over-expression in *H. vulgare* epidermis cells	DH5α
O623	pGY1 mCherry-*Hv*RACB T20N	Over-expression in *H. vulgare* epidermis cells	DH5α
O191	pGY1 mCherry-*Hv*RACB D121N	Over-expression in *H. vulgare* epidermis cells	DH5α
R756	pGBKT7 EV	Gateway-compatible empty vector for expression in *S. cerevisiae* nucleus for Y2H	DH5α
R755	pGADT7 EV	Gateway-compatible empty vector for expression in *S. cerevisiae* nucleus for Y2H	DH5α

Table 9: List of additional Plasmids used in this Dissertation.

Glycerol ID	Plasmid name	Description	Host Strain
O315	pGBKT7 *Hv*RACB WT ΔC	Y2H bait construct of *Hv*RACB lacking C-terminal prenylation (CSIL) domain (+ myc-tag) for expression in *S.cerevisiae* nucleus	DH5α
O317	pGBKT7 *Hv*RACB G15V ΔC	Y2H bait construct of constitutively activated *Hv*RACB-G15V lacking C-terminal prenylation (CSIL) domain (+ myc-tag) for expression in *S. cerevisiae* nucleus	DH5α
O373	pGBKT7 *Hv*RACB T20N ΔC	Y2H bait construct of dominant negative *Hv*RACB-T20N lacking C-terminal prenylation (CSIL) domain (+ myc-tag) for expression in *S. cerevisiae* nucleus	DH5α
O319	pGBKT7 *Hv*RACB D121N ΔC	Y2H bait construct of low nucleotide affinity *Hv*RACB-D121N lacking C-terminal prenylation (CSIL) domain (+ myc-tag) for expression in *S.cerevisiae* nucleus	DH5α
O035	pGY1 GFP	Gateway compatible GFP for over-expression in *H. vulgare* epidermis cells	DH5α
O279	pGY1 *Hv*RIC171-mCherry	Over-expression in *H. vulgare* epidermis cells	DH5α
	pGWB *Hv*CRIB46-mCherry	Transient plant transformation via *A. tumefaciens* (used for FRET-FLIM)	GV3101
O874	pGWB6 meGFP-*Hv*RACB WT	Transient plant transformation via *A. tumefaciens* (used for FRET-FLIM)	GV3101

Table 9: List of additional Plasmids used in this Dissertation.

Glycerol ID	**Plasmid name**	**Description**	**Host Strain**
O875	pGWB6 meGFP-*Hv*RACB G15V	Transient plant transformation via *A. tumefaciens* (used for FRET-FLIM)	GV3101
Y940	pGWB2 GST-mCherry	Transient plant transformation via *A. tumefaciens* (used for FRET-FLIM)	GV3101
Y105	pGWB2 *Hv*CRIB46-mCherry	Transient plant transformation via *A. tumefaciens* (used for FRET-FLIM)	GV3101
Y231	pBin61 p19	Transient plant transformation via *A. tumefaciens* (used for FRET-FLIM)	GV3101

3. Results

3.1. PRONE-GEFs in *H. vulgare*

3.1.1. *H. vulgare* genomic resources

To identify potential ROP activators in *H. vulgare*, the available genomic resources were screened. The *H. vulgare* genome of cultivar MOREX was first published in 2012 and annotated three times in the versions 1, 2 and 3 (International Barley Genome Sequencing Consortium, 2012). In versions 1 and 2 there were eight PRONE-domain containing proteins annotated. This list has been extended to a total of eleven *H. vulgare* PRONE-GEFs in the latest annotation (Morex version 3, International Barley Genome Sequencing Consortium (2012)). The sequences of all eleven *Hv*PRONE-GEFs were used for the work performed in this dissertation. A summary of all *Hv*GEF identifiers can be found in Table S13.

3.1.2. Annotation and Phylogeny of *H. vulgare* PRONE-GEFs

The eleven PRONE-domain containing proteins of the most recent *H. vulgare* genome annotation (Mascher et al., 2021) have not been characterised until now. In order to keep a consistent nomenclature for PRONE-GEFs, the *H. vulgare* proteins were annotated according to PRONE GEFs in *A. thaliana* (Berken et al., 2005) after a phylogenetic analysis. However, not every *H. vulgare* PRONE-GEF corresponded to a single *A. thaliana* orthologue. To further unbundle the phylogeny of *H. vulgare* PRONE-GEFs, the primary sequences of PRONE GEFs from the more closely related monocot *O. sativa* were added to the alignment of *H. vulgare* and *A. thaliana* PRONE-GEFs. In *O. sativa*, likewise eleven proteins harbour the conserved PRONE domain. Since the existing nomenclature of *Os*GEFs had not been consistent in literature, a new phylogenetic analysis was performed with all 14 *At*GEFs and 11 *Os*GEFs (Figure S14). A maximum likelihood (ML) analysis was performed based on previous MUSCLE alignment and all *Os*GEFs were numbered according to their corresponding *At*GEF orthologues. This consistent nomenclature ensures comparability of publications and between different species. Based on this analysis, *At* and *Os* PRONE-GEFs form three clades that separate with high confidence (bootstrap value of 100). The bootstrap values on the phylogenetic branches report statistical confidence by calculating 100 replicates and recording their outcomes. The bootstrap value then indicates in how many of these repetitions the branching was exactly as shown in the resulting tree (Figure S14).

Subsequently, *H. vulgare* PRONE-GEFs were aligned with *A. thaliana* and *O. sativa* PRONE-GEFs (Figure S15). The alignment offers the possibility to observe differences on an amino acid level but the phylogenetic relationship between these PRONE-GEF isoforms is not easily visible. Therefore, another ML analysis was performed that also resulted in

three clades of PRONE-GEFs. Clade I includes PRONE-GEFs 1-7 with three potential orthologues of *At*GEF3 in the monocot species named *Os* or *Hv* GEF3a-c according to their decreasing distance in the tree to *At*GEF3. Analogously, PRONE-GEF7 of *At* corresponds to each two potential orthologues in *Os* and *Hv* which are denoted GEF7a and 7b.

The next clade (II) summarises PRONE-GEFs 8-13. The analysis showed that monocotyledonous PRONE-GEFs of clade II only contain GEF 9 and 10 with each three isoforms of GEF9.

Clade III is completely separate from the first two clades and only encompasses PRONE-GEF14 from all three species. In addition, clades I and II are more similar to each other than to clade III which branches off at the base of the tree with a bootstrap value of 100 (Figure 3).

This phylogenetic tree provides an overview of *Hv*GEFs and establishes a consistent nomenclature for *Hv*GEFs. In addition, it highlights corresponding orthologues in *A. thaliana* and *O. sativa*, the two plant species in which PRONE-GEFs have been studied mostly until now.

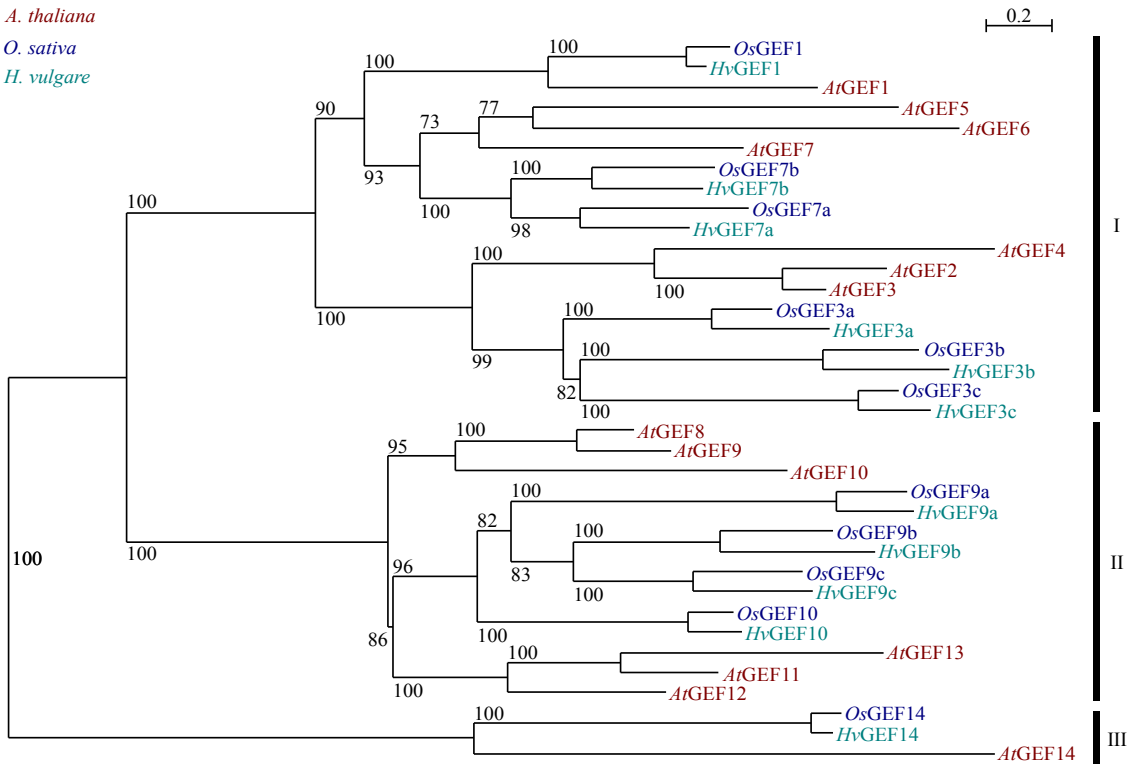

PhyML ln(L)=-27900.7 736 sites LG 100 replic. (TBE) 4 rate classes

Figure 3: PRONE GEFs of *A. thaliana* (*At*, red), *O. sativa* (*Os*, blue) and *H. vulgare* (*Hv*, green) cluster in three clades. Phylogenetic tree based on MUSCLE alignment and ML analysis with 100 replicates performed in Seaview. Bootstrap values indicated on branching points. Figure adapted from Trutzenberg et al. (2022).

3.1.3. Alignment of *Hv*GEFs highlights the conserved PRONE domain and conserved amino acids

A MUSCLE alignment was performed with all eleven primary sequences to compare the predicted PRONE domains and conserved amino acids of the *H. vulgare* GEF protein family (Figure 4). There are no overall conserved amino acids in the N- and C- terminal variable regions. However, the primary sequence of all *Hv*GEFs is largely conserved in the PRONE domain. In accordance with previous publications (Berken et al., 2005; Shin et al., 2009; Kawasaki et al., 2009), the only conserved motifs can be found in the PRONE-domain which is summarised in Figure 4.

Highlighted in blue are amino acids that were published to be important in GEF homomerisation, such as F133 and the consecutive leucines L136, L137, L138 (Figure 4). Other conserved amino acids are located in the PRONE domain and were previously published to be important for GEF-ROP heteromerisation (in purple): N161, Q206, E215 , M217, W275, W276, L434, R460 Figure 4, for details see Table S14).

In addition to these residues important for interaction, serine 394 was shown to be a possible phosphorylation site in *At*GEF14 (Mergner et al., 2020). This site is also conserved in the *H. vulgare* homologue and highlighted in turquoise (Figure 4).

Figure 4: Alignment of *H. vulgare* PRONE-GEFs annotated with predicted PRONE domain in grey, conserved GEF-GEF (blue, see also Figure 8) and ROP-GEF (purple, see also Figure 8) interaction sites and a predicted phosphorylation residue in *Hv*GEF14 in green based on Mergner et al. (2020). Figure adapted from Trutzenberg et al. (2022).

To further compare all *Hv*GEF primary sequences, a *Hv*PRONE-GEF consensus sequence was calculated after the alignment (Table 10). Interestingly, the primary sequence of *Hv*GEF14 differs most from all other *H. vulgare* GEFs with 30 % variation in amino acids when compared to the consensus sequence (Table 10). Even though, the four amino acids involved in GEF homomerisation and eight amino acids of GEF-ROP heteromerisation are still conserved. It is also apparent, that some *Hv*GEF sequences, such as *Hv*GEF3a and *Hv*GEF3b, end with the PRONE domain and do not possess additional amino acids in their C-terminal region.

Table 10: *Hv*GEF14 is least similar to the *H. vulgare* PRONE-GEF consensus sequence. After MUSCLE alignment, a *H. vulgare* PRONE-GEF consensus sequence was calculated. Non-conserved amino acids denoted by dots.

Consesnus sequence: MFLLLRHPLCPPLRHHHR.....M.....P.SSV.....S..... ....TWEEGSQSDYADLDDDDMPMERQRGGVLR.....P....SRGK....LP..... .....R.....LSE...MKERF.KLLLGEDMSG.GKGV..ALA.SNAITNL.ATVFG...RLEP L.P..K..W..EMDWLLSV.D.IVEFVP...Q...DGG...E.M.T..RSD...NLPAL.KLD.MLL..LDSF ....EFWYV.....SSS...S.R....R...KWW.P.P.VP..GL....R..LQ.....NQILKAAMAIN...L. EM.IPE.Y...LPK.GR..LGD..YR.IT....F.P..LL...DLS.EH..L....R.EA....W.RK.....LGR.....S WG..VK....AADDGG..EK.....RAE.LL..LK.RFPGL.QT.LD.SKIQYNKDVG.AILESYSR VLESLA....SRI.DVL.AD.....FVTA.....P..... .....D.....LMW.			
*Hv*GEF	aa overlap with consensus sequence	variable aa	percent variable aa
1	214	21	10%
3a	216	30	14%
3b	259	30	12%
3c	204	35	17%
7a	209	20	10%
7b	213	15	7%
9a	202	30	15%
9b	208	19	9%
9c	217	27	12%
10	204	26	13%
14	214	64	30%

3.1.4. Gene expression of *H. vulgare* PRONE GEFs

The initial *H. vulgare-Bgh* interaction takes place between conidiospores of the fungus and epidermal cells of *H. vulgare* leaves. Therefore, all predicted *Hv PRONE-GEF*s were specifically analysed for their expression in *H. vulgare* leaf epidermis. To get an overview of *H. vulgare PRONE-GEF* expression in different plant tissues, fragments per million kilobase (FMPK) were extracted from RNAseq experiments published by the James Hutton Institute (https://ics.hutton.ac.uk/barleyGenes).

Due to the fact that *HvGEF3b*, *HvGEF3c* and *HvGEF7* had no data in the JHI publication, these *HvGEF*s are listed in grey (Table 11). The expression of all other *HvGEFs* is summarised in Table 11. In addition to the FPKM counts, the expression level was visualised in a colour code for every individual tested tissue in increasing shades from white (no expression) to dark green (highest expression in that tissue). That way, the *HvGEF* with the highest expression in each respective tissue can be identified by the darkest colour.

Strikingly, *HvGEF1* and *HvGEF14* transcripts are ubiquitously found across the tested tissues and *HvGEF14* is the highest expressed *HvGEF* in most tissues. The further survey of RNAseq results showed that few of the *H. vulgare PRONE-GEFs* are expressed in epidermal peels. In four week old plants, only five *HvGEF*s were recorded to be epidermis expressed. More specifically, *HvGEF7a*, *HvGEF9b* and *HvGEF9c* were measured with only 1 fragment per million kilobase. However, *HvGEF1* was recorded with 4 FPKM and the highest expression in the epidermis was measured for *HvGEF14* (Table 11).

Table 11: Tissue specific expression of *HvGEFs* based on RNA sequencing extracted from James Hutton Institute. Colour code from white (lowest FPKM in the respective tissue) to dark green (highest FPKM in the respective tissue). Grey boxes denote *HvGEFs* with no available data.

	FPKM															
HvGEF	4-day embryos from germinating grains	Etiolated seedling (10 days)	Shoots from the seedlings (10 cm shoot stage)	Peeled epidermis (4 weeks)	Roots from the seedlings (10 cm shoot stage)	Root (4 weeks)	Developing tillers at six leaf stage, 3rd internode	Rachis (5 weeks pa)	Young developing inflorescences (5mm)	Developing inflorescences (1-1.5 cm)	Developing grain, bracts removed (5 DPA)	Developing grain, bracts removed (15 DPA)	Lemma (6 weeks pa)	Lodicule (6 weeks pa)	Palea (6 weeks pa)	Senescing leaf (2 months)
1	10	7	5	4	8	8	9	17	21	23	16	15	7	9	12	0
3a	5	0	0	0	1	2	0	0	0	0	0	0	0	0	0	0
3b																
3c																
7a	6	1	3	1	4	11	1	6	14	11	2	1	1	2	1	1
7b																
9a	0	0	0	0	0	0	0	0	0	0	0	0	9	0	17	0
9b	1	0	1	1	1	1	0	0	0	0	0	0	12	1	19	1
9c	1	7	1	1	1	1	5	8	1	1	1	1	13	3	14	0
10	2	0	0	0	1	0	0	0	0	0	1	1	6	1	10	0
14	11	20	14	9	6	7	21	23	31	35	39	11	31	12	34	0

In conclusion, The *H. vulgare* PRONE GEFs are comparable with those from other plant species. The annotation of *Hv*GEFs can be performed on the basis of *At* and *Os*GEFs and functionally important conserved amino acids can be found in the primary structure. Finally, the expression pattern of *Hv*GEFs provides candidates to investigate further.

3.2. Barley Guanine Nucleotide Exchange Factor 14

Since *HvGEF14* has been shown to be well expressed in *H. vulgare* epidermal peels, it was an interesting candidate PRONE-GEF to be important during the interaction of *H. vulgare* with the powdery mildew fungus. In a next step, *HvGEF14* gene expression had to be verified and tested for possible response to *Bgh* inoculation. In addition, it was important to establish whether *Hv*GEF14 might be involved in *Hv*RACB-dependent susceptibility or if it has an other function. To that end, protein-protein interaction between *Hv*GEF14 and *Hv*ROPs was tested and a novel GEF activity assay was established *in planta*.

3.2.1. *HvGEF14* is expressed in Golden Promise epidermis and down-regulated after *Bgh* inoculation

Even though it was known that *HvGEF14* was expressed in *H. vulgare* epidermis in 4-weeks old leaves (Table 11), it had not been established whether the gene expression is different during *Bgh* attack. This is why *HvGEF14* expression was also measured in epidermal peels from seven day old seedlings of the cultivars Ingrid, Pallas and Golden Promise un-inoculated and after *Bgh* inoculation by qRT-PCR of whole leaves and epidermal peels. As housekeeping gene, *HvGAPDH* was used as the gene expression showed the least variation across cultivars, tissues and treatments tested. In addition, *HvGAPDH* primers were predicted to not target fungal genes via the si-Fi prediction software. Figure S16 reports normalised threshold cycles (dCt) of qRT-PCR experiments. Since the threshold cycle indicates the earliest detection of the amplified transcript, the higher the dCt the lower is the expression of the measured gene. The three different cultivars show an enrichment of *HvGEF14* transcripts in the epidermis, independent of the cultivar and a decrease in *HvGEF14* transcript after *Bgh* inoculation (Figure S16).

Comparing the different *H. vulgare* cultivars, the most reproducible results were obtained with Golden Promise. Since the sample constitution change when only using one cultivar, the housekeeping gene had to be assessed again. For the samples collected from Golden Promise, *HvUbiquitin* served as a better housekeeping gene because *HvGAPDH* expression was not as uniform across the different sample types. Using the $2^{(-\Delta\Delta\ Ct)}$ method by Livak and Schmittgen (2001) to transform raw cycle threshold values (Ct) to foldchanges, it became apparent that the *HvGEF14* expression was on average 4.5 fold higher in epidermal peels of Golden Promise leaves when compared to the transcript level in whole leaves (Figure 5A).

In addition, *HvGEF14* expression decreased 0.5 fold in epidermal peels after *Bgh* inoculation in comparison to unchallenged epidermis (Figure 5B). Efficiency of *HvGEF14* (Table 7) primers was evaluated via the slope of a dilution curve of pooled cDNA from all tested treatments (Figure 5C) and amplicon specificity was checked during melt curve analysis after every qRT-PCR run (Figure 5D).

These results indicate the importance of *HvGEF14* expression in the tissue of plant-fungus interaction as well as hint to a possible role in the plant's response to *Bgh*.

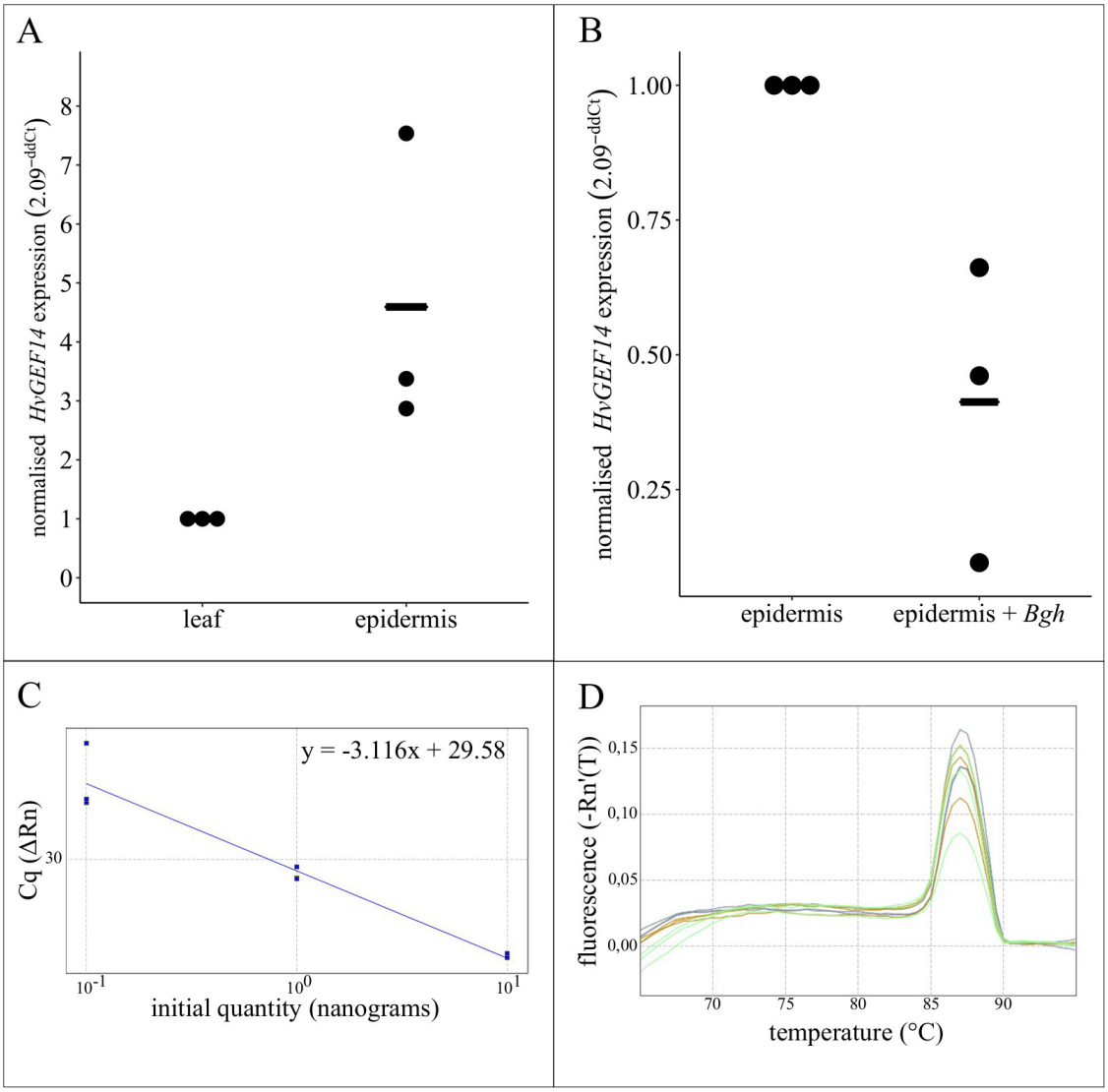

Figure 5: *HvGEF14* is expressed in *H. vulgare* epidermis and down-regulated upon *Bgh* inoculation. (A) *HvGEF14* transcript levels from epidermal peels normalised to whole leave samples in three independent biological replicates. (B) *Bgh*-inoculated epidermal peels normalised to non-inoculated epidermis shows decreased gene expression of *HvGEF14* after fungal challenge. (A-B) Cycle thresholds were extracted from the AriaMx software and normalised to *HvUbiquitin* as housekeeping gene via the $2^{(-ddCt)}$ method by Livak and Schmittgen (2001). (C) Dilution curve of *HvGEF14* transcripts in cDNA pool of all treatments to establish primer efficiency. (D) Melt curves of *HvGEF14* primers show target specificity.
Figure adapted from Trutzenberg et al. (2022).

3.2.2. *Hv*GEF14 interacts with *Hv*ROPs of type I and II

To understand if *Hv*GEF14 is indeed a *H. vulgare* guanine nucleotide exchange factor, its interaction with *H. vulgare* ROPs was tested via three different protein-protein interaction methods. First, Yeast-two-Hybrid (Y2H) was performed to test if *Hv*GEF14 can interact with *Hv*ROPs. In a next step, Bimolecular Fluorescence Complementation (BiFC) was used to identify proteins of close proximity *in planta*. Lastly, to confirm direct protein-protein interaction *in planta*, Foerster Resonance Energy Transfer (FRET) with subsequent Fluorescence Lifetime Imaging (FLIM) was performed.

Since other studies have shown the importance of the PRONE domain in interaction of GEFs and ROPs, both full length and PRONE domain of *Hv*GEF14 were analysed. In addition, during Y2H, ROPs have to be tested without their C-terminal lipidation motifs in order to allow movement into the yeast nucleus. Therefore, the type I ROP *Hv*RACB was tested without the last four amino acids of the C-terminus (ΔCSIL) and the type II ROP *Hv*RAC1 was truncated at the C-terminus by seven amino acids (ΔC). The results show that *Hv*GEF14 interacts with different *Hv*RACB and *Hv*RAC1 variants in similar ways.

Full length and PRONE domain (amino acids 124-485) constructs of *Hv*GEF14 interact with the three *Hv*RACB ΔCSIL variants WT, the constitutively activated G15V and low nucleotide affinity D121N on yeast interaction-selective media (-L-W-H). Yeast growth did not occur when co-transformed with *Hv*GEF14 and *Hv*RACBΔCSIL-T20N, indicating that the GEF does not interact with this (domiant negative) mutant (Figure 6A). Similar results were obtained for the wild type and constitutively activated (G23V) variants of *Hv*RAC1. Figure 6B shows a representative Y2H dropout on stringent interaction-selective medium (-L-W-H-Ade) between *Hv*GEF14 and *Hv*RAC1 ΔC. Again, there was no interaction observed between the two *Hv*GEF14 variants and the dominant negative mutant *Hv*RAC1-T28N. Protein stability of all bait and prey constructs was tested via protein extraction from transformed yeast and subsequent Western Blot (Figure 6C-D).

The results of Y2H indicate that *Hv*GEF14 can interact with *H. vulgare* ROPs and pave the way to further verify this interaction *in planta*.

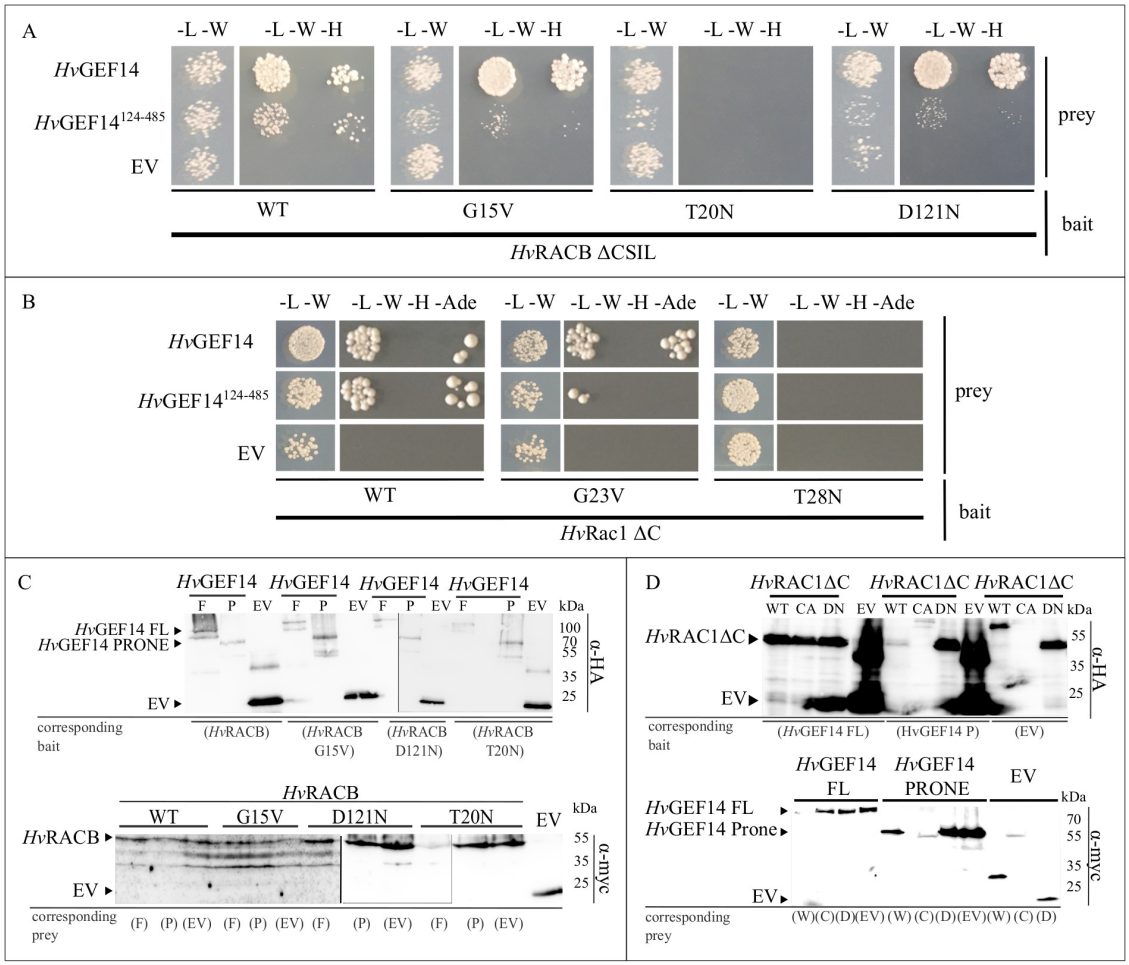

Figure 6: *Hv*GEF14 interacts with *Hv*ROPs. (A) Yeast-two-hybrid showing the interaction of *Hv*GEF14 full length and PRONE (amino acids 124-485) with *Hv*RACB ΔCSIL variants wild type (WT), constitutively activated (G15V), low nucleotide affinity (D121N), and dominant negative (T20N). No yeast growth was observed using the empty vector (EV) as negative control. Successful transformation was validated on selective medium lacking the amino acids leucine and tryptophan (-L-W) and protein-protein interaction was tested on dropout medium without leucine, tryptophan, and histidine (-L-W-H) in two dilutions (1, 1:10). The assay was repeated a least three times with the same results. (B) Yeast-two-hybrid dropout of *Hv*GEF14 full length and PRONE domain (124-485) and *Hv*RAC1 wild type (WT), G23V (constitutively activated), and T28N (dominant negative) each lacking the C-terminal lipidation motif (ΔC). No yeast growth was observed using the empty vector (EV) as negative control. Successful transformation was validated on selective medium lacking the amino acids leucine and tryptophan (-L-W) and protein-protein interaction was tested on dropout medium without leucine, tryptophan, histidine and adenine (-L-W-H-Ade) in two dilutions (1, 1:10). The assay was repeated a least three times with the same results. (C) Western blot of HA-*Hv*GEF14 full length (F) or PRONE (P) and myc-*Hv*RACBΔCSIL proteins expressed in yeast strain AH109 for Y2H. α-HA showing protein stability of prey proteins (HA-*Hv*GEF14 or HA-EV) detected via chemiluminescence and DURA substrate. α-myc showing protein stability of bait proteins (myc-*Hv*RACBΔCSIL or myc-EV) detected with chemiluminescence and FEMTO substrate. Proteins visualised on several gels as indicated by grey lines. (D) Western blot of myc-*Hv*GEF14 and HA-*Hv*RAC1ΔC -wild type (W), -G23V (C) or -T28N (D) proteins expressed in yeast strain AH109 for Y2H. α-HA showing protein stability of prey proteins (HA-*Hv*RAC1ΔC or HA-EV). Detection via chemiluminescence and DURA substrate. α-myc showing protein stability of bait proteins (myc-*Hv*GEF14 or myc-EV). Detection with chemiluminescence and FEMTO substrate.
Figure adapted from Trutzenberg et al. (2022).

In planta interaction of *Hv*GEF14 with *Hv*RACB was confirmed via ratiometric BiFC and FRET-FLIM. Since fluorescently tagged *Hv*PRONE14 constructs were not stable after transient transformation into *H. vulgare* epidermis cells or protoplasts, all further experiments were performed with full length *Hv*GEF14. By transiently over-expressing YFP_N-*Hv*GEF14 full length and YFP_C -*Hv*RACB variants in *H. vulgare* epidermis cells, the results observed in Y2H were reproduced (Figure 7A-B). YFP fluorescence complementation was observed in cells containing *Hv*GEF14 and *Hv*RACB-WT as well as -G15V. However, fluorescence intensity was not as strong as with the positive control between *Hv*RACB and its known interactor *Hv*RIC171 (Schultheiss et al., 2008). All three interacting combinations were, however, statistically different (Table S12) to the non-interacting control of *Hv*RIC171 and *Hv*RACB-T20N (Schultheiss et al., 2008). *Hv*GEF14 and *Hv*RACB-T20N did not interact just as in Y2H (compare Figures 6A and 7). Representative images of YFP_N-*Hv*GEF14 with the three YFP_C-*Hv*RACB variants WT, G15V and T20N showed fluorescence complementation for interacting proteins. YFP fluorescence was observed mainly at the cell periphery, indicating an interaction of *Hv*GEF14 with *Hv*RACB at this localisation (Figure 7B).

Further, the protein-protein interaction of *Hv*GEF14 full length with *Hv*RACB variants was tested via FRET-FLIM at the cell periphery. Monomeric enhanced GFP (meGFP) was N-terminally fused to *Hv*GEF14 and mCherry to *Hv*RACB wild type and previously studied mutants (Figure 7C-D). Representative false colour images show that the meGFP-*Hv*GEF14 lifetime was decreased in the presence of mCherry-*Hv*RACB-WT, -G15V or -D121N. The co-expression of meGFP-*Hv*GEF14 and mCherry-*Hv*RACB-T20N resulted in a GFP fluorescence lifetime that was not decreased when compared to the control. This indicates that, like in Y2H and BiFC, *Hv*RACB-T20N does not interact with *Hv*GEF14 *in planta* (Figure 7C).

Average meGFP lifetimes over at least three independent biological replicates indicated significantly lower values when meGFP-*Hv*GEF14 was co-expressed with either mCherry-*Hv*RACB WT, -G15V or -D121N. Amongst these tested combinations, the strongest interaction was observed of *Hv*GEF14 with constitutively activated *Hv*RACB-G15V. The lifetime of meGFP-*Hv*GEF14 was however not significantly different from the negative control (mCherry only) when *Hv*GEF14 was co-expressed with mCherry-*Hv*RACB-T20N (Figure 7D). In total, at least 30 cells were analysed for each combination, except for the interaction of meGFP-*Hv*GEF14 and mCherry-*Hv*RACB-T20N since fewer cells were observed with mCherry fluorescence (Figure 7D).

In summary, the protein-protein interaction of *Hv*GEF14 with *Hv*ROPs, especially *Hv*RACB wild type, -G15V and -D121N , could be established in *H. vulgare* epidermis cells.

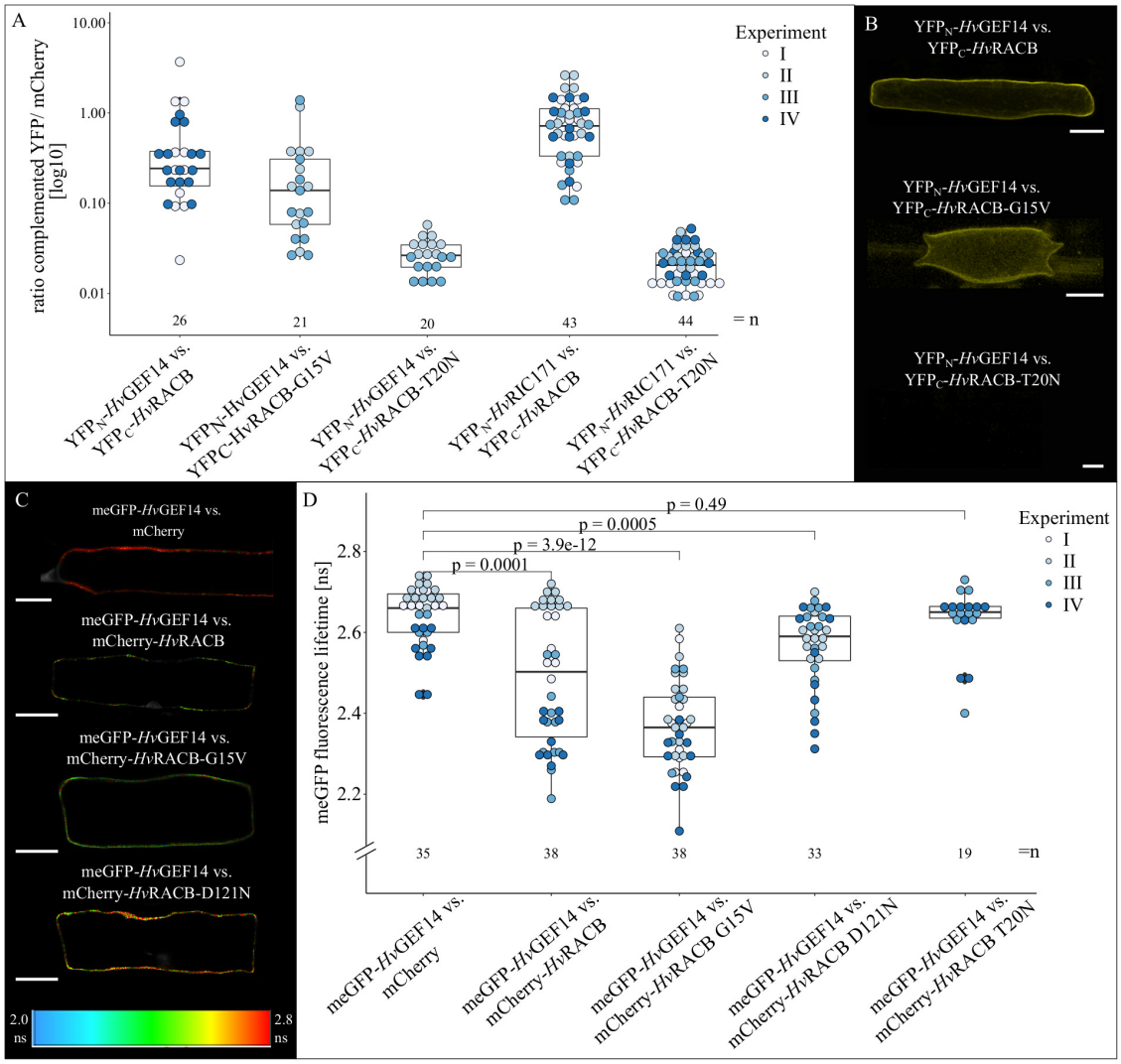

Figure 7: *Hv*GEF14 interacts with *Hv*RACB *in planta*. (A) Complemented YFP fluorescence intensity normalised to cytosolic mCherry shows interaction of *Hv*GEF14 with WT and G15V-*Hv*RACB but not with *Hv*RACB-T20N by comparison with positive control (*Hv*RIC171 interaction with *Hv*RACB) and negative control (*Hv*RIC171 interaction with *Hv*RACB-T20N obtained from Schultheiss et al. (2008)). For statistical analysis see Table S12. (B) Representative images of complemented YFP fluorescence of *H. vulgare* epidermis cells recorded as z-stacks with 2 μm increments. Scale bars 30 μm. (C) False colour images of *H. vulgare* epidermis cells show meGFP lifetime of different combinations tested in FRET-FLIM. Scale bars 30 μm. (D) FRET-FLIM of meGFP-*Hv*GEF14 full length with *Hv*RACB variants fused to mCherry. Cytosolic mCherry was used as negative control. Statistical analysis performed in Rstudio (version 1.2.5033): Shapiro-Wilk test was used to test data distribution and pairwise comparison with bonferroni adjustment for multiple testing returned the reported p-values.
Figure adapted from Trutzenberg et al. (2022).

3.2.3. *Hv*GEF14 and *Hv*RACB probably form a hetero-tetramer

Since the interaction of *Hv*GEF14 with *Hv*RACB could be established *in planta*, computational modelling was used to observe the interacting proteins *in silico*. Using the available crystal structure of *At*PRONE8 interacting with *At*ROP7 (2wbl.1 Thomas et al. (2009)) as reference, a computational model of *Hv*GEF14 and *Hv*RACB was created via SWISS-MODEL with a Global Model Quality Estimate (GMQE) score of 0.59 and qualitative model energy analysis with consensus-based distance constraint (QMEANDisCo, Studer et al. (2019)) score of 0.73 $\pm$ 0.05. The GMQE score reports the reliability of the model created. The QMEANDisCo score integrates absolute quality estimates for the overall structure and per residue. Both scores range from 0 (lowest) to 1 (highest).

The secondary structure of *At*PRONE8 has been shown to consist of mostly α helices with one outward oriented β-sheet. An other characteristic of the *At*PRONE8 crystal structure is a so called WW-loop harbouring two conserved tryptophanes (Thomas et al., 2007). The β-arm and WW-loop both have interaction interfaces with ROPs and are therefore important structural cues to GEF functionality (Thomas et al., 2007, 2009). The modelling reveals that the *Hv*PRONE14 domain also consists of 13 alpha-helices, a protruding β-sheet and the WW-loop between α4 and α5 (Figure 8A-B). This very close modelling to *At*PRONE8 also results in the conformation of a dimer by two PRONE-domains with the interaction interface between the two α1-helices as indicated by the white arrows. Interacting residues on the two α1-helices are highlighted in blue (Figures 8A for front view and 8B for birds eye view). This homodimer of two *Hv*PRONE14 domains can interact with the model of *Hv*RACB at the highlighted purple residues that are conserved amongst *Hv*GEFs (Figure 4 and Figures 8C-D). The hetero-tetramer of two *Hv*PRONE14 (green and turquoise) in interaction with two *Hv*RACB (beige) proteins can be seen in Figure 8C where the white arrow points to the *Hv*GEF14-*Hv*GEF14 interaction sites. This ROP-GEF model is based on the published crystal structure of the unmodified *At*ROP7 and the PRONE domain of *At*GEF8 without nucleotide attachment and has previously been termed "butterfly" (Thomas et al., 2007) for its wing-like shapes formed by one PRONE domain and one ROP on each side. A closer view of the predicted ROP-GEF interaction interface can be seen in Figure 8D where the white arrows point to conserved residues of *Hv*PRONE14 highlighted in purple that were predicted to interact with *Hv*RACB. This view also shows that the protruding β-sheets of the green *Hv*PRONE14 interact with the same *Hv*RACB protein as the interaction residues on the turquoise *Hv*PRONE14 located in its α-helices (Figure 8D).

This model of *Hv*GEF14-*Hv*RACB interaction highlights the possible conformation in a heterotetramer and provides important interaction interfaces to be tested further for functionality. Since this GEF-ROP model is reminiscent of the already published *A. thaliana* orthologues, it can be hypothesized that the *H. vulgare* GEFs might have a similar biological function.

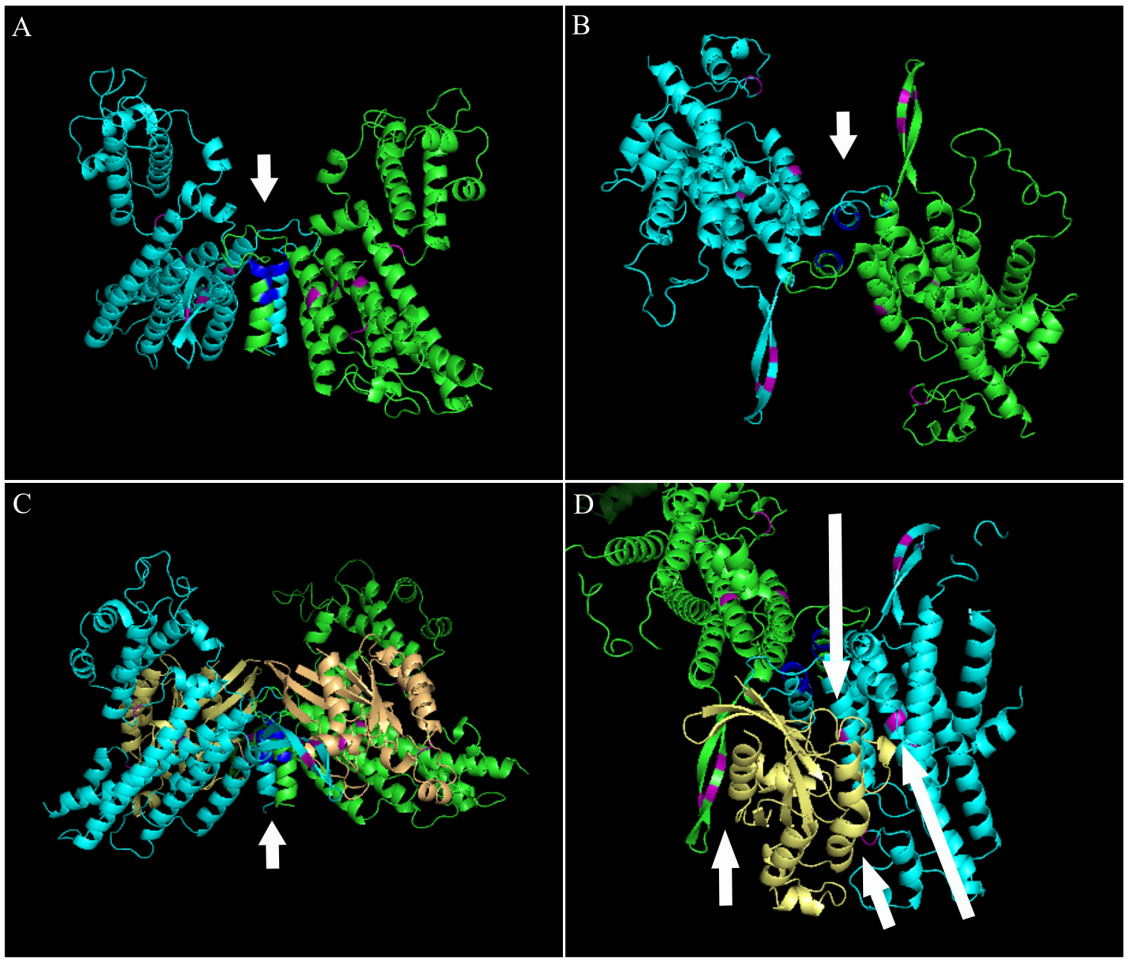

Figure 8: Protein model of *Hv*GEF14 PRONE domain dimer in interaction with two *Hv*RACB proteins based on SWISS-MODEL 2wbl.1 (GMQE: 0.59; QMEANDisCo global: 0.73 ± 0.05). (A) Homo-dimer of the PRONE domain of two *Hv*GEF14 in green and turquoise interacting at N-terminal α-helices (white arrow) based on the hetero-tetramer model 2wbl. (B) *Hv*GEF14 PRONE homo-dimer tilted 90 °to the front. Interaction region indicated with white arrow (based on 2wbl). (C) Hetero-tetramer of two *Hv*GEF14 PRONE domains interacting with two *Hv*RACB proteins (in beige). Interacting α-helices of *Hv*GEF14 indicated with arrow. (D) *Hv*GEF14 in turquoise and green interacting with *Hv*RACB in beige at highlighted interaction sites in magenta. One *Hv*RACB interacts with both *Hv*GEF14 PRONE domains.
Conserved interaction residues highlighted in blue, GEF-ROP interaction sites in purple.

3.2.4. *Hv*GEF14 is a susceptibility factor in the interaction with *Bgh*

A crucial step in characterising *Hv*GEF14 was the analysis of its biological function during the *H. vulgare*-*Bgh* interaction. The effect of *Hv*GEF14 on *Bgh* penetration success was therefore analysed with fixed cell microscopy of single transformed cells in interaction with *Bgh*.

Transient transformation of *H. vulgare* leaves was performed with a marker gene expressing the GUS enzyme. *H. vulgare* leaves were GUS stained after *Bgh* inoculation and fixed in Ethanol (EtOH) at 48 hours post inoculation (hpi). Figure 9A summarises five experiments in which *Hv*GEF14 was transiently over-expressed. In each experiment, at least 50 plant-fungus interactions could be counted. Compared to the cells transformed with the

empty vector, *Hv*GEF14 over-expression consistently leads to a significant increase in *Bgh* penetration into *H. vulgare* epidermis cells.

The knock-down (KD) via RNAi was designed with a hairpin-construct of a complementary 600 bp stretch within the PRONE domain (bp 601- bp 1201 of the full length gene coding for amino acids 201-401) of *HvGEF14* that showed no off-targets in *H. vulgare* and *Bgh* using the si-Fi prediction software. Transient transformation with this construct, decreases the penetration efficiency of *Bgh* in all six repetitions (Figure 9).

Due to the fact that *HvGEF14* RNAi was performed via single cell transformation, the silencing efficiency was previously tested via simultaneous over-expression of GFP-*Hv*GEF14 and *Hv*GEF14 RNAi in *H. vulgare* epidermis cells. Compared to the empty vector control, *HvGEF14* RNAi resulted in 52% lower fluorescence intensity of the tagged GEF (Table S15). Taken together, these results indicate a role of *Hv*GEF14 in the susceptibility of *H. vulgare* towards *Bgh*.

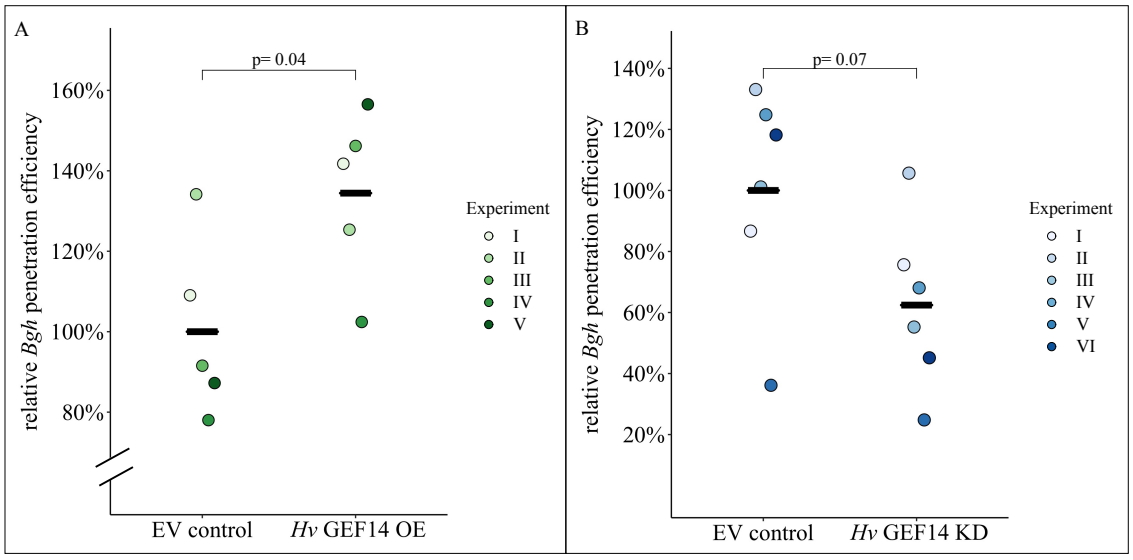

Figure 9: *Hv*GEF14 is a susceptibility factor in the interaction with *Bgh*. (A) Transient over-expression (OE) of *Hv*GEF14 in *H. vulgare* epidermis cells leads to 34 % significantly higher susceptibility when compared to the empty vector (EV) control at 2 dpi. (B) Transient knock-down (KD) of the *HvGEF14* transcript was performed in *H. vulgare* epidermis cells via bombardement with a hairpin-loop construct. Transformed cells were 38 % more resistant on average when compared to the corresponding EV control at 2 dpi and 4 dpt. Data points represent relative penetration efficiency of at least 50 observed interactions in every experiment. Statistical significance determined by *t* test after determination of normal distribution by Shapiro-Wilk test (both in Rstudio version 1.2.5033). Figure adapted from Trutzenberg et al. (2022).

Barley susceptibility is not influenced by the over expression of *Hv*GEF14 phosphorylation mutants

A serine residue at the C-terminus of the *At*GEF14 PRONE domain was published to be a phosphorylation site (Mergner et al., 2020). Due to the similarity in primary sequence with the *H. vulgare* orthologue, the corresponding S394 in *Hv*GEF14 was identified. The serine residue was mutated during gene synthesis to either alanine (S394A) creating a

phosphoablation mutant or aspartic acid (S394D) for a phosphomimic mutant. Subsequently, the penetration efficiency of *Bgh* was scored on cells transiently over-expressing either *Hv*GEF14-S394A or *Hv*GEF14-S394D. In five independent experiments, both mutations lead to increased susceptibility of *H. vulgare* towards *Bgh* by 14-18 % but statistical analysis by Kruskal-Wallis test confirmed that the effect of these two *Hv*GEF14 mutants are neither significantly different from the control nor from the wild type (Figure S18). In addition, compared to the over-expression of wild type *Hv*GEF14, the susceptibility inducing effect of both mutants was reduced by 40% (Figure S18).
These results establish, that serine 394 in *Hv*GEF14 is probably not a functionally important amino acid for the role of *Hv*GEF14 in susceptibility towards *Bgh* on its own. However, these results did not allow for any conclusion on as to whether S394 is perhaps a residue of *Hv*GEF14 with protein-regulatory function by posttranslational modification.

3.2.5. *Hv*GEF14 can activate *Hv*ROPs *in planta*

The ROP activity status can be determined *in planta* by different methods. To investigate how *Hv*ROPs get activated in *H. vulgare* epidermis cells, two strategies were employed based on the protein's interaction with downstream executers. The scaffold protein *Hv*RIC171 was shown to preferably interact with activated *Hv*RACB at the plasma membrane (Schultheiss et al., 2008; Li et al., 2020). Therefore, the localisation of fluorescently tagged *Hv*RIC171 was observed as well as its interaction with *Hv*RACB in presence of *Hv*GEF14.

*Hv*GEF14 over expression leads to recruitment of mCherry-*Hv*RIC171 to the cell periphery

Firstly, the scaffold protein *Hv*RIC171 was tested for its localisation in *H. vulgare* epidermis cells while simultaneously over-expressing *Hv*RACB variants or *Hv*GEF14.
mCherry-*Hv*RIC171 was recruited to the cell periphery during co-expression with *Hv*GEF14 as can be seen on the representative image in Figure 10A. In the z-stack as well as in a section of the cell imaged at the equatorial plane, the mCherry-RIC171 fluorescence is much stronger at the periphery when *Hv*GEF14 is expressed in access, when compared to the EV control. Even though mCherry-*Hv*RIC171 fluorescence is not excluded from the periphery in the control, the zoomed in image shows uneven distribution at the cell periphery (Figure 10A). This observation was quantified by measuring mCherry-*Hv*RIC171 fluorescence at the equatorial plane and normalising it to the cytosolic marker GFP and cytosolic fluorescence of mCherry*Hv*RIC171 over the whole cell (Figure 10B). mCherry-*Hv*RIC171 further shows consistent localisation to the plasma membrane when co-expressed with untagged *Hv*RACB-G15V and cytosolic localisation when *Hv*RACB-T20N is co-expressed. The over-expression of *Hv*GEF14 hence lead to the same outcome as the over-expression of constitutively activated *Hv*RACB-G15V (Figure 10B).

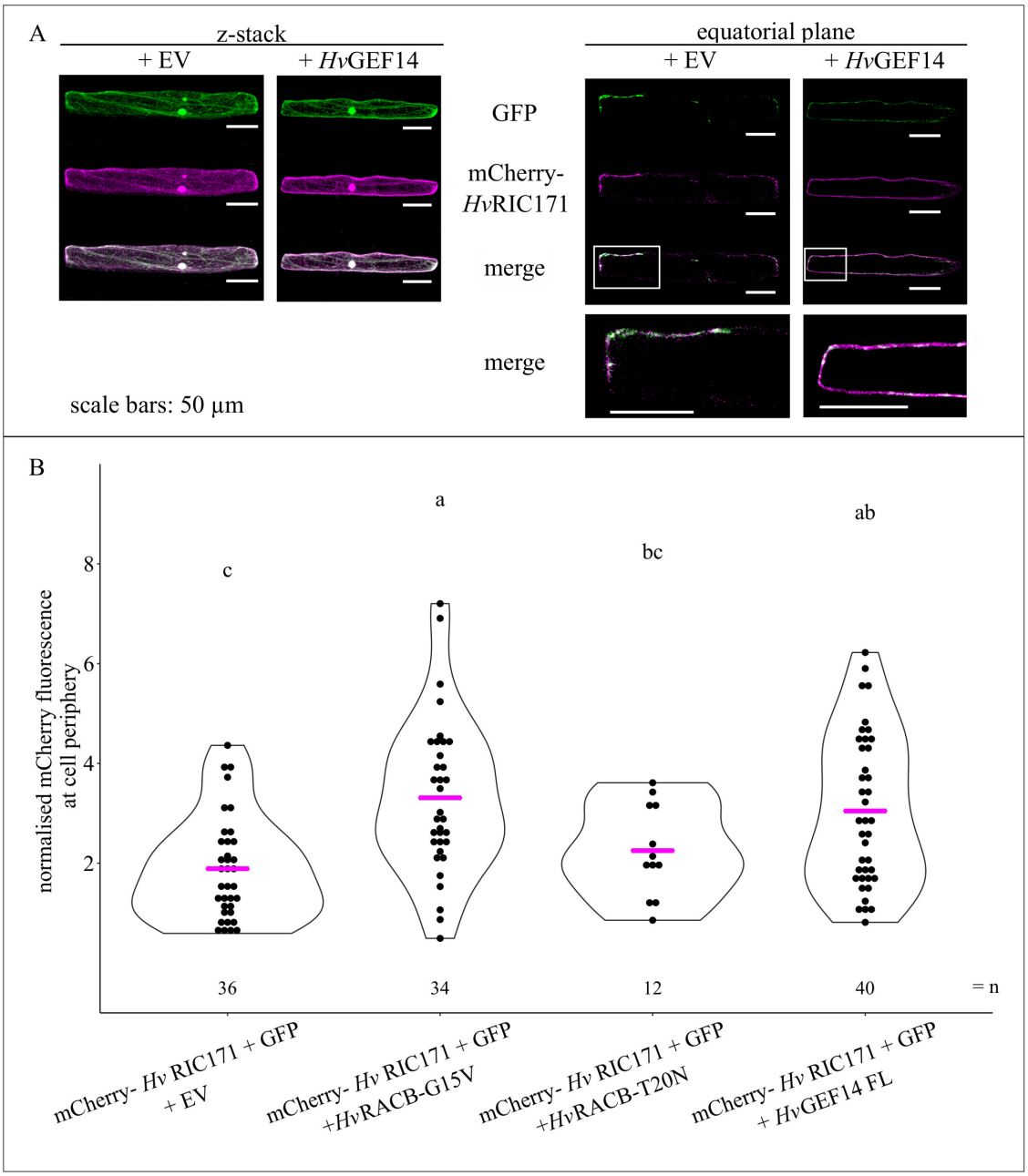

Figure 10: *Hv*GEF14 leads to cell-periphery localisation of mCherry-*Hv*RIC171. (A) Confocal microscopy images of mCherry-*Hv*RIC171 and cytosolic GFP transiently over expressed in addition to either empty vector (EV) or *Hv*GEF14. mCherry-*Hv*RIC171 is recruited to the cell periphery during the over expression of *Hv*GEF14 but not empty vector (EV). Z-stacks on the left in 2μm increments starting from equatorial plane to top of the cell. Images taken 24 hours after transformation. (B) Quantification of mCherry-*Hv*RIC171 recruitment by measurement of fluorescence intensity at the cell periphery (equatorial plane) relative to whole cell fluorescence (z-stack) and normalised to GFP fluorescence. *Hv*RACB-G15V serves as positive, *Hv*RACB-T20N as negative control for mCherry-*Hv*RIC171 recruitment by activated ROPs. Figure adapted from Trutzenberg et al. (2022).

***In planta Hv*RACB activity sensor**

Measuring the ROP activity status *in planta* has been shown to work on the basis of a FRET-FLIM sensor. In these previously published setups, one FRET-fluorophore was attached to the wild type ROP and a corresponding fluorophore to an interactor of activated ROP (Kawano et al., 2010; Hamers et al., 2014; Wang et al., 2018). Based on these reports, a *Hv*RACB activity sensor was developed using *H. vulgare* specific protein combinations fused to FRET-fluorophores. Wild type *Hv*RACB was tested for interaction with different known executors in *H. vulgare* epidermis cells: *Hv*RIC171, *Hv*RIC157 or *Hv*CRIB46. *Hv*RIC171 and *Hv*RIC157 are signalling proteins in the *Hv*RACB-mediated susceptibility pathway (Schultheiss et al., 2008; Engelhardt et al., 2021) and *Hv*CRIB46 is a 46 amino acid long fragment of *Hv*RIC171 which includes the ROP-interacting domain CRIB. Interestingly, all three executers showed interaction with not only CA-*Hv*RACB but also WT-*Hv*RACB without any added stimulus in *H. vulgare* (unpublished data from by Michaela Kopischke). To counteract the effect of possible endogenous *Hv*RACB activators, the experiment was moved to a heterologous plant system, *N. benthamiana*. The Agrobacterium-mediated co-transformation with binary vectors containing meGFP-*Hv*RACB and *Hv*CRIB46-mCherry showed a reasonable dynamic range of GFP lifetimes across a number of tested cells in *N. benthamiana* (unpublished data by Lukas Weiss). The interaction of these two partners can therefore reliably indicate *Hv*RACB activity status: the interaction of meGFP-*Hv*RACB with *Hv*CRIB46-mCherry decreases the measured GFP lifetime and reports *Hv*RACB activation (Figure 11A). This *Hv*RACB activity sensor was then used to observe the effect of co-expressed 3xHA-*Hv*GEF14 on ROP activity. All transformed proteins were successfully expressed in *N. benthamiana* as shown by Western Blotting (Figure 11B-D). Figure 11E summarises three independent repetitions of this FRET-FLIM-based ROP activity sensor with meGFP-*Hv*RACB as the donor and *Hv*CRIB46-mCherry as the acceptor fluorophore. meGFP-*Hv*RACB does not interact with the negative control, GST-mCherry, but meGFP-CA-*Hv*RACB strongly interacts with *Hv*CRIB46-mCherry. Though the interaction of meGFP-*Hv*RACB with *Hv*CRIB46-mCherry is significantly different from the non-interacting control, the interaction is not as strong as with the constitutively activated *Hv*RACB. Interestingly, the additional overexpression of 3xHA-*Hv*GEF14 decreases the meGFP-lifetime significantly (Figure 11E). This suggests that *Hv*GEF14 can activate *Hv*RACB in order for it to interact with the CRIB-containing downstream executer.

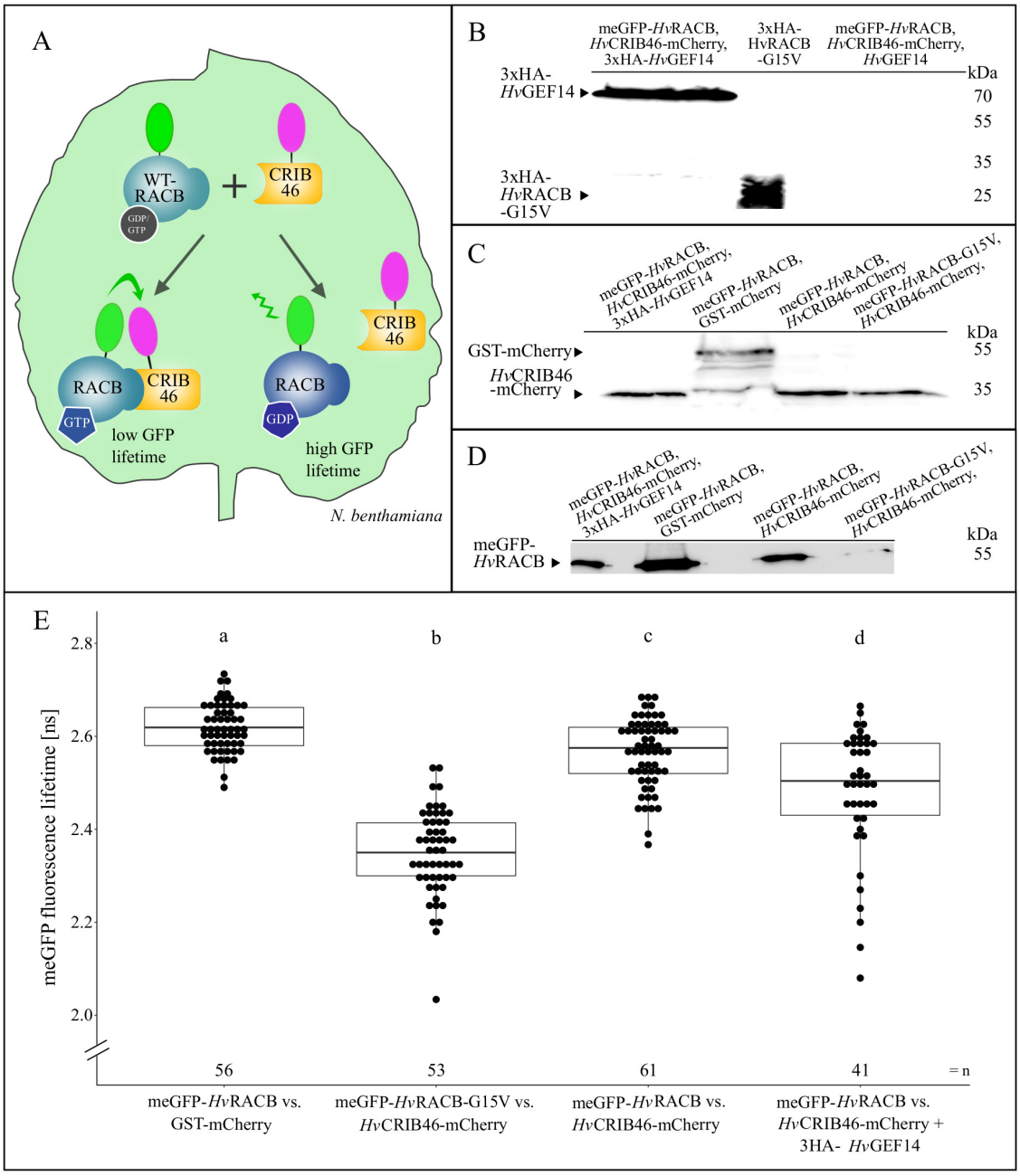

Figure 11: *Hv*GEF14 can activate *Hv*RACB. (A) Scheme of FRET-based *Hv*RACB activity sensor in *N. benthamiana*. (B-D) Proteins were extracted from transformed *N. benthamiana* leaf discs and visualised via Western Blotting and subsequent immunodetection. (B) Proteins were labelled with anti-HA-HRP during Western Blotting. (C) Proteins were labelled with anti-RFP-rat mAb and anti-rat antibodies. (D) Proteins were labelled with anti-GFP and m-IgGκ BP-HRP antibodies. (E) FRET-FLIM of *Hv*RACB and *Hv*CRIB46 in *N. benthamiana* leads to decreased GFP lifetimes in presence of *Hv*GEF14. *Hv*RACB interaction with GST-mCherry used as negative control and CA-*Hv*RACB interaction with *Hv*CRIB46 as positive control.

3.3. Dimerisation of susceptibility pathway proteins

3.3.1. *Hv*GEF14 can homo-dimerise

According to reports from literature and structural prediction, PRONE-GEFs form signalling active dimers. Therefore, the homo-dimerisation capacity of *Hv*GEF14 was tested via Y2H. *Hv*GEF14 full length and PRONE domain (amino acids 124-485) were tested against each other in bait and prey constructs. Interaction was observed between all combinations of *Hv*GEF14 full length and PRONE while the negative controls (EV) show expected results (Figure 12A-B). This result is an other hint that *Hv*GEF14 functions in a similar manner to already published PRONE-GEFs that were shown to require homo-dimerisation for proper GEF activity (Thomas et al., 2007).

3.3.2. Homo- and hetero-dimerisation of epidermis expressed *Hv*RICs

Interestingly, other *Hv*RACB interactors were also shown to homo- and hetero-dimerise. In Y2H, *Hv*RIC157 and *Hv*RIC171 homo-dimerise in three independent repetitions (representative image in Figure 12C) but were both not detectable on α-myc Western Blot (Figure 12D). HA-*Hv*RIC157 stayed elusive even in the α-HA immunodetection after many attempts while HA-*Hv*RIC171 could be detected (Figure 12D).

Subsequently, the hetero-dimerisation amongst all epidermis expressed *Hv*RIC proteins (Engelhardt et al., 2018), was observed (Figure 13A-D). On selective media, yeast transformed with *Hv*RIC171 in combination with *Hv*RIC157 or *Hv*RIC193 grew. In addition, the transformation with *Hv*RIC163 and *Hv*RIC194 lead to growth of yeast colonies. These results indicate that *Hv*RIC171 can interact with *Hv*RIC157 and *Hv*RIC163. In addition, *Hv*RIC194 only interacts with *Hv*RIC163. Since *Hv*RIC157 also only interacts with *Hv*RIC171, two pairs of exclusively interacting *Hv*RICs can be established from these assays: *Hv*RIC157 and *Hv*RIC171 on the one hand plus *Hv*RIC163 and *Hv*RIC194 on the other hand.

In addition to the results obtained in Y2H, the dimerisation of *Hv*RIC171 and *Hv*RIC157 was tested *in planta* via FRET-FLIM (Figure 13E). Indeed, the reduction in measured GFP fluorescence lifetime was significant when GFP-*Hv*RIC157 and mCherry-*Hv*RIC171 were transiently co-expressed in *H. vulgare* epidermis cells. This indicates direct protein-protein interaction of these *Hv*RACB executers *in planta*.

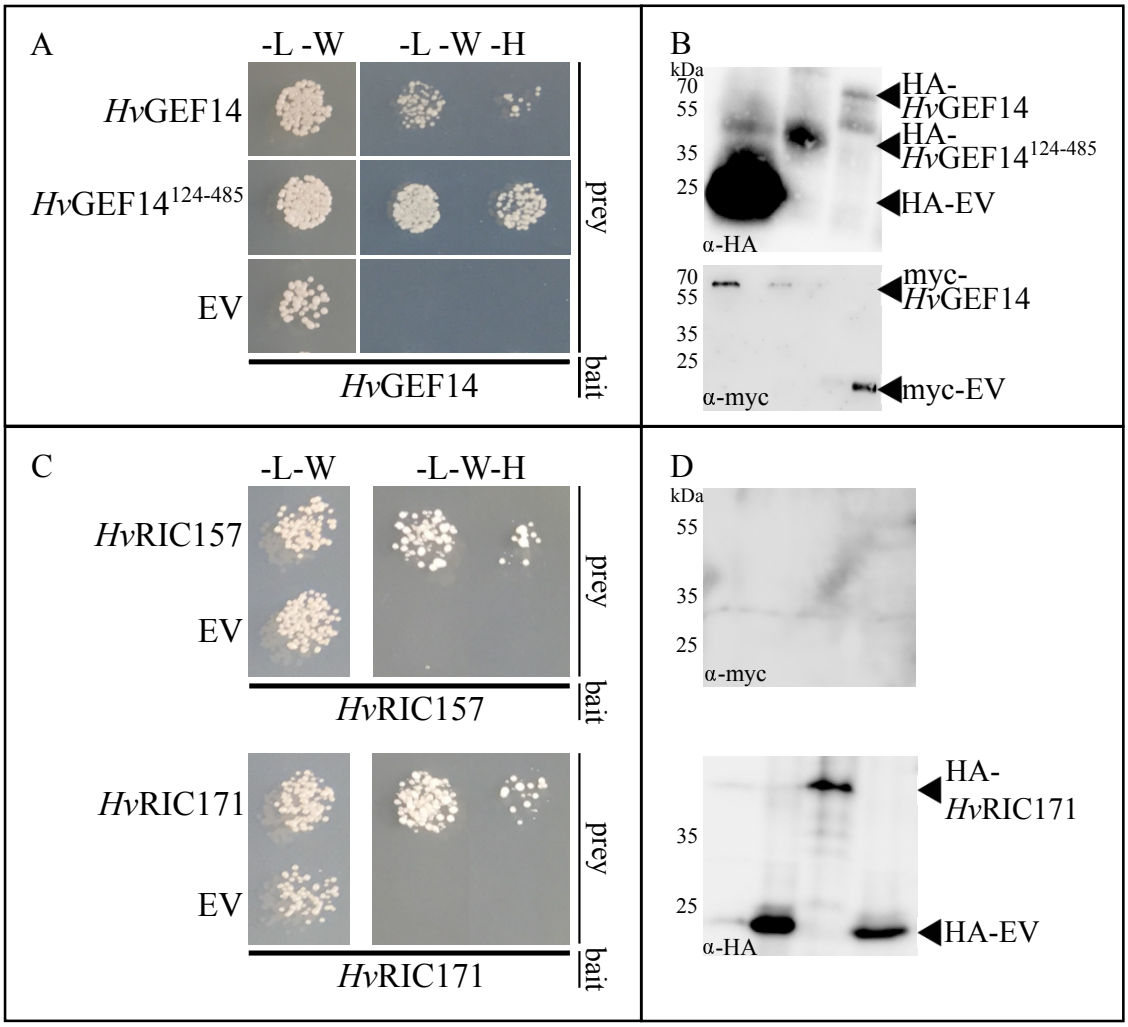

Figure 12: *Hv*RACB interactors can homo-dimerise.
(A) Representative images of yeast transformed with *Hv*GEF14 full length and PRONE domain (amino acids 124-485) show growth on selective media for successful transformation (-L-W) and protein-protein interaction (-L-W-H). Empty vector (EV) was used as a negative control and the experiment was repeated at least three times with the same results. (B) Western Blot of transformed yeast confirms expression of full length prey (α-HA) and bait (α-myc) proteins. (C) Representative images of yeast transformed with *Hv*RIC157 and *Hv*RIC171. Growth observed on selective media for successful transformation (-L-W) and protein-protein interaction (-L-W-H). EV was used as a negative control and the experiment was repeated three times with the same results. (D) Only *Hv*RIC171 and EV were detectable in α-HA Western Blot even though yeast growth was observed when transformed with *Hv*RIC157 in all cases on transformation selective medium.
Figure adapted from Trutzenberg et al. (2022).

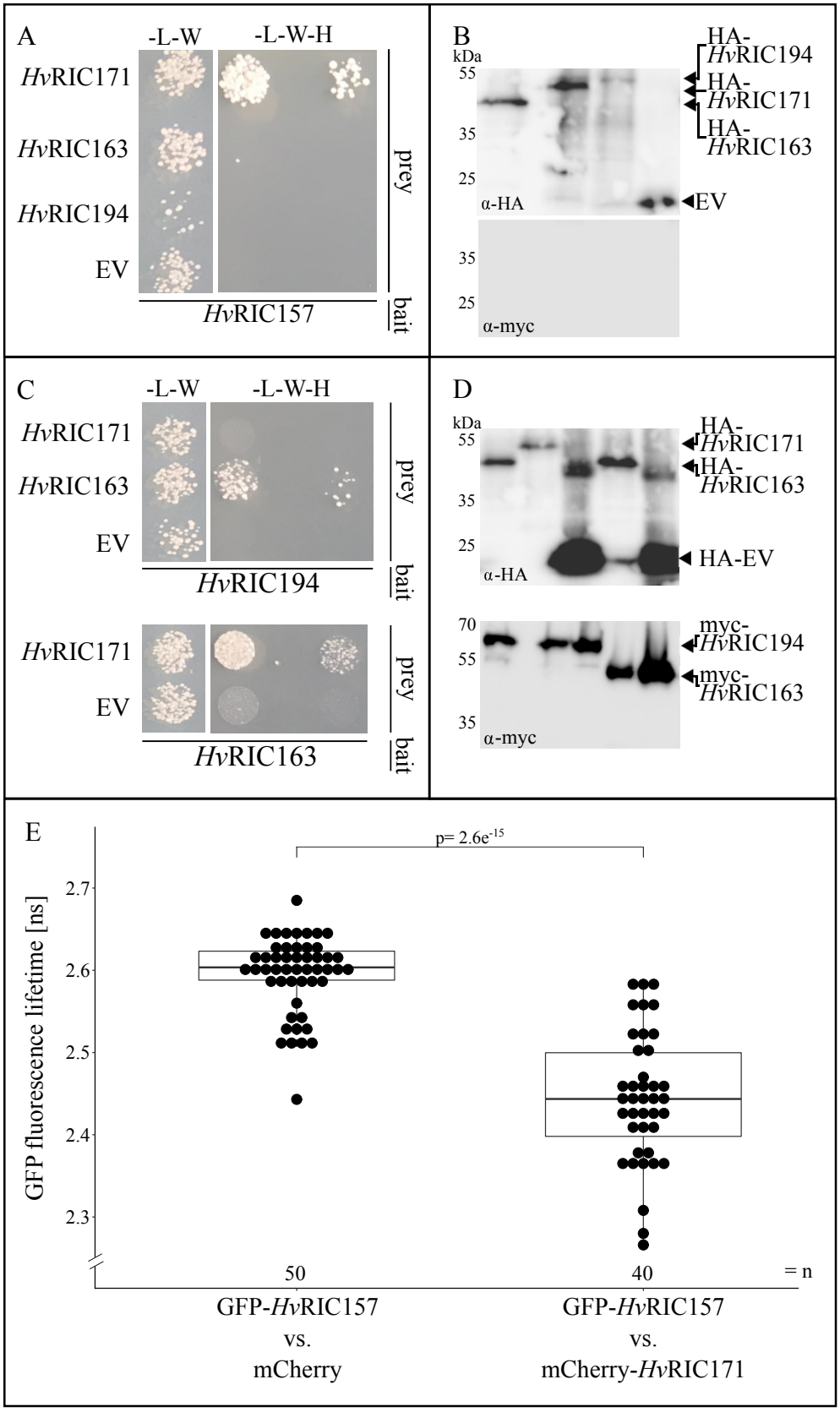

Figure 13: Hetero-dimerisation between two epidermis expressed *Hv*RICs. (A, C) Y2H show interaction of *Hv*RIC157 with *Hv*RIC171 and interaction of *Hv*RIC163 with *Hv*RIC194 and *Hv*RIC171. (B, D) *H. vulgare* proteins expressed in yeast and visualised after Western Blot via immunodectection of HA- and myc-tag for prey and bait proteins, respectively. (E) *In planta* interaction of meGFP-*Hv*RIC157 and mCherry-*Hv*RIC171 observed with FRET-FLIM in transiently transformed *H. vulgare* epidermis cells. Pairwise comparison t-test performed in R studio after test for data distribution.

4. Discussion

Plant ROPs are important signalling proteins that steer a variety of processes in development and immunity. The *H. vulgare* ROP *Hv*RACB has been of special interest in the last decades due to its role as susceptibility factor in the interaction with the powdery mildew fungus *Bgh*. The molecular switch *Hv*RACB aids in fungal accommodation when in its activated form. Despite scientific advances in understanding the molecular interplay of activated *Hv*RACB with downstream interactors, the activation mechanism of *Hv*RACB itself had not been elucidated until now. To bridge this gap of knowledge, the work presented in this dissertation provides evidence of *H. vulgare* PRONE GEFs as activators of *H. vulgare* ROPs.

More specifically, the PRONE-domain containing protein *Hv*GEF14 is presented as an epidermis-expressed and *Bgh*-regulated ROP activator. The results show that *Hv*GEF14 can interact with different types of *H. vulgare* ROPs and activate the susceptibility factor *Hv*RACB *in planta*. In addition, evidence is presented of *Hv*GEF14 as a susceptibility factor due to its typical effect on *Bgh* infection success during functional studies.

The role of PRONE-type guanine nucleotide exchange factors in plant development, polar growth and immunity has been studied in many plant species. After the initial discovery in *Arabidopsis thaliana* by Berken et al. (2005) and parallel reports in *Solanum lycopersicum* by Kaothien et al. (2005), PRONE-GEFs have also been studied in crop pants like *Oryza sativa* (Akamatsu et al., 2013) and *Glycine max* (Gao et al., 2021b). In addition, the protein family has been reported in bryophytes, such as *Marchantia polymorpha* and *Physcomitrium patens* (Hiwatashi et al., 2019; Le Bail et al., 2019). Increasingly more accurate annotations of the sequenced *H. vulgare* genome as well as advances in *Bgh* genome and proteome mapping have built the basis to understand the interaction of *H. vulgare* with *Bgh* on a molecular level.

4.1. An organised Family Tree: Annotation and Phylogeny of PRONE-GEFs

In order to gain an overview of PRONE GEFs in *H. vulgare*, it was important to establish a consistent nomenclature. In the first report on PRONE-GEFs by Berken et al. (2005), the members of this new class of proteins were numbered from 1-14. Since then, this nomenclature has however not always been used due to previous names or new numbering in following publications. When investigating PRONE-GEFs in other plants than *A. thaliana*, however, it is vital to have consistent nomenclature to ease research and avoid misunderstandings. This is especially important when working with species that have less PRONE-GEFs encoded in their genome, such as grasses. This is why the nomenclature of

the eleven PRONE-GEFs in *H. vulgare* are numbered 1-14 in this dissertation as well.

Protein families evolve with time and environmental pressure. In order to gain insight into evolutionary development as well as functional differences between the members of the PRONE GEF protein family, a phylogenetic analysis was performed comparing PRONE GEFs of the dicotyledonous model organism *A. thaliana* and monocotyledonous *O. sativa* with PRONE GEFs of the species of interest, *H. vulgare*. The phylogenetic analysis published in this dissertation reports three clades of plant GEFs. Previous publications have observed different phylogenetic relationships of PRONE-GEFs but most are in accordance with the results shown in Figure 3. Even though a number of plant GEFs have been reported to function in distinct molecular pathways, there are no strictly clade- specific functions to be observed. PRONE GEFs are rather implicated in a number of similar signal pathways across the phylogenetic tree. This might be due to the fact that GEFs are central molecular components important for ROP-mediated signalling, which in itself is important for vital processes. In addition, many PRONE GEFs have not been researched until now, especially in plants other than *A. thaliana* so that more functions might still be discovered.
However, some characteristics of the three clades can be highlighted: Clade I encompasses GEFs 1-7 which have been identified by others to function in immunity and plant development (Akamatsu et al., 2013; Xu et al., 2021; Denninger et al., 2019; Huang et al., 2018b). The most prominent member of this clade is GEF1 due to the fact that it has been extensively studied in *O. sativa* as well as *A. thaliana* (Akamatsu et al., 2015; Duan et al., 2010; Li et al., 2018b; Huang et al., 2018a; Gu et al., 2004; Li et al., 2018a).
Clade II (GEFs 8-13) includes another prominent PRONE-GEF, *At*GEF8, which has been crystallised and therefore serves as a model to structurally explore other PRONE GEFs (Thomas et al., 2007). Other members of this clade were reported to have roles in various polar growth processes and lipid metabolism (Yoo et al., 2011; Takeuchi and Higashiyama, 2016; Li et al., 2020; Cao et al., 2017).
Finally, it is intriguing that PRONE GEFs of clade III are least similar to all other GEFs in the phylogenetic analysis. Clade III is formed by only GEF14 proteins. This distribution is reminiscent of outgroups that are normally used in phylogenetic analyses to resolve a certain branch of the phylogenetic tree (Pavlopoulou et al., 2019). However, in the analysis of GEFs from the three different species, no outgroup was included. The fact that all three species are represented in clade III therefore highlights the unique sequence of GEF14 proteins compared to the other GEFs in the family.

However, comparing *Hv*GEFs to other PRONE-type GEFs, it is apparent that they possess the same structure of primary sequence. All PRONE-GEFs published until now have the characteristic three sub-domains of increased conservation within PRONE (Berken et al., 2005). In addition, just as *At* and *Os* GEFs, *Hv*GEFs are equipped with conserved amino

acids for protein-protein interactions between GEFs and with ROPs (Table S14). Based on that, *Hv*GEFs probably homo-dimerise and are able to interact with *H. vulgare* ROPs just like their counterparts in *A. thaliana* and *O. sativa* (Thomas et al., 2007; Fricke and Berken, 2009). In this dissertation, first evidence was presented in Y2H that *Hv*GEF14 indeed homo-dimerises. In combination with the protein-protein interaction assays that show *Hv*GEF14-*Hv*RACB interaction, it is likely that the two *H. vulgare* proteins interact as previously published in *A. thaliana*. This is further supported by high support values for a structural model of the *Hv*GEF14-*Hv*RACB heterotetramer (Figure 8).

4.2. *H. vulgare* Guanine Nucleotide Exchange Factor 14 is a representative of *Hv*GEFs

The aim of this dissertation is to give an overview on *H. vulgare* GEFs with a special focus on *Hv*GEF14. In this study, *HvGEF14* was characterised to be expressed in the epidermis and in addition, *H. vulgare* epidermal cells respond to the inoculation with *Bgh* by down-regulating the *HvGEF14* transcript (Figure 5). This reduction of expression upon fungal stimulus in *H. vulgare* epidermis provided a first hint towards a function of *HvGEF14* in the *H. vulgare-Bgh* interaction. At the example of *Hv*GEF14, this dissertation also shows how PRONE-GEFs can activate the *Hv*RACB-dependent susceptibility pathway to a fungal pathogen in *H. vulgare*. Though there might be other GEFs to perform a similar function, *Hv*GEF14 shows all characteristics of a PRONE-GEF and is potentially linked to *H. vulgare* susceptibility via the *Hv*RACB signalling pathway.

At the beginning of this study, little was known about *Hv*GEFs and GEF14 in particular has only been studied in the model species *A. thaliana*. Interaction partners have been found to be the small GTPases *At*ROP1 (including the *At*ROP1 mutants G15V and D121A/C188S) during *in vitro* pull-down assays (Gu et al., 2006) and *At*ROP6 *in planta* via immunoprecipitation (IP) from transgenic plants. In the same study, the RLK *At*FER was also found to be an interaction partner of *At*GEF14 (Lin et al., 2021). In earlier studies, *At*FER was shown to be a susceptibility factor n the interaction of *A. thaliana* with the powdery mildew fungus (Kessler et al., 2010). Put together, these studies indicate that susceptibility towards powdery mildews might be regulated via a FER-GEF14-ROP pathway. The hypothesis arises whether in *H. vulgare* these proteins might also play a role in the interaction with *Bgh* and it highlights the hypothesised position of GEFs in the signalling cascade as a bridge between cell surface receptors and ROPs.

It was also shown that *At*GEF14 plays a role in polar growth processes like pollen tube

elongation (Gu et al., 2006), epidermal cell shape (Lin et al., 2021), the development of root hairs (Denninger et al., 2019), but also during the sensing of mechanical stimuli (Tang, 2022). In addition, the protein can be found localised to the apical region in *N. tabacum* pollen tubes (Gu et al., 2006) and resides in the RHID during early polarisation events of root hair growth (Denninger et al., 2019), which hints at a mechanism behind its function in polar growth processes.

To get a better overview on *H. vulgare* GEFs in general, and *Hv*GEF14 in particular, the expression of their corresponding genes was analysed. Due to their many functions, it is not surprising that *HvGEFs* are expressed in all observed tissues as published by the JHI (Table 11). The same has also been shown for *A. thaliana GEFs*. RT-PCR of different plant tissues showed for example that *AtGEF1*, *AtGEF3*, *AtGEF5*, *AtGEF6* and *AtGEF7* were expressed in most examined tissues. More specific expression was however observed for *AtGEF4*, which was only detected in roots and *AtGEF8*, *AtGEF9*, *AtGEF11*, *AtGEF12* and *AtGEF13* which showed transcripts mostly in reproductive organs. In the same study, *AtGEF14* was found to be expressed in seedlings, leafs and unpollinated pistils (Zhang and McCormick, 2007). A tissue specific expression pattern was also reported a few years later by another group but with slightly different results. In the study by Shin et al. (2009), *AtGEF1*, *AtGEF4*, *AtGEF5* and *AtGEF11* show transcripts in all analysed tissues, whereas *AtGEF7*, *AtGEF8*, *AtGEF9* and *AtGEF13* were mostly expressed in flowers. Interestingly, *AtGEF14* expression responded to abiotic stresses applied by down-regulation of the transcript. There are other examples of how different study designs report varying expression patters of *GEFs* depending on the aim of the research. Therefore, it is important to report gene expression in the tissue and at the time point of interest. To that end, the expression of *HvGEF*s was measured in young leaves, epidermal peels and after *Bgh* inoculation for this study.

The JHI data provides a variety of samples tested at time points that might be of highest interest. The data shows that in *H. vulgare* only two *HvGEFs* are ubiquitously expressed: *HvGEF1* and *HvGEF14*. Other GEFs, such as *HvGEFs 3a, 9a-c* and HvGEF10 were recorded to have increased transcript counts in a fraction of tested tissues.
The qRT-PCR assay presented in this dissertation (Figure 5) was performed with two week old leaves and epidermal peels since other measurements, such as protein-protein interaction, localisation and susceptibility towards *Bgh* were assessed at the same leaf age. With this assay, increased *HvGEF14* expression in the epidermis could be confirmed. In addition, the down-regulation after inoculation with *Bgh* of the *HvGEF14* transcript was observed (Figure 5). This reduction of expression upon fungal stimulus in *H. vulgare* epidermis points to a function of *HvGEF14* in the *H. vulgare-Bgh* interaction. The expression of only *HvGEF14* was measured due to the fact that many *HvGEF*s are weakly expressed in leaf tissue. Therefore the establishment of qRT-PCR for *HvGEF*s posed

several obstacles and the focus stayed on the *HvGEF* with highest reported expression in epidermal peels. Therefore, the results presented in this dissertation do not exclude that *HvGEF*s other than *HvGEF14* could also show *Bgh*-responsive gene expression and function in susceptibility or resistance.
Other studies have shown before that the expression of plant *GEF*s responds to external stimuli. In 2009 for example, Shin et al. (2009) published a gene expression analysis on *AtGEFs* in response to abiotic stresses like temperature, drought and salt. In accordance with the data published in this dissertation, the authors found that *AtGEF14* is expressed in leaves, stem, flowers and pollen. The same study also reported that the plant responds to salt stress with up-regulation of *AtGEF14* and to increased heat by down-regulation of the transcript (Shin et al., 2009). This shows a general mechanism of *GEF* transcript regulation after the perception of environmental stimuli. It is important to stress, however, that even though tissue- and stimulus-dependent gene expression is a prerequisite for translation, it does not predict protein function. Therefore, further studies have to show the functionality of proteins in signalling pathways that result in a plant's response to its environment. For *At*GEF14, it was shown that it can interact with *At*ROPs (Gu et al., 2006) as well as *At*RLKs (Lin et al., 2021) and functions in root hair development (Denninger et al., 2019). Taken together, the gene expression and protein functional studies indicate a role for *At*GEF14 in the plant's response to external stress stimuli, possibly by linking perception via RLKs to intercellular ROP-signalling.
In *H. vulgare*, there have been reports on differential gene expression during the interaction with *Bgh* (Hückelhoven et al., 2001; Douchkov et al., 2014; Schnepf et al., 2018). Just as *HvGEF14*, some genes linked to primary metabolism, secretion or gene expression where reported to be down-regulated after *Bgh* inoculation in epidermis and whole leaf (Douchkov et al., 2014). These processes are basic developmental pathways and their down-regulation might be part of a transcriptional reprogramming from growth to pathogen defense. However, the molecular function in *H. vulgare* of proteins corresponding to these genes has not been elucidated further.

Although the transcriptional abundance of *HvGEF14* does not directly correspond to the functionality of the mature protein, one may speculate that the down-regulation can either be the result of a fungal virulence strategy or a response by the plant to defend itself against *Bgh* attack.
Knowing that the results from *Hv*GEF14 functional studies classify the protein as a susceptibility factor, the down-regulation of the *HvGEF14* transcript upon *Bgh* inoculation might be the result of an underlying susceptibility mechanism. In that way, the transcript abundance of *HvGEF14* might be directly or indirectly controlled by fungal effectors to support penetration of the plant cell. An example of a similar mechanism was presented by Yuan et al. (2021), who showed that the fungal effector CSEP0027 targets *H. vulgare* catalase 1 that had been implicated in the plant's immunity. Through protein-protein interaction of the *Bgh* effector and the *H. vulgare* immunity regulator, the function of the

host protein is disturbed.
On the other hand, the corresponding gene of the susceptibility factor *Hv*GEF14 might be down-regulated by the plant in order to protect itself against the fungal invader. More specifically, if a possible function of *Hv*GEF14 during plant development is redirected during *Bgh* attack to be important for plant susceptibility, the down-regulation of the gene could be a resistance mechanism.
Though, differential gene expression after *Bgh* inoculation of other susceptibility genes has not been an indicator for protein function in *H. vulgare* in other publications. The transcript of the susceptibility factor *HvBAX inhibitor-1*, for example, is constitutively expressed in the plant but gene expression increases after *Bgh* inoculation (Hückelhoven et al., 2001, 2003). In addition, transcripts of the susceptibility factor *HvRACB* were only slightly regulated upon *Bgh* inoculation and the transcript levels of its downstream executer *Hv*RIPb not at all (Schultheiss et al., 2002; McCollum et al., 2020). So a possible connection between *HvGEF14* down-regulation and protein function can only be speculated.
An other explanation might be that *Bgh* targets *Hv*RACB directly to keep it signalling active which in turn might result in decreased *HvGEF14* expression through a possible, yet unknown negative feedback loop. In addition, GEFs have been shown to be redundant in function (Denninger et al., 2019). Therefore, the down-regulation of a specific *GEF* might be a way to protect the plant from *Bgh* infection while at the same time this does not harm possible GEF function in other signalling pathways.

4.2.1. The exchanger and the switch: *Hv*GEF14 interaction with ROPs

Further investigation of the *Hv*GEF14 protein showed that the GEF interacts with different types of *H. vulgare* ROPs. *Hv*GEF14 might therefore act in different ROP pathways. Both interacting ROPs, *Hv*RAC1 and *Hv*RACB are expressed in the epidermis and function in plant pathogen interaction (Schultheiss et al., 2003; Pathuri et al., 2008).
PRONE GEFs have been shown to stabilise a nucleotide- and cation-free ROP conformation by first facilitating the release of Mg^{2+} from the ROP-GDP-complex. Subsequently, structural changes in the switch regions result in GDP dissociation. Therefore, GEFs are not responsible for strictly GDP to GTP exchange but their binding to ROPs leads to nucleotide dissociation which makes it possible for an other nucleotide to bind. Since the concentration of GTP is high in the cell, the result of GEF-ROP association is usually a GDP to GTP exchange (Thomas et al., 2007). In summary, structural orientation of the switch regions, nucleotide binding as well as Mg^{2+} binding are important prerequisites for GEF-ROP interaction.
The specific interaction with *Hv*RACB and *Hv*RAC1 mutants shows a comparable pattern: *Hv*GEF14 interacts with wild type ROPs, so called constitutively activated but not dominant negative variants. On a first glance, these observations are puzzling because GEFs are known activators of ROPs and should in theory associate with the non-signalling conformation of the GTPase in order to activate it. However, previously published work is partially in accordance with the data presented in this dissertation. *At*GEF14, for exam-

ple, interacts with *At*ROP1 in pull-down assays, independent of its nucleotide loading (Gu et al., 2006). This shows that GEFs have the capacity to interact with different conformations of ROP proteins in these experimental setups. *In vitro* studies of the *At*ROP1-D121 mutant, however, have shown that the amino acid substitution with asparagine decreases nucleotide affinity and increases GEF binding capacity when compared to the wild type (Cool et al., 1999; Berken et al., 2005). Plant GEFs have further been shown to preferably interact with nucleotide-free ROP variants (Berken et al., 2005; Gu et al., 2006). The data presented in this dissertation show a similar effect of the G15V substitution in *Hv*RACB as was obtained with *At*ROP1-D121. This raises the question, if in *H. vulgare*, G15V might not be GTP bound but in a nucleotide free conformation. Until now, there has not been direct evidence that the *Hv*RACB-G15V mutant is bound to GTP. Therefore, the G15V variant might not have the exact same protein fold as the activated wild type ROP and the two might therefore show different binding capacities to GEFs.
Structurally, the used ROP amino acid substitutions are located at different parts of the protein that have been shown to be involved in various functions. While the D121N substitution resides in the nucleotide binding motif and was therefore reported to have increased GEF affinity (Berken et al., 2005), G15V might sustain *Hv*GEF14 interaction due to other reasons. Glycine 15 is part of a *Hv*GEF-oriented loop but this does not alone indicate that the residue is important for the interaction with *Hv*GEF14. The amino acids threonine 20 and aspartic acid 121 are both located in the *Hv*RACB α-helices. While the α-helix containing threonine 20 points towards the *Hv*ROP-*Hv*GEF-interaction interface, aspartic acid 121 is part of a stretch that points away from it (Figure 8). A mutation in a *Hv*GEF-facing α-helix might therefore disturb the interaction capability of the two proteins while the G15V mutation seems not to be as disruptive.

In planta interaction of *Hv*GEF14 and *Hv*RACB was confirmed by two assays: BiFC and FRET-FLIM. Both methods have been widely used to study protein-protein interaction *in planta*. While BiFC offers great visualisation of the localisation of possible protein-protein interactions, it has shown to be unspecific and the assay design requires powerful controls in order to interpret the data correctly (Horstman et al., 2014). FRET-FLIM, on the other hand, has been shown to reliably report protein-protein interactions of molecules in close proximity (Lampugnani et al., 2018).
The results of these *in planta* methods are in accordance with the data obtained in Y2H. In particular, *Hv*GEF14 interaction with *Hv*RACB wild type, as well as with the variants -G15V and -D121N was confirmed *in planta* (Figures 6 and 7).
In contrast to the interaction studies in yeast, both *in planta* interaction assays were recorded at the plant cell periphery. In Y2H, the ROPs had to be C-terminally truncated in order to provide the ability to avoid prenylation and hence to interact in the yeast nucleus. The fact that all three assay types were recorded to have the same result, points to the hypothesis that membrane association is not a basis for the interaction of *Hv*GEF14 with *Hv*RACB.

Based on literature (Thomas et al., 2007; Wu and Lew, 2013; Kawano et al., 2014b) and the computational model of GEF-ROP interaction (Figure 8), one can speculate that the hetero-tetramer composed of a GEF dimer interacting with two ROPs, is probably part of a larger complex that includes other ROP regulatory proteins. In addition, because ROPs shuffle between two signalling states it can be hypothesised that the protein interactions within such a ROP complex are dynamic. Just as *Hv*GEF14, *At*GEF14 has also been shown to interact with a number of *At*ROPs as well. As discussed earlier, Gu et al. (2006) published the interaction of *At*GEF14 with *At*ROP1 D121A/C188S *in vitro* and Lin et al. (2021) with *At*ROP6 wild type *in planta*.
The observation that GEFs can interact with different ROPs leads to a number of hypotheses. In the case of *Hv*GEF14, it might be possible that the exchanger does not specifically but ubiquitously interact with *H. vulgare* ROPs dependent on subcellular localisation of the interactors. Whereas some publications report the interaction of distinct GEFs with a specific ROP (Akamatsu et al., 2013; Tang, 2022), other studies have shown that GEFs can indeed interact with a number of different ROPs to perform specific functions. For example, in *O. sativa* it was shown that *Os*GEF2 interacts with *Os*RAC1-3 and *Os*RAC5-7 to signal during floral organ development (Huang et al., 2018b). Shin et al. (2010) tested the interaction of *At*GEF11 with *At*ROPs in pull-down assays and found that the GEF also interacts with more than one ROP (*At*ROP2, *At*ROP6 and *At*ROP8). For *At*GEF8 it was shown in structural studies to interact with *At*ROPs 4 and 7 (Thomas et al., 2007, 2009). An interesting GEF-pathway including more than one ROP was published by Cao et al. (2017). The authors reported that phosphatidic acid (PA) activates *At*GEF8 which in turn interacts with *At*ROPs 7 and 10. Interestingly, even though *At*GEF8 is able to interact with both *At*ROPs, only *At*ROP7 was activated by PA signalling via *At*GEF8. These results pose the question whether the interaction with *At*ROP10 was unspecific or if the interaction of *At*GEF8 and *At*ROP10 is involved in a different signalling pathway.

One interpretation of the data presented in this dissertation would therefore be that *Hv*GEF14 functions in different pathways depending on upstream signals. A similar idea was put forward for the *O. sativa* small GTPase *Os*RAC1, which functions in ETI and PTI (Akamatsu et al., 2021). The GTPase can be targeted by both, *Os*GEF1 and *Os*GEF2 (Akamatsu et al., 2013, 2015). An other example for this phenomenon are the pollen expressed *Os*GEFs 2, 3, 6 and 8 that can all activate *Os*RACB *in vitro*. However, when analysed further, *Os*GEF3 had the strongest effect on the ROP activity in *in vitro* activity assays (Xu et al., 2021). This shows that it is important to consider not only the capability of a GEF to interact with a ROP but also their joined function.
It has to be shown whether *Hv*GEF14 is in complex with different ROPs at the same time. Earlier research on the GEF-ROP complex showed a crystal structure of two ROPs with two GEFs in a heterotetramer. However, in these *in vitro* assays, only *At*GEF8 and

either *At*ROP4 or *At*ROP7 were used (Thomas et al., 2007, 2009). It would be interesting to see a possible protein complex in living plant cells, however, there is no report on the interaction of one GEF interacting simultaneously with several ROPs. The same is true for polar domains at membranes. It is hypothesized that different ROPs may cluster together in active signalling hubs at the membrane (Smokvarska et al., 2021).

Regarding GEF dimerisation, the data in this dissertation also show that *Hv*GEF14 can interact with itself (Figures 8 and Figure 12A-B). The ability to homo-dimerise has been reported to be important for GEF function before. For example, it has been proven for mammalian DH-PH GEFs that their oligomerisation is a vital step to facilitate the activating function of these GEFs (Zhu et al., 2001). Also in the case of plant GEFs, it was reported that a mutant of *At*GEF1 which is unable to dimerise was also not able to interact with the upstream interactor *At*AGC1.5, thus stopping the signal cascade during pollen tube growth (Li et al., 2018a). In addition, for *O. sativa*, it was reported that *Os*GEF1 and *Os*GEF2 can homo- and hetero-dimerise in order to fulfil their function in plant immunity (Akamatsu et al., 2015). Thus giving rise to the idea that the homo-dimerisation of *Hv*GEF14 could also be important as a regulatory mechanism. In addition, it is possible to speculate that *Hv*GEF14 might be able to hetero-dimerise with other *Hv*GEFs.
In a similar manner, the dimerisation of ROP downstream elements, for example GAPs and RICs, has been shown to be required for their function (Schaefer et al., 2011). Data provided in this dissertation show that certain *Hv*RICs can dimerise with each other and themselves (Figures 12C-D and Figure 13). Just as with ROP-upstream interactors, these results provide a hint towards a possible regulatory mechanism based on the oligomerisation of ROP interactors. It seems hence worth testing in future whether *Hv*GEFs may also interact with *Hv*RICs or other *Hv*ROP interactors to elucidate possible functions of protein oligomerisation in ROP signalling.

4.2.2. *Hv*GEF14 can lead the way: A new susceptibility factor for *Bgh*

Susceptibility factors are host proteins that support pathogen success (Hückelhoven, 2005). In *H. vulgare*, a number of proteins have been found to fulfil this function, one of the most prominent being *Hv*RACB (Schultheiss et al., 2002). Patho-assays in which candidate proteins are either down-regulated or over-expressed can be used to identify host proteins as susceptibility factors. There are different ways of host plant transformation: in model organisms such as *A. thaliana*, test plants often stably carry the genetic modification, whereas transient transformation of single cells can be used to circumvent possible pleiotropic effects of full knock-out mutants.

Due to the fact that the initial interaction of *H. vulgare* and *Bgh* occurs with epidermal cells of the plant, single *H. vulgare* epidermis cells were transiently transformed for this study. *H. vulgare* susceptibility towards *Bgh* has successfully been scored previously

by analysis of plant cell penetration normalised to all observed interactions (Schweizer et al., 1999; Hückelhoven et al., 2003). Figure 9 shows that *Hv*GEF14 over-expression and knock-down induce the same response to *Bgh* as activated and inactivated *Hv*RACB does, respectively. *Hv*GEF14 increases susceptibility of *H. vulgare* when over-expressed and resistance when knocked down (Figure 9). The statistical analysis verifies that especially the results for over-expression are significantly different from the controls. However, the resulting p-value of the *HvGEF14* knock-down does not match the commonly accepted criteria for significance. This might be due to the fact that knock-down via RNAi does not eliminate all transcribed mRNAs and therefore residual concentration of the targeted protein will still be present in the transformed cells. For *Hv*GEF14, it was shown in this study that the hairpin construct used for down regulation only reduces the fluorescence of GFP-*Hv*GEF14 by 53% (Table S15). Even though, the statistical analysis does not account for the observed natural variation amongst individual experiments which results in higher variability of data collected in the different experiments. However, a reduction in penetration efficiency was still observed in all repeats. Considering these points, the data support that the knock-down of *HvGEF14* indeed induces resistance in single *H. vulgare* epidermal cells. Since interaction of *Hv*GEF14 and *Hv*RACB had been observed *in planta*, it can be assumed that the over-expression of the nucleotide exchange factor *Hv*GEF14 leads to activation of *Hv*RACB which further supports fungal penetration. In the case of other PRONE-GEFs it had previously been reported that phosphorylation by RLKs is required for GEF activation (Kaothien et al., 2005; Gu et al., 2006; Zhang and McCormick, 2007). However, for *Hv*GEF14, no such phosphorylation site was found so far. It can therefore be speculated that *Hv*GEF14 might be auto-active as a nucleotide exchanger. An other possible explanation is that endogenous *Hv*GEF14 activators also perform their function when the GEF is over-expressed in epidermis cells. An other possible role of *Hv*GEF14 in the susceptibility pathway might be the direct or indirect targeting by fungal effectors. Even though no effector has been found to target *Hv*GEF14 so far, there might be an analogous mechanism as has been observed in other plant species. In *O. sativa* for example, the immunity-supportive DH-PH GEF, *Os*SWAP70, was shown to be indirectly targeted by a pathogenic effector in order to decrease the plant's defenses. The effector enhances interaction between the GEF and a negative regulator of immunity in order to diverge the GEF from the immunity pathway (He et al., 2018). In a similar way, a *Bgh* effector could facilitate the interaction of *Hv*GEF14 and *Hv*RACB in order to turn on the susceptibility pathway in *Bgh* attacked *H. vulgare* cells.

Published downstream interactors of *Hv*RACB show a similar capacity to enhance fungal penetration success when over-expressed *in planta*. This observed phenotype has been used to propose proteins as susceptibility factors in the *Hv*RACB-dependent pathway (Schultheiss et al., 2008; Engelhardt et al., 2021; McCollum et al., 2020).

Thus, *Hv*GEF14 can also be seen as susceptibility factor in the interaction of *H. vulgare* with the powdery mildew fungus *Bgh*. This is the first report of a *Hv*GEF as possible regulatory protein in *H. vulgare* immunity. However, the biological function in susceptibility and interaction capacity with *Hv*RACB alone are not enough to confidently establish

*Hv*GEF14 as an activator of *Hv*RACB.

4.2.3. Signal on: *Hv*GEF14 activates *Hv*ROPs *in planta*

To characterise and establish the function of PRONE-GEFs as ROP activators, two methods were established in this dissertation for use *in planta*. Since the biological function of *Hv*RACB in *H. vulgare* susceptibility had been established before, this ROP was used to further study *Hv*GEF14 activating capacity. As introduced earlier, *in vivo* ROP activity has been measured either via subcellular RIC localisation or direct interaction with RICs as proxy for ROP activity.

Indeed, using mCherry-*Hv*RIC171 localisation, the data shows that *Hv*GEF14 activates *Hv*ROPs. Figure 10 shows mCherry-*Hv*RIC171 localisation at the cell periphery as an indicator of activated *Hv*ROPs in those cells, as previously shown by Schultheiss et al. (2008). mCherry-*Hv*RIC171 cell periphery localisation was observed either when simultaneously over-expressing CA-*Hv*RACB or *Hv*GEF14. This is evidence for a similar underlying mechanism in both experimental designs. Localised activation of *At*ROPs has been visualised that way by others before. For example, by monitoring the localisation of GFP-*At*RIC4 at the apical cap of pollen tubes to indicate domains of activated ROPs (Hwang et al., 2005). In plants, the activity of ROPs has also been shown to be closely related to their plasma membrane association (Smokvarska et al., 2021). Though, observing interactors of activated ROPs instead of ROP localisation itself, is not a direct observation of activity. However, it offers the possibility to indirectly observe ROP activation without having to manipulate the molecular switch directly.
In addition to the visual data, a quantification was performed in this dissertation by taking the ratio of mCherry-*Hv*RIC171 fluorescence at the cell periphery in relation to the fluorescence signal of the whole cell. Including stringent normalisation to the fluorescence of the cytosolic marker GFP, it was possible to compare all cells imaged. Even though normalisation of specialised fluorescence to a cytosolic marker is common (for example in Schultheiss et al. (2008); Reiner et al. (2016)), this is the first publication that quantifies fluorescence intensity of a ROP-GTP interactor at the cell periphery. With this new method, it is possible to obtain not only visual data on ROP-GTP interactors but also perform statistical analyses on the data generated.
Since it has been shown that mCherry-*Hv*RIC171 interacts with activated *Hv*RACB at the plasma membrane and CA *Hv*RACB recruits *Hv*RIC171 to the cell periphery, it is assumed that this localisation reports *Hv*RACB activation (Schultheiss et al., 2008). As mCherry-*Hv*RIC171 also localises to the cell periphery during over-expression of *Hv*GEF14, it can be hypothesised in turn that the GEF activates the susceptibility factor *Hv*RACB. Though, the localisation of mCherry-*Hv*RIC171 can also indirectly be influenced by other unknown factors and it does not give direct evidence for the activation of *Hv*RACB by *Hv*GEF14. Another possible explanation for the observed mCherry- *Hv*RIC171 localisation could be a direct interaction and recruitment of *Hv*RIC171 by *Hv*GEF14. If the two proteins in-

teract and are both expressed in excess in the epidermal cell, the same phenotype might be observed if *Hv*GEF14 is localised to the plasma membrane without the interaction with activated *Hv*ROPs. However, this scenario is unlikely due to the fact that *Hv*GEF14 interacts strongly with activated *Hv*RACB and over-expression of fluorescently tagged *Hv*GEF14 in *H. vulgare* cells alone, showed the protein's localisation in the cytosol (Figure S19). Therefore, mCherry-*Hv*RIC171 localisation and its quantification are valuable tools to monitor *Hv*ROP activation in *H. vulgare* epidermis cells.

As a second method, a FRET-based activity sensor measured interaction of wild type, switchable *Hv*RACB with *Hv*CRIB46, the *Hv*RACB-GTP-interacting fraction of *Hv*RIC171 (Schultheiss et al., 2008). This approach of observing ROP-GTP executers in order to determine ROP activity status, was recently published in the model plant *A. thaliana*. Via the pull-down of GST-*At*RIC1, the activity of *At*ROP6-FLAG was estimated in transgenic plants. This method is also very good to observe overall GEF activity *in planta* (Gao et al., 2021a). Though, so far the ROP activity status had not been shown in intact plant epidermal cells.

FRET-based Raichu sensors have increased our understanding of specific *in planta* activation of ROPs (Kawano et al., 2010; Platre et al., 2019). However, plant Raichu probes established in *O. sativa* have consisted of a single plasmid containing both fluorophores together with the respective ROP and a binding domain obtained from *H. sapiens* PAK1. This setup may lead to several problems. First, the Raichu probe resides on one plasmid which gives room for unspecific signals resulting from close proximity of the FRET pair. Secondly, introducing a non-native ROP binding partner may lead to inconclusive interpretation of the data obtained. Another criticism of the previous studies might be the expression in *O. sativa* protoplasts and not in intact plant cells. Even though it is an easier system to transform and image, proteins might interact differently than in their normal cellular environment. Especially because epidermis expressed proteins were observed in this dissertation, protoplasts extracted from mesophyll cells were not the right cellular environment.

To my knowledge, there have only been two previous publications that showed the activation of ROPs by GEFs *in planta* via the Raichu sensor. Akamatsu et al. (2013) and Wang et al. (2018) made use of the already published FRET-probe consisting of CFP-*Os*RAC1 and *Hs*CRIB-Venus in protoplasts. The ratio of Venus/CFP increased during co-expression of the *O. sativa* GEFs *Os*GEF1 (Akamatsu et al., 2013) or *Os*SPK1 (Wang et al., 2018), leading to the conclusion that each GEF can activate *Os*RAC1.

For this study, a ROP activity sensor was therefore further developed supported by Michaela Kopischke (Hückelhoven laboratory) to specifically show *Hv*RACB activity *in planta*. Benefits of the here published FRET-sensor include the use of a *Hv*RACB-specific CRIB domain that has been shown to interact with constitutively activated *Hv*RACB-G15V by FRET-FLIM (unpublished data by Michaela Kopischke). However, in *H. vulgare* bombarded cells also wild type *Hv*RACB interacted with *Hv*CRIB46 without addition of

any stimulus, possibly indicating high endogenous GEF activity in those *H. vulgare* epidermal cells. This issue was solved by the use of *N. benthamiana* as expression system, possibly due to exclusion of endogenous *Hv*RACB activation that otherwise would have provoked constitutive interaction of *Hv*CRIB46 and wild type *Hv*RACB. In addition, *Hv*RACB, *Hv*CRIB46 and *Hv*GEF14 as well as the controls were over-expressed on individual vectors. Another way to improve the sensor was to change FRET compatible fluorophores from the earlier used CFP/YFP to the more efficient pair GFP/mCherry (Denay et al., 2019).

In order to validate the results obtained in FRET-FLIM in presence of *Hv*GEF14, it was important to over-express *Hv*GEF14 tagged with a non-fluorescent label to not interfere with the FRET-FLIM measurements. This setup, however, only allowed confirmation of general 3HA-*Hv*GEF14 expression from transfected *N. benthamiana* leaf discs by Western Blotting and not the expression in individual cells measured in FRET-FLIM. Though, since the co-expression efficiency of fluorescently labelled proteins was very high and the FRET-FLIM measurements were performed in biological repeats with many measured individual cells, there is a high probability that the observed *N. benthamiana* cells did indeed express all proteins intended. The observed enhanced interaction of *Hv*CRIB46 and switchable wild type *Hv*RACB upon co-expression of *Hv*GEF14 strongly suggests, that *Hv*GEF14 can facilitate *Hv*RACB activation *in planta* (Figure 11).
Previously, the activity of *A. thaliana* and *O. sativa* GEFs has been reported to be regulated by RLKs through phosphorylation at the GEF C-terminus (Kaothien et al., 2005; Gu et al., 2006; Zhang and McCormick, 2007). *Hv*GEF14, however seems to be active without any induced post translational modification. Most of the activity and susceptibility assays in this dissertation have been performed in *H. vulgare* epidermis cells and with wild type *Hv*GEF14, where possible endogenous activators were also present. However, in the heterologous system, *N. benthamiana*, *Hv*GEF14 was also able to activate *Hv*RACB. Following the same logic, that *Hv*GEF14 has to be activated in order to associate with *Hv*RACB, endogenous *N. benthamiana* activators must have also been present. However, so far, no post-translational modifications of *Nb*GEFs are known. In addition, without known *Nb*GEF modulators, it was not possible to determine whether the introduced *H. vulgare* GEF might have been modified. On the other hand, even if *Nb*GEFs are post-translationally modified, the *Nb* molecular machinery might not function with *Hv*GEFs. Therefore, it can be hypothesized that wild type *Hv*GEF14 can interact with and activate *Hv*RACB without the need for prior activation via RLKs. However, these results are still in accordance with previously published activity assays of PRONE GEFs. For example, Wang et al. (2017) proved that both, the wild type and the isolated PRONE domain of *At*GEF2 activate *At*ROPs in signalling processes related to light sensing and gas exchange. Even though the PRONE domain itself was more effective in activating the ROPs, the full length protein could perform the same function. Unfortunately, in the case of *Hv*GEF14, the isolated PRONE domain was unstable after transformation and could not be tested *in planta*. Therefore the activity assays could only be performed with full

length *Hv*GEF14.
Next to using the isolated PRONE domain in these assays, an other approach to create auto-active *Hv*GEF14 was to look for potential phosphorylation sites that could be manipulated. In *A. thaliana* and *O. sativa* PRONE-GEF activity was shown to require phosphorylation of conserved serines located in the variable C-terminus (Berken et al., 2005; Zhang and McCormick, 2007; Akamatsu et al., 2013). Since especially in *Hv*GEF14 the primary sequence differs from other *H. vulgare* GEFs, no conserved possible phosphorylation sites could be determined. Even when comparing the primary sequence of *Hv*GEF14 to the well studied *Os*GEF1, that was shown to be regulated by C-terminal phosphorylation (Akamatsu et al., 2013), no predictions on possible phosphorylation sites could be made (Figure S20).

Taken together, based on the data published in this dissertation, *Hv*GEF14 is an activator of *Hv*RACB. However, the action by *Hv*GEF14, or GEFs in general might not be the only *Hv*RACB activating mechanism.
Host susceptibility proteins are potential targets of fungal effectors. The *Bgh* effector CSEP0027 for example, interacts with the *H. vulgare* catalase *Hv*CAT1 which increases fungal virulence when knocked down (Yuan et al., 2021). In addition, the susceptibility factor *Hv*RACB itself was observed to be manipulated by the *Bgh* effector ROPIP1 (Nottensteiner et al., 2018).
Although, the activation of ROPs by PRONE-GEFs has been documented extensively and is therefore an important molecular pathway to be considered in *H. vulgare* susceptibility. One interesting observation is the fact that ROP signalling cascades often involve a large number of regulatory proteins, creating the hypothesis that the signalling mechanisms are complex. Therefore it is perceivable that *Hv*RACB-mediated susceptibility towards *Bgh* might also not be only facilitated by *Hv*GEF14 but other, yet unknown *Hv*GEFs. Other studies have highlighted that a number of different GEFs can fulfil the same function on the same ROP. For example, in *O. sativa*, the ROP *Os*RACB has been shown to be activated by several *Os*GEFs (Xu et al., 2021)). In *H. vulgare* leaves, one if the other activator candidates for *Hv*RACB is *Hv*GEF1.
Even though in this dissertation the expression of *HvGEF1* was not measured, the data provided by the JHI (Table 11) indicate comparably high transcript levels of this gene in various tissues, including epidermal peels. Other candidate GEFs to play a role in *Bgh* susceptibility are the epidermis expressed *HvGEF7a*, *HvGEF9b* and *HvGEF9c*. However, the recorded fragment counts for these three *Hv*GEFs are rather low when compared to *HvGEF14* and *HvGEF1*. On the expression data it is possible to speculate, however, that there might be crosstalk amongst several *Hv*GEFs in epidermal cells. *Hv*GEF14 might interact with other *Hv*GEFs like it was reported for *Os*GEF1 and *Os*GEF2 (Akamatsu et al., 2015). This interaction could have positive or negative regulatory effects. In earlier publications, GEF-ROP interaction partners were often assumed to be specific for single signalling pathways (Zhang and McCormick, 2007; Yoo et al., 2011) but the fact that

interaction studies showed association of several GEFs with the same ROP paved the way for more in depth studies on GEF -ROP signalling specificity (for example in Denninger et al. (2019); Li et al. (2020)).
It is imagined that ROPs are master regulators for various signal cascades while different activating GEFs form the basis for regulation of these cascades. The same might be true for ROP downstream executers which have been shown to perform different functions while interacting with the same ROP (Wu et al., 2001; Gu et al., 2004).

4.2.4. Two sides of the same coin? ROP signalling in different plant-microbe interactions

Cellular rearrangements during the colonisation of plants by biotrophic pathogens is reminiscent of their invasion by beneficial fungi, such as mycorrhiza. Especially when comparing the accommodation of fungal haustoria on the one hand and arbuscular mycorrhiza on the other, the similarity in structure becomes apparent. Indeed, on a molecular level, the two processes share common signalling components.
One example is the already introduced chitin receptor *Os*CERK1 that functions in both, plant defense and arbuscular mycorrhiza symbiosis (Akamatsu et al., 2016). The fact that the same receptor can function in perception of pathogens and symbionts might also be a possible explantation why the colonisation of beneficial microbes protects plants from harmful invaders due to competition for the same receptor. This might be one of the mechanism underlying the protective function of the mycorrhiza *Piriformospora indica* from *H. vulgare* colonisation with pathogenic microbes (Deshmukh et al., 2006). However, it does not mechanistically explain how *P. indica* induces systemic resistance to *Bgh*.

In both species, *H. vulgare* and *O. sativa*, it was shown that the interaction with pathogens and the subsequent response by the plant requires ROP signalling (Engelhardt et al., 2020; Akamatsu et al., 2021). However, the role of ROPs in plant-symbiont relationships has been documented mainly in legumes (see section 1.3.3). Consequently, PRONE-GEFs might be important signalling components as ROP-activators. Recently, the first reports on the role of PRONE-GEFs in symbiosis between rhizobia and the legumes *G. max* and *M. truncatula* have been published. Both studies show that Nod-factor sensing receptors phosphorylate PRONE-GEFs which in turn activate type II ROPs which are positive regulators of nodule symbiosis (Gao et al., 2021b; Wang et al., 2021). This is reminiscent of the function of PRONE-GEFs in *O. sativa* in response to pathogenic fungi (Akamatsu et al., 2015). These results also open up the hypothesis that *Hv*GEFs might play a role in the symbiosis of *H. vulgare* with beneficial microbes. Based on the expression data summarised in Table 11, *HvGEF1*, *HvGEF7a* and *HvGEF14* are potential candidates to activate ROP signalling in *H. vulgare* roots upon Myc-factor perception. However, in other plant species, no homologue of these *Hv*GEFs have yet been published to function in plant-microbe symbiosis until now.

Interestingly, known common symbiosis genes were also found to act like susceptibility factors in *A. thaliana* (Ried et al., 2019), linking the underlying molecular machinery of symbiosis and immunity. As discussed, in *H. vulgare*, ROPs have been mainly studied for their role in susceptibility. Considering this data on susceptibility factors in *A. thaliana*, it is interesting to note that the susceptibility factor BAX inhibitor-1 is important in the colonisation of the beneficial fungus *P. indica* in *H. vlugare* roots (Deshmukh et al., 2006).
In addition, *H. vulgare* ROP signalling also plays a role in root growth and symbiosis. Indeed, it was shown that root hair development relies on ROP function because *Hv*RACB RNAi transgenic plants were observed to be defect in root hair outgrowth (Scheler et al., 2016). In other species, root hair development has been linked to be central for root nodule symbiosis and also relies on GEF-mediated activation of ROPs (Denninger et al., 2019). *H. vulgare* has been shown to interact with beneficial root bacteria (Lupwayi et al., 2004). In the interaction with the rhizobium R*r*F4, it was recently discovered that a known regulator of *H. vulgare* immunity also acts in the establishment of these beneficial bacteria (Kumar et al., 2021), linking plant defense and symbiosis on a molecular level. If ROP-signalling is indeed required for *H. vulgare* root symbiosis with beneficial microbes, their corresponding GEFs might also link cell surface perception of microbial factors to downstream ROP-signalling.

Taken together, although there has not been direct evidence that GEF-mediated ROP signalling underlies the interaction of *H. vulgare* with beneficial bacteria or fungi, it is an interesting field to study based on the results obtained in other closely related plant species, such as *O. sativa*. ROP signalling might therefore be a common link between polar growth processes that are required in the plant's interaction with all kinds of microbes.

4.3. Concluding Remarks

It is clear that we only know a fraction of how ROP signalling in *H. vulgare* is regulated and how different regulatory proteins work together to fulfil the functions that are visible to us. This dissertation provides first evidence for a ROP-regulatory role of the PRONE-GEF *Hv*GEF14 and its involvement in *H. vulgare* susceptibility towards *Bgh*.

Even though, *Hv*RACB function has mostly been studied in its role as a susceptibility factor, the GTPase is also important in cytoskeleton organisation. These two functions of *Hv*RACB are hypothesised to work in an integrated manner such that the ROP's action on the cytoskeleton is a prerequisite for its susceptibility function (Engelhardt et al., 2020). This dissertation contributes a molecular and cell biological insight into *Hv*GEF14 as a *Hv*RACB regulator. Based on the knowledge provided, further research might show that *Hv*RACB and its activator *Hv*GEF14 also play a role in other molecular pathways related

to plant development.

The described *Hv*GEF14-induced activation mechanism of *Hv*RACB helps to further elucidate molecular mechanisms of *Hv*RACB susceptibility. However, most immunity pathways rely on the transduction of signals following external stimuli. Literature reports many examples of the role of RLKs in ROP-dependent signalling pathways. The cell wall sensing *At*FER and the chitin co-receptor *Os*CERK1 are just two prominent examples (Lin et al., 2021; Akamatsu et al., 2021). Future studies may investigate *H. vulgare* susceptibility-related RLKs (Schnepf et al., 2018; Douchkov et al., 2014) for their interaction with *Hv*GEF14 and functionality in *H. vulgare* susceptibility. *Hv*GEF14 therefore is a candidate to link signal perception at the cell surface with intercellular ROP-signalling. Since RLKs have been shown to play an important role in signal perception during PTI in *O. sativa* (Akamatsu et al., 2021), it will be further interesting to test the involvement of *Hv*GEF14 in PAMP triggered immunity pathways in *H. vulgare*. In the case of fungal pathogens, the cell wall component chitin is a standard pathogenic pattern used to unravel PTI responses in plants. Therefore, transcriptional analysis of *HvGEF14* after chitin treatment might shed light on the exchanger's role in pattern triggered immunity.

Finally, the observation that *Hv*GEF14 influences *H. vulgare* susceptibility could make it a target for plant breeding. Although the stable knock-down of *HvRACB* makes *H. vulgare* more resistant to *Bgh*, it might also make the crop less viable due to a loss of root hair development (Scheler et al., 2016). While *HvRACB* knock-down leads to pleiotropic effects in polar growth processes it is yet to be investigated if this also holds true for stable transgenic knock-down or knock-out of *HvGEF14*. Root hairs provide important surfaces for plants to obtain nutrients and interact with beneficial soil microbes (Grierson et al., 2014). The function of *At*GEFs in root hair development has been elucidated recently by Denninger et al. (2019). Their study shows that *At*GEF3 is important as an initiator for root hair emergence, a function that can also be performed by *At*GEF14. If this redundancy in function is also present in *H. vulgare*, manipulating *Hv*GEF14 might provide plants with increased immunity without disturbing proper development of organs or cells, such as root hairs. If only the function of *Hv*GEF14 in *H. vulgare* susceptibility can be targeted, and other *Hv*GEFs would still be able to fulfil their function in plant development, this strategy offers new possibilities for increased plant health. It can therefore be speculated that a stable knock-down of *HvGEF14* has a protective effect towards *Bgh* but not a strong root hair phenotype. This makes it an interesting target as an alternative in *Bgh*-resistance breeding or biotechnology of *H. vulgare*.

5. Appendix

5.1. Supplementary Figures

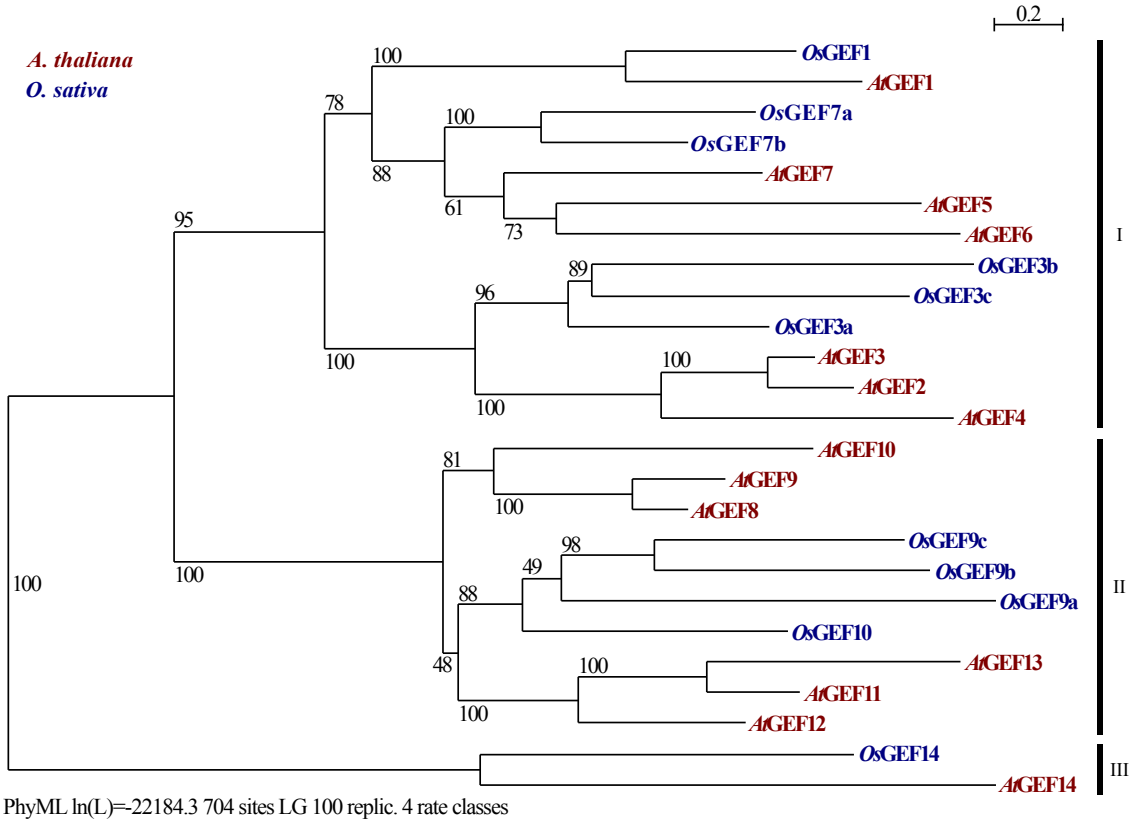

Figure S14: *O. sativa* (*Os*) PRONE-GEF annotation based on *A. thaliana* (*At*) PRONE-GEFs published in Berken et al. (2005). Phylogenetic tree was calculated based on MUSCLE alignment and via maximum likelihood analysis with 100 replicates performed in Seaview. Bootstrap values indicated on branchin points. Species specific colouring was added in InkScape.

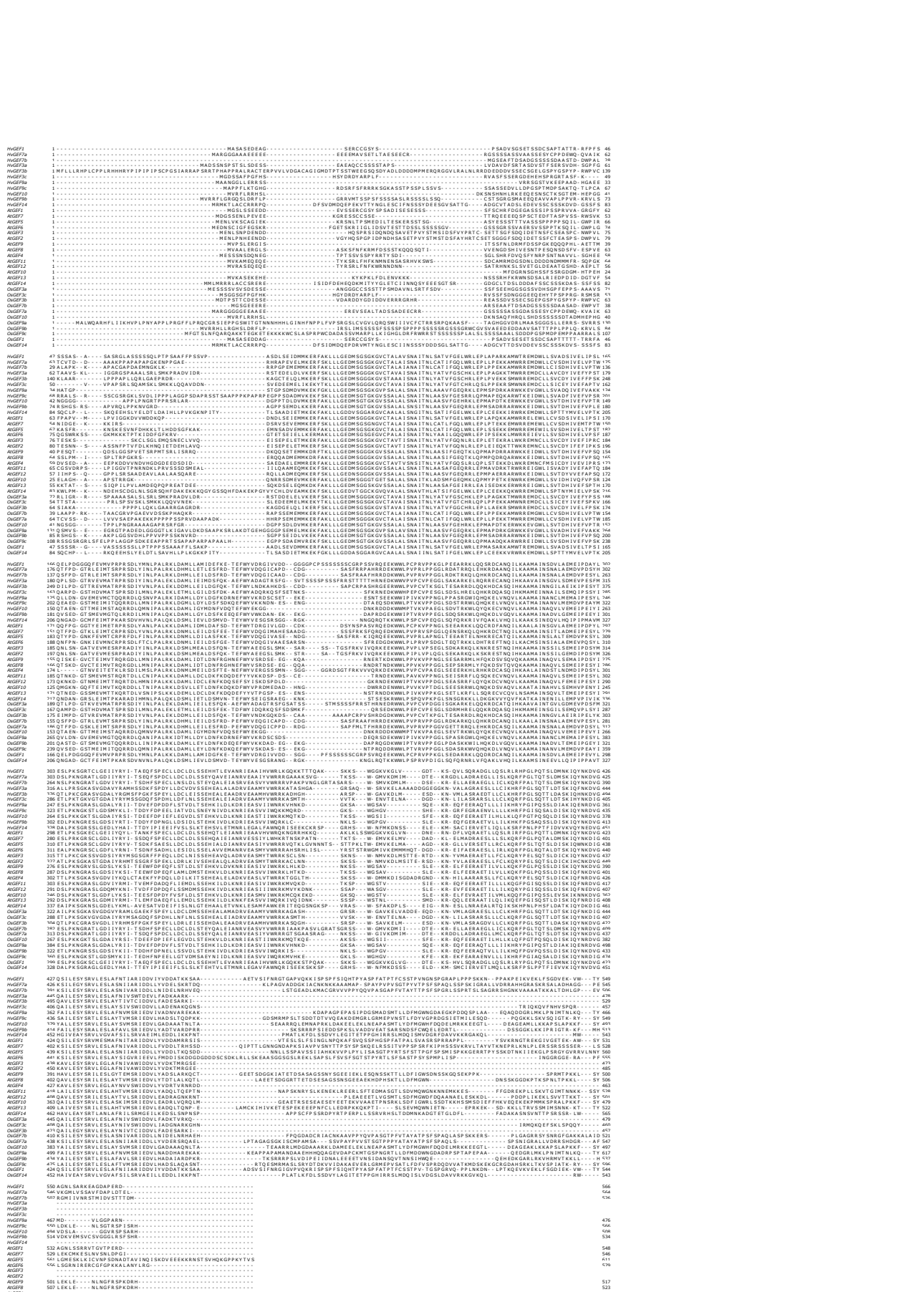

Figure S15: MUSCLE alignment of ***A. thaliana*** (***At***), ***O. sativa*** (***Os***) and ***H. vulgare*** (***Hv***) **GEF primary sequences was used as basis for phylogenetic analysis in Figure 3.** The alignment was performed in Jalview.

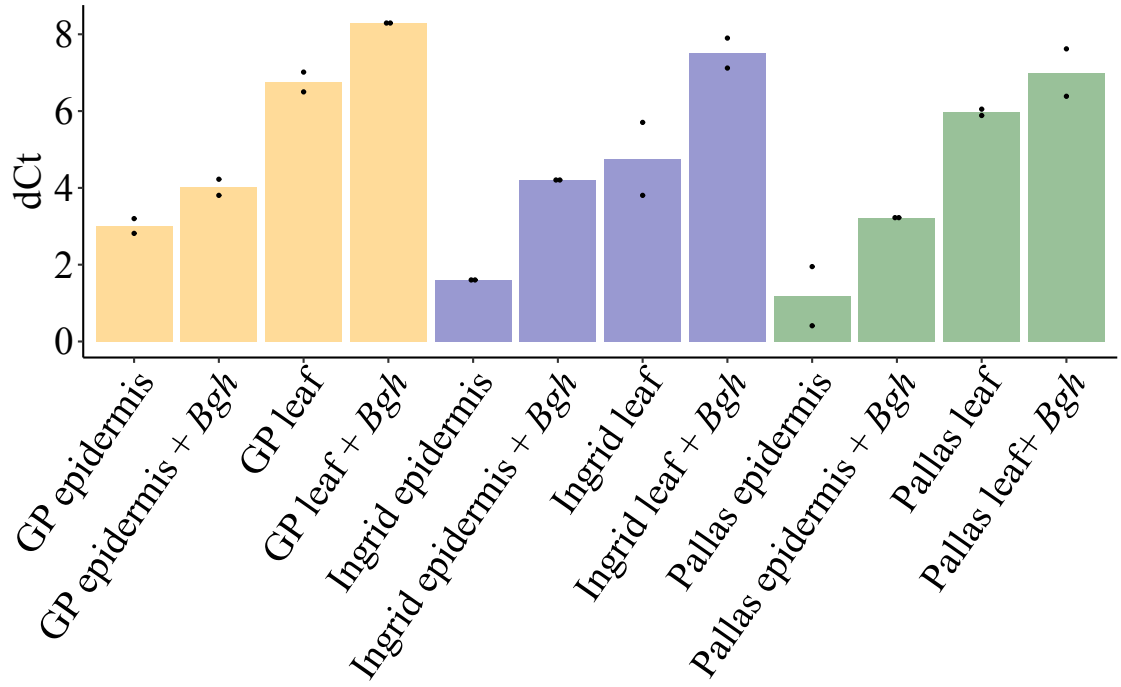

Figure S16: Threshold cycles of *HvGEF14* transcript after normalisation to the housekeeping gene *HvGAPDH* (dCt) show the same pattern in all three cultivars: Golden Promise (GP), Ingrid and Pallas. The summary of two independent biological replicates shows highest expression in epidermal peels and reduced *HvGEF14* expression after *Bgh* inoculation in every cultivar.

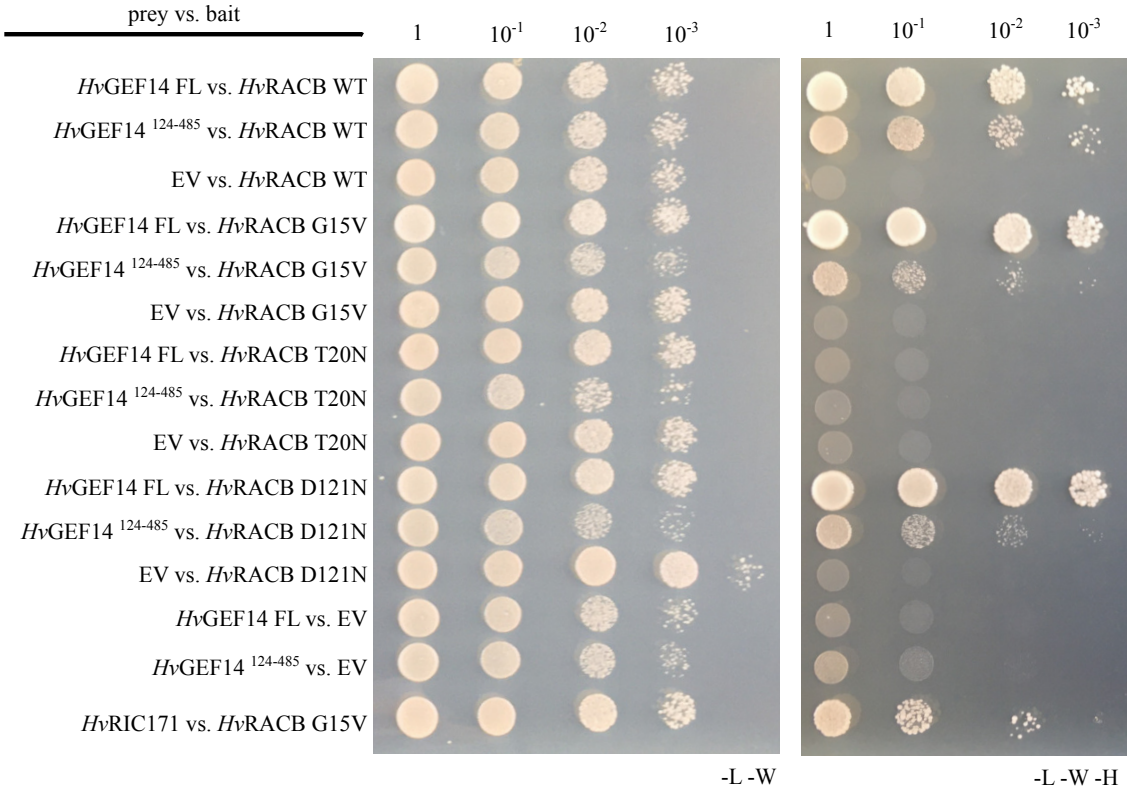

Figure S17: Original image Y2H *Hv*GEF14 vs. *Hv*RACB. Same data as in Figure 6A but uncropped. All dilution steps shown from undiluted (1) to most diluted (10^{-3}).

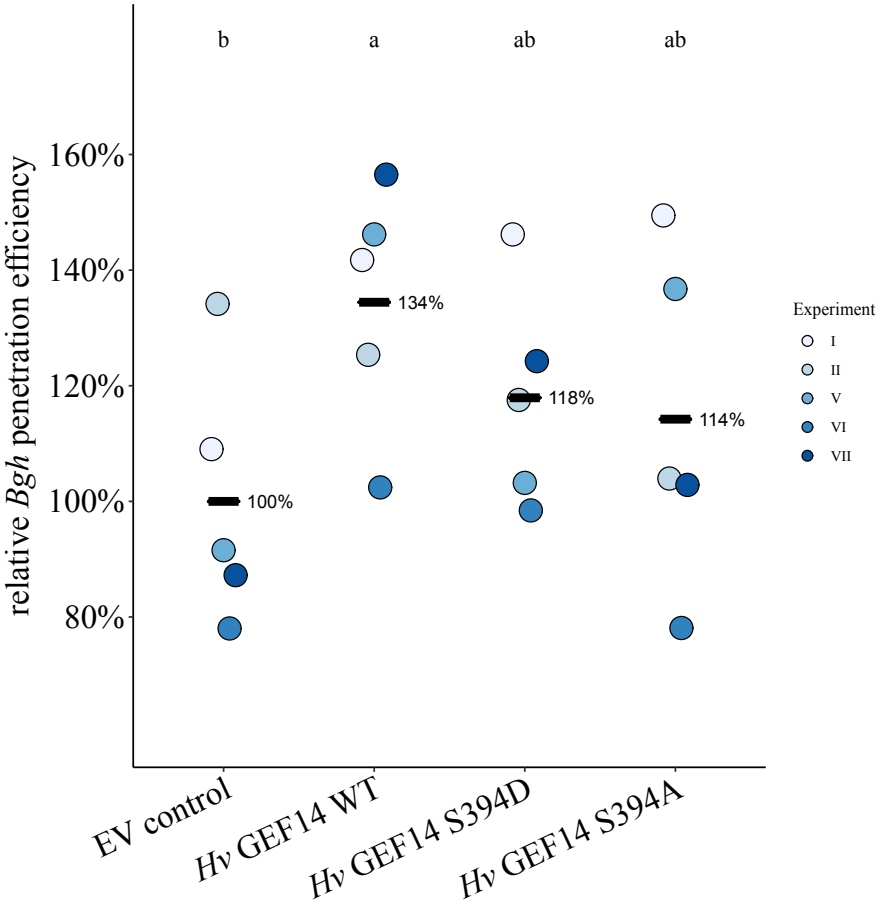

Figure S18: *Hv*GEF14 phospho-mimic (S394D) and phospho-ablation (S394A) variants do not significantly change susceptibility towards *Bgh*. Relative *Bgh* penetration efficiency of five independent biological replications compared to empty vector (EV) control. Experiments colour coded in shades of blue. Only valid experiments shown with at least 50 interactions each. Statistical analysis performed in Rstudio: Kruskal Walis test.

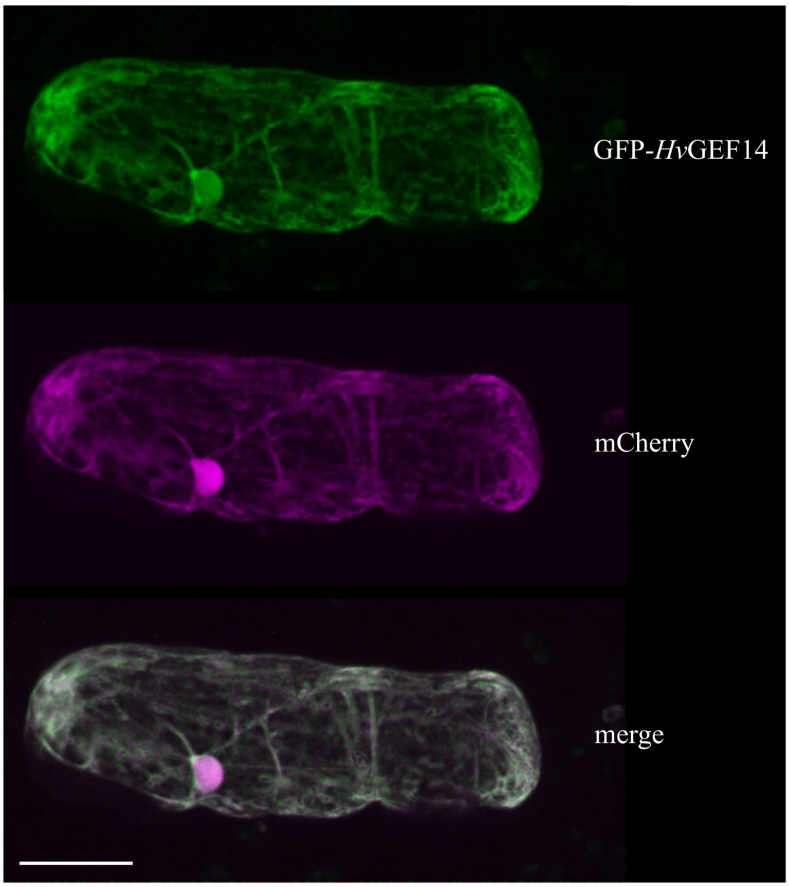

Figure S19: GFP-*Hv*GEF14 shows cytoplasmic localisation. Transient transformation of *H. vulgare* epidermal cell with GFP-*Hv*GEF14 and mCherry as cytosolic marker. Image taken as z-stack with 1.5 μm increments. Scale bar 50 μm.

```
                                10        20        30        40        50        60        70        80
HvGEF14      1 MRMKTLACCRRRPQDFSVDMDQEPEKVTTYNGLESCIFNSSSYDEESGVSATTGADGCVTADSLEDEVSSCSSSSKDVDGSSFSSQCL  87
OsGEF1       1 -------MASASEDD-----------------AGSERC---CGSYSPSADVSESETSSDCSAPTTTTTTRRFASSSSRGVASSSSSSLL  62

                    90        100       110       120       130       140       150       160       170
HvGEF14     88 PLSKQEEHSLYELDTLDAIHLLPVKGKNPITYTLSAADIETMKEKFAKLLLGDDVSGGARGVCAALALSNGITNLSATIFGELWKLE 174
OsGEF1      63 PTPPPSSAAAFFLSAKPAADL-----------------SEVDMMKERFAKLLLGEDMSGSGKGVCTALAISNAITNLSATVFGELWRLE 134

                          180       190       200       210       220       230       240       250       260
HvGEF14     175 PLCEEKKIRWRKEMDWLLSPTTYMVELVPTKQNGAD-GCMFEIMTPKARSDVHVNLPALQKLDSMLIEVLDSMVDTEYWYVESG---  257
OsGEF1      135 PMASARKAMWTREMDWLLSVADSIVELTPSIQELPDGGGQFEVMVPRPRSDLYMNLPALKKLDAMLLAMIDGFKETEFWYVDRGIVV  221

                               270       280       290       300       310       320       330       340
HvGEF14     258 SRSGGRGKNNGQ-------RQTKKWWLPSPCVPEQGLSQFQRKRIVFQAKLVHQILKAAKSINEQVLHQIPIPMAVMDALPKSGRSS  337
OsGEF1      222 DDSGGPFSSSSSSCGRPSVRQEEKWWLPCPRVPPKGLSEDARRKLQQDRDCANQILKAAMAINSDVLAEMEIPEVYLESLPKSGKSC  308

                    350       360       370       380       390       400       410       420       430
HvGEF14     338 LGEDLYHAITTDYIPIEEIFVSLSLKTEHSVLETMNRLEGALFAWNQRISEEKCKRSPGRHSW-NFMKDNSSELEKMSACIERVETL  423
OsGEF1      309 LGEIIYRYITAEQFSPECLLDCLDLSSEHHTLEVANRIEAAIHVWRLKGQKKSTPQAKSKKSWGGKVKGLVGDTEKSHVLSQRADGL  395

                          440       450       460       470       480       490       500       510       520
HvGEF14     424 IQLLKSRFPNLPPTFIDVVKVQYNEDVGHGIVEAYSRVLVGVAFSILSRVAEIMLEDDLIKKPNTPMATLKFDLSSDVYLE------  504
OsGEF1      396 LQSLRLRYPGLPQTSLDMNKIQYNKDVGQSILESYSRVLESLAFNIIARIDDVIYVDDATKKSAAADSVSIFNRGIGVPVQKRISPS  482

                               530       540       550       560       570       580       590       600
HvGEF14     505 --GITETP-------------------PGHIRRSLMDQISMVDGRFDAVVKK--RGAKQLMW-------------------  543
OsGEF1      483 PFSIQHTPYASPFATPTFCSSTPVTGSPGRVQPPLNKD--NLPTKQEVKVEKLFSGDIEKVWTYAGNLSARKDAGDAPERD  561
```

Figure S20: Alignment of *Hv*GEF14 and *Os*GEF1 shows no conservation of functional phosphorylation site. S459 of *Os*GEF1 is required for GEF activity and function in *O. sativa* (Akamatsu et al., 2015) but not conserved in *Hv*GEF14. MUSCLE alignment of primary sequences performed in Jalview.

5.2. Supplementary Tables

Table S12: Statistical Analysis of BiFC between *Hv*RACB and *Hv*GEF14. Pairwise comparison via Wilcoxon Test of data points collected on same experimental days with Bonferroni adjustment performed in Rstudio. Summary of all data points in Figure 7A.

Group 1	**Group 2**	**p**	**p.adj**	**p.format**	**p.signif**	**Exp.**
*Hv*RACB WT + *Hv*GEF14	*Hv*RACB WT + *Hv*RIC171	0.00154	0.0046	0.0015	**	I, IV
*Hv*RACB WT + *Hv*GEF14	*Hv*RACB DN + *Hv*RIC171	2.3 e-12	6.9 e-12	2.3 e-12	****	I, IV
*Hv*RACB CA + *Hv*GEF14	*Hv*RACB WT + *Hv*RIC171	0.0002	0.0005	0.0002	***	II, III
*Hv*RACB CA + *Hv*GEF14	*Hv*RACB DN + *Hv*RIC171	1.01 e-8	3.0 e-8	1.0 e-8	****	II, III
*Hv*RACB DN + *Hv*GEF14	*Hv*RACB WT + *Hv*RIC171	1.45 e-11	4.4 e-11	1.5 e-11	****	II, III
*Hv*RACB DN + *Hv*GEF14	*Hv*RACB DN + *Hv*RIC171	0.271	0.81	0.27	ns	II, III

Table S13: Summary of *Hv*GEF identifiers, PRONE domain prediction and protein length.

***Hv* GEF**	**Accession No.**	**Prot. ID**	**HORVU ID Morex v1**	**HORVU ID Morex v2**	**HORVU ID Morex v3**	**JHI ID**	**MLOC ID**	**Uni Prot ID**	**PRONE domain (amino acids)**	**Protein length (amino acids)**
1	AK 376075	BAK 07270, GI: 3265 18036, KAE 8771 684	HOR VU 5Hr 1G0 85510 .1	HOR VU. MO REX. r2. 5HG0 416790	HOR VU. MO REX. r3. 5HG0 501980	JLOC 148 704	73178	F2 EIU8 HOR VV	84-458 (374)	566

Table S13: Summary of *Hv*GEF identifiers, PRONE domain prediction and protein length.

***Hv* GEF**	**Accession No.**	**Prot. ID**	**HORVU ID Morex v1**	**HORVU ID Morex v2**	**HORVU ID Morex v3**	**JHI ID**	**MLOC ID**	**Uni Prot ID**	**PRONE domain (amino acids)**	**Protein length (amino acids)**
3a	AK 362448	BAJ 93652 .1, GI: 3265 33360	HOR VU 1Hr 1G0 53350	HOR VU. MO REX. r2. 1HG0 044050	HOR VU. MO REX. r3. 1HG0 055850	JLOC 137 154	57351	F2 DEY1 HOR VV	99-478 (379)	478
3b			HOR VU 2Hr 1G0 96430 .13	HORVU. MO REX. r2. 2HG0 156020	HOR VU. MO REX. r3. 2HG0 188380				168-528 (360) prediction by AT	529
3c		KAE 8779 824	HOR VU 6Hr 1G0 92860 .4	HOR VU. MO REX. r2. 6HG0 525180	HOR VU. MO REX. r3. 6HG0 631600				81-438 (357)	458
7a	AK 358686	BAJ 89898, GI: 3264 88119	HOR VU 1Hr 1G0 72910.3	HOR VU. MO REX. r2. 1HG0 059830	HOR VU. MO REX. r3. 1HG0 073950	JLOC 132 912	51507	F2 D477 HOR VV	95-459 (364)	564
7b		KAE 876 7369		HOR VU. MO REX. r2. 3HG0 251900	HOR VU. MO REX. r3. 3HG0 301980		59655		56-424 (368)	526

Table S13: Summary of *Hv*GEF identifiers, PRONE domain prediction and protein length.

***Hv* GEF**	**Accession No.**	**Prot. ID**	**HORVU ID Morex v1**	**HORVU ID Morex v2**	**HORVU ID Morex v3**	**JHI ID**	**MLOC ID**	**UniProt ID**	**PRONE domain (amino acids)**	**Protein length (amino acids)**
9a	AK 377118	BAK 08312, GI: 3265 30065	HORVU 3Hr 1G0 73200.7	HORVU.MOREX.r2.3HG0241090	HORVU.MOREX.r3.3HG0290250	JLOC 15637	8484	F2ELU0 HORVV	43-394 (355)	476
9b	AK 376239	BAK 07434, GI: 3265 20351	HORVU 3Hr 1G0 62030.1	HORVU.MOREX.r2.3HG0231670	HORVU.MOREX.r3.3HG0279570	JLOC 18733	12953	F2EJB2 HORVV	99-445 (346)	534
9c	AK 367803	BAJ 99006, GI: 3265 02756, KAE 8786 946	HORVU 1Hr 1G0 86590.2	HORVU.MOREX.r2.1HG0071520	HORVU.MOREX.r3.1HG0086820	JLOC 134357	53471	F2DV85 HORVV	120-467 (347)	566
10	AK 365068	BAJ 96271, GI: 3265 14568	HORVU 6Hr 1G0 50860.4	HORVU.MOREX.r2.6HG0488080	HORVU.MOREX.r3.6HG0588520	JLOC 147493	71455	F2DMF0 HORVV	68-412 (344)	508

Table S13: Summary of *Hv*GEF identifiers, PRONE domain prediction and protein length.

***Hv* GEF**	**Accession No.**	**Prot. ID**	**HORVU ID Morex v1**	**HORVU ID Morex v2**	**HORVU ID Morex v3**	**JHI ID**	**MLOC ID**	**UniProt ID**	**PRONE domain (amino acids)**	**Protein length (amino acids)**
14	AK 371648	BAK 02846, GI: 326504120, KAE 8778 486	HORVU 6Hr1G0 68660.4	HORVU. MOREX. r2. 6HG0 503340	HORVU. MOREX. r3. 6HG0 607130	JLOC 140909	62513	F2E674 HORVV	124-485 (361)	543

Table S14: Published amino acids of PRONE-GEFs important for function and corresponding *Os*- and *Hv*GEF sites. List organised from N- to C-terminus. Conserved amino acids in *Hv*GEF14 in bold letters.

***At* GEF**	***Os* GEF**	***Hv* GEF14**	**Function**	**Source**	***Hv*GEF**									
					1	**3a**	**3b**	**3c**	**7a**	**7b**	**9a**	**9b**	**9c**	**10**
K13 (GEF8)			binding of phosphatidic acid	Cao et al. (2017)										
K18 (GEF8)			binding of phosphatidic acid	Cao et al. (2017)										
S51 (GEF1)			phosphorylation by *At*CPK4 and subsequent degradation (induced by ABA)	Li et al. (2018b)										
F93 (GEF8)		**F133**	GEF homodimerisation (supportive)	Thomas et al. (2007)	93	107	176	90	103	64	52	108	129	77
L96 (GEF8)		**L136**	GEF homodimerisation	Thomas et al. (2007)	96	110	179	93	106	67	55	111	132	144
L97 (GEF8)		**L137**	GEF homodimerisation	Thomas et al. (2007)	97	111	180	94	107	68	56	112	133	145

Table S14: Published amino acids of PRONE-GEFs important for function and corresponding *Os*- and *Hv*GEF sites. List organised from N- to C-terminus. Conserved amino acids in *Hv*GEF14 in bold letters.

***At* GEF**	***Os* GEF**	***Hv* GEF14**	**Function**	**Source**	***Hv*GEF**									
					1	**3a**	**3b**	**3c**	**7a**	**7b**	**9a**	**9b**	**9c**	**10**
L98 (GEF8)		**L138**	GEF homo-dimerisation (essential)	Thomas et al. (2007)	98	112	181	95	108	69	57	113	134	82
L103 (GEF1)		**L138**	Interaction with ROPs, dimerisation, important for function	Li et al. (2018a)	98	112	181	95	108	69	57	113	134	82
M102 (GEF8)		V142	GEF-ROP interaction	Thomas et al. (2007)										
N121 (GEF8)		**N161**	GEF-ROP interaction	Thomas et al. (2007)	121	135	204	118	131	92	80	136	157	105
S125 (GEF8)		T165	GEF-ROP interaction	Thomas et al. (2007)										
Q166 (GEF8)		**Q206**	GEF-ROP interaction	Thomas et al. (2007)	166	180	-	163	176	137	125	181	202	150

Table S14: Published amino acids of PRONE-GEFs important for function and corresponding *Os*- and *Hv*GEF sites. List organised from N- to C-terminus. Conserved amino acids in *Hv*GEF14 in bold letters.

***At* GEF**	***Os* GEF**	***Hv* GEF14**	**Function**	**Source**	***Hv*GEF**									
					1	**3a**	**3b**	**3c**	**7a**	**7b**	**9a**	**9b**	**9c**	**10**
M177 (GEF8)		**M217**	GEF-ROP interaction	Thomas et al. (2007)	178	191	260	174	187	148	136	192	213	161
D218 (GEF8)			GEF-ROP interaction	Thomas et al. (2007); Fricke and Berken (2009)										
W234 (GEF8)		**W275**	ROP interaction, role in confirm change of ROP, part of WW-loop	Thomas et al. (2009)	250	263	323	233	250	211	194	249	270	211
W235 (GEF8)		**W276**	ROP interaction, role in confirm change of ROP, part of WW-loop	Thomas et al. (2009)	251	264	324	234	251	212	195	250	271	212
S258 (GEF1)		**S258**	Theoretical p-site, found to be not important	Li et al. (2018a)	-	276	T 336	246	-	-	-	262	283	224

Table S14: Published amino acids of PRONE-GEFs important for function and corresponding *Os*- and *Hv*GEF sites. List organised from N- to C-terminus. Conserved amino acids in *Hv*GEF14 in bold letters.

***At* GEF**	***Os* GEF**	***Hv* GEF14**	**Function**	**Source**	***Hv*GEF**									
					1	**3a**	**3b**	**3c**	**7a**	**7b**	**9a**	**9b**	**9c**	**10**
Q265 (GEF8)			GEF-ROP interaction	Thomas et al. (2007)										
T299 (GEF1)		A329	Theoretical p-site, found to be not important	Li et al. (2018a)										
S333 (GEF1)		K363	PM localisation, phosphorylated by AGC kinase	Li et al. (2018a)										
G383 (GEF8)		N433	GEF-ROP interaction	Fricke and Berken (2009)										
L384		**L434**	GEF-ROP interaction	Thomas et al. (2007)	409	427	477	388	408	373	-	-	-	-
S388 (GEF8)			GEF-ROP interaction	Thomas et al. (2007); Fricke and Berken (2009)										

Table S14: Published amino acids of PRONE-GEFs important for function and corresponding *Os*- and *Hv*GEF sites. List organised from N- to C-terminus. Conserved amino acids in *Hv*GEF14 in bold letters.

***At* GEF**	***Os* GEF**	***Hv* GEF14**	**Function**	**Source**	***Hv*GEF**									
					1	**3a**	**3b**	**3c**	**7a**	**7b**	**9a**	**9b**	**9c**	**10**
S404 (GEF14)		**S394**	Predicted P-site	Data J. Mergner *A.thaliana* proteomics	-	-	-	-	-	T 333	-	-	-	-
T409 (GEF1)		**T437**	Theoretical p-site, found to be not important	Li et al. (2018a)	412	430	480	391	411	376	S 347	S 399	S 421	S 364
R410		**R460**	GEF-ROP interaction	Thomas et al. (2007)	435	453	503	414	434	399	370	422	444	387
E413 (GEF8)			GEF-ROP interaction	Thomas et al. (2007)										
S460 (GEF1)		**T488**	C-term. P-site	Chang et al. (2013)	-	-	-	442	-	-	-	-	-	-
S480 (GEF1)		G505	C-term. P-site	Chang et al. (2013)	488	-	-	-	-	-	409	-	-	-
	S480 (Os-GEF1)	E508	no difference in activating capacity	Akamatsu et al. (2013)	-	-	-	-	488	-	-	-	483	-

Table S14: Published amino acids of PRONE-GEFs important for function and corresponding *Os*- and *Hv*GEF sites. List organised from N- to C-terminus. Conserved amino acids in *Hv*GEF14 in bold letters.

***At* GEF**	***Os* GEF**	***Hv* GEF14**	**Function**	**Source**	***Hv*GEF**									
					1	**3a**	**3b**	**3c**	**7a**	**7b**	**9a**	**9b**	**9c**	**10**
S510 (GEF12)			P-site in C-terminus, phosphorylated by RLK (PRK2), important for autoinhibition	Zhang and McCormick (2007)	-	-	-	-	-	-	-	530	561	503
	S549 (OsGEF1)	-	involved in *Os*RAC1 activation and rice immunity	Akamatsu et al. (2013)	554	-	-	-	552	-	-	-	-	-

Table S15: *Hv*GEF14 hairpin construct efficiently reduces *Hv*GEF14 protein amounts.

Constructs	**mean GFP Fluorescence Intensity**	**mean mCherry Fluorescence Intensity**	**normalised GFP Fluorescence Intensity**	**RNAi efficiency**
mCherry + GFP-*Hv*GEF14 + pIPKTA30N EV	20.49667	43.20189	0.474439	
mCherry + GFP-*Hv*GEF14 + pIPKTA30N *HvGEF14* RNAi	7.7036	34.2094	0.22519	0.525356

5.3. Buffers

Table S16: Alkaline Lysis Buffers for plasmid preparation (Birnboim, 1983).

Buffer P1

sucrose	30g
0.5 M EDTA pH 8	40 ml (50 mM)
1M Tris-HCl pH 8	20ml (50mM)
RNase A	1 ml (0.3 mg/ml)
H_2O	to final volume 200 ml
HCl to adjust pH to 8	

Buffer P2

NaOH	200 mM
SDS	1 %
H_2O	to final volume

Buffer P3

glacial acetic acid	11.5 %
5M K-Acetate	60 %
H_2O	to final volume
pH 5.2	

Table S17: LiAc Buffer used in yeast tranformation during Y2H (Yeastmaker™ Transformation System 2, Clontech.)

Reagent	**amount for 2ml**
10x LiAc	200 μl
10x TE Buffer	200 μl
H_2O	1600 μl

Table S18: PEG Buffer used in yeast transformation during Y2H (Yeastmaker^{TM} Transformation System 2, Clontech).

Reagent	**amount for 10ml**
10x LiAc	1 ml
10x TE Buffer	1 ml
50 % PEG (sterile filtered)	8 ml

Table S19: Tris-EDTA (TE) Buffer used in yeast transformation during Y2H (Yeastmaker^{TM} Transformation System 2, Clontech).

Reagent	**Concentration**
1M TRIS-Cl ph 8.0	10 mM
0.5 M EDTA pH 8.0	1 mM
H_2O	to final volume

Table S20: Recipe for PBS-T Buffer used in Western Blot (adapted from Laemmli (1970)).

NaCl	80 g
KCl	2 g
Na_2HPO4 (dibasic anhydrous)	14 g
KH_2PO4 (monobasic anhydrous)	2.4 g
Tween	0.05 %
H_2O	fill up to 1000 ml
adjust pH to 7.4	
Sterilisation by autoclaving 20 min at 121 °C	

Table S21: Recipe for 4x SDS Buffer used for proteins in SDS-PAGE (adapted from Laemmli (1970)).

Tris-HCl	250mM
SDS	10 %
Bromophenol blue	0.008 %
β-mercaptoethanol	20 %
glycerol	40 %
adjust pH to 6.8	

Table S22: Recipe for 10x Running Buffer for SDS-PAGE. Use 1x while running the gel (adapted from Laemmli (1970)).

Tris-HCl	250mM
SDS	1 %
glycerol	2.5M %

5.4. Media

Table S23: Recipe for 800ml yeast peptone dextrose adenine (YPDA) culture medium used for yeast transformation (Yeastmaker™Transformation System 2, Clontech).

Bacto yeast extract	8 g
Bacto peptone	16 g
Glucose monohydrate	16 g
Adenine hemisulfate	40 mg
Agar	16 g
H_2O	fill up to 800 ml
pH= 5.8	
sterilisation by autoclaving (121°C for 13 min.)	

Table S24: Recipe for 800ml synthetic defined (SD) dropout culture medium used in Y2H (Yeastmaker™Transformation System 2, Clontech).

Bacto yeast extract	8 g
Bacto peptone	16 g
Glucose monohydrate	16 g
Adenine hemisulfate	40 mg
Agar	16 g
H_2O	fill up to 800 ml
pH= 5.8	
sterilisation by autoclaving (121°C for 13 min.)	

Table S25: Recipe for 1l Lysogeny Broth (LB) culture medium used for *E.coli* in cloning.

Peptone	10 g
$NaCL_2$	10 g
Yeast Extract	5 g
Agar	15 g
H_2O	fill up to 800 ml
antibiotics (as needed)	according to desired concentration
sterilisation by autoclaving (121°C for 20 min.)	

Table S26: Media *A. tumefaciens* transformation of *N. benthamiana* (Yang et al., 2000).

AB medium 1l (sterilise by autoclaving at 121°C for 20 min)	
MES	3.9 g
Glucose	10 g
dH_2O	940 ml
adjust pH to 5.5 with KOH	

20 x AB salts 200 ml (sterilise by autoclaving at 121°C for 20 min)	
NH_4Cl	20 g/l
$MgSO_4$-7 H_2O	6 g/l
KCl	3 g/l
$CaCl_2$	0.2 g/l
$FeSO_4$-7 H_2O	50 mg/l

20 x AB buffer 200 ml (sterilise by autoclaving at 121°C for 20 min)	
K_2HPO_4	60 g/l
NaH_2PO_4	20 g/l

Induction Medium 10 ml (prepare freshly)	
AB medium	9.4 ml
AB salts	0.5 ml
AB buffer	0.1 ml
antibiotics (gentamicin, kanamycin, rifampicin)	10 μl
acetosyringone 100 mM	10 μl

Infiltration Medium 50 ml (prepare freshly)	
1M $MgSO_4$	0.5 ml
0.5M MES pH 5.5	1 ml
100 mM acetosyringone stock (add after washing according to remaining volume)	final concentration 150 μM

Bibliography

Aguilar, G. B., Pedersen, C., and Thordal-Christensen, H. (2016). Identification of eight effector candidate genes involved in early aggressiveness of the barley powdery mildew fungus. *Plant Pathology*, 65(6):953–958.

Ahmed, A. A., Pedersen, C., and Thordal-Christensen, H. (2016). The barley powdery mildew effector candidates csep0081 and csep0254 promote fungal infection success. *PLoS One*, 11(6):e0157586.

Aist, J. R. and Bushnell, W. R. (1991). *Invasion of Plants by Powdery Mildew Fungi, and Cellular Mechanisms of Resistance*. The Fungal Spore and Disease Initiation in Plants and Animals. Springer, Boston, MA.

Akamatsu, A., Fujiwara, M., Hamada, S., Wakabayashi, M., Yao, A., Wang, Q., Kosami, K.-I., Dang, T. T., Kaneko-Kawano, T., Fukada, F., Shimamoto, K., and Kawano, Y. (2021). The small gtpase *Os*rac1 forms two distinct immune receptor complexes containing the prr *Os*cerk1 and the nlr pit. *Plant and Cell Physiology*, 62(11):1–14.

Akamatsu, A., Shimamoto, K., and Kawano, Y. (2016). Crosstalk of signaling mechanisms involved in host defense and symbiosis against microorganisms in rice. *Current Genomics*, 17:297–307.

Akamatsu, A., Uno, K., Kato, M., Wong, H. L., Shimamoto, K., and Kawano, Y. (2015). New insights into the dimerization of small gtpase rac/rop guanine nucleotide exchange factors in rice. *Plant Signaling and Behavior*, 10(7):e1044702.

Akamatsu, A., Wong, H. L., Fujiwara, M., Okuda, J., Nishide, K., Uno, K., Imai, K., Umemura, K., Kawasaki, T., Kawano, Y., and Shimamoto, K. (2013). An oscebip/oscerk1-osracgef1-osrac1 module is an essential early component of chitin-induced rice immunity. *Cell Host and Microbe*, 13(4):465–476.

Ausubel, F. M. (2005). Are innate immune signaling pathways in plants and animals conserved? *Nature Immunology*, 6(10):973–9.

Badr, A., Müller, K., Schäfer-Pregl, R., El Rabey, H., Effgen, S., Ibrahim, H. H., Pozzi, C., Rohde, W., and Salamini, F. (2000). On the origin and domestication history of barley (hordeum vulgare). *Molecular Biology and Evolution*, 14(4):499–510.

Berken, A., Thomas, C., and Wittinghofer, A. (2005). A new family of rhogefs activates the rop molecular switch in plants. *Nature*, 436(7054):1176–1180.

Berken, A. and Wittinghofer, A. (2008). Structure and function of rho-type molecular switches in plants. *Plant Physiology and Biochemistry*, 46(3):380–393.

Berkey, R., Zhang, Y., Ma, X., King, H., Zhang, Q., Wang, W., and Xiao, S. (2017). Homologues of the rpw8 resistance protein are localized to the extrahaustorial membrane that is likely synthesized de novo. *Plant Physiology*, 173(1):600–613.

Bindschedler, L. V., Burgis, T. A., Mills, D. J. S., Ho, J. T. C., Cramer, R., and Spanu, P. D. (2009). In planta proteomics and proteogenomics of the biotrophic barley fungal pathogen blumeria graminis f. sp. hordei. *Molecular and Cellular Proteomics*, 8(10):2350–67.

Birnboim, H. (1983). A rapid alkaline extraction method for the isolation of plasmid dna. *Methods in Enzymology*, 100:243–255.

Bloch, D. and Yalovsky, S. (2013). Cell polarity signaling. *Current Opinion in Plant Biology*, 16(6):734–742.

Boller, T. and Felix, G. (2009). A renaissance of elicitors: perception of microbe-associated molecular patterns and danger signals by pattern-recognition receptors. *Annual Review of Plant Biology*, 60:379–406.

Both, M., Csukai, M., Stumpf, M. P. H., and Spanu, P. D. (2005). Gene expression profiles of blumeria graminis indicate dynamic changes to primary metabolism during development of an obligate biotrophic pathogen. *The Plant Cell*, 17(7):2107–2122.

Brugnera, E., Haney, L., Grimsley, C., Lu, M., Walk, S. F., Tosello-Trampont, A.-C., Macara, I. G., Madhani, H., Fink, G. R., and Ravichandran, K. S. (2002). Unconventional rac-gef activity is mediated through the dock180-elmo complex. *Nature Cell Biology*, 4(8):574–82.

Cao, C., Wang, P., Song, H., Jing, W., Shen, L., Zhang, Q., and Zhang, W. (2017). Phosphatidic acid binds to and regulates guanine nucleotide exchange factor 8 (gef8) activity in arabidopsis. *Functional Plant Biology*, 44(10):1029–1038.

Cerione, R. and Zheng, Y. (1996). The dbl family of oncogenes. *Current Opinion in Cell Biology*, 8:216–222.

Chandran, D. (2015). Co-option of developmentally regulated plant sweet transporters for pathogen nutrition and abiotic stress tolerance. *International Union of Biochemistry and Molecular Biology Life*, 67(7):461–71.

Chang, F., Gu, Y., Ma, H., and Yang, Z. (2013). Atprk2 promotes rop1 activation via ropgefs in the control of polarized pollen tube growth. *Molecular Plant*, 6(4):1187–1201.

Chen, M., Liu, H., Kong, J., Yang, Y., Zhang, N., Li, R., Yue, J., Huang, J., Li, C., Cheung, A. Y., and Tao, L.-Z. (2011). Ropgef7 regulates plethora-dependent maintenance of the root stem cell niche in arabidopsis. *The Plant Cell*, 23(8):2880–2894.

Chomczynski, P. and Sachhi, N. (1987). Single-step method of rna isolation by acid guanidinium thiocyanate-phenol-chloroform extraction. *Analytical Biochemistry*, 162:156–159.

Cool, R. H., Schmidt, G., Lenzen, C. U., Prinz, H., Vogt, D., and Wittinghofer, A. (1999). The ras mutant d119n is both dominant negative and activated. *Molecular and Cellular Biology*, 19(9):6297–6305.

Denay, G., Schultz, P., Hansch, S., Weidtkamp-Peters, S., and Simon, R. (2019). Over the rainbow: A practical guide for fluorescent protein selection in plant fret experiments. *Plant Direct*, 3(12):1–14.

Denninger, P., Reichelt, A., Schmidt, V. A. F., Mehlhorn, D. G., Asseck, L. Y., Stanley, C. E., Keinath, N. F., Evers, J.-F., Grefen, C., and Grossmann, G. (2019). Timing of polar protein accumulation and signaling in arabidopsis thaliana. *Current Biology*, 29(11):1854–1865.

Deshmukh, S., Huckelhoven, R., Schafer, P., Imani, J., Sharma, M., Weiss, M., Waller, F., and Kogel, K. H. (2006). The root endophytic fungus piriformospora indica requires host cell death for proliferation during mutualistic symbiosis with barley. *Proceedings of National Academy of Science USA*, 103(49):18450–7.

Devoto, A., Piffanelli, P., Nilsson, I., Wallin, E., Panstruga, R., Heijne, G. v., and Schulze-Lefert, P. (1999). Topology, subcellular localization, and sequence diversity of the mlo family in plants. *Journal of Biological Chemistry*, 274(49):34993–35004.

Dodds, P. N. and Rathjen, J. P. (2010). Plant immunity: towards an integrated view of plant-pathogen interactions. *Nature Reviews Genetics*, 11(8):539–48.

Doermann, P., Kim, H., Ott, T., Schulze-Lefert, P., Trujillo, M., Wewer, V., and Hückelhoven, R. (2014). Cell-autonomous defense, re-organization and trafficking of membranes in plant-microbe interactions. *The New phytologist*, 204(4):815–822.

Douchkov, D., Lueck, S., Johrde, A., Nowara, D., Himmelbach, A., Rajaraman, J., Stein, N., Sharma, R., Kilian, B., and Schweizer, P. (2014). Discovery of genes affecting resistance of barley to adapted and non-adapted powdery mildew fungi. *Genome Biology*, 15(518).

Duan, Q., Kita, D., Li, C., Cheung, A. Y., and Wu, H.-M. (2010). Feronia receptor-like kinase regulates rho gtpase signaling of root hair development. *Proceedings of National Academy of Science USA*, 107(41):17821–17826.

Eklund, D. M., Svensson, E. M., and Kost, B. (2010). Physcomitrella patens: a model to investigate the role of rac/rop gtpase signalling in tip growth. *Journal of Experimental Botany*, 61(7):1917–1937.

Engelhardt, S., Kopischke, M., Hofer, J., Probst, K., McCollum, C., and Hückelhoven, R. (2021). Barley ric157 is involved in racb-mediated susceptibility to powdery mildew. *BioRxiv*, (848226).

Engelhardt, S., Stam, R., and Hückelhoven, R. (2018). Good riddance?: Breaking disease susceptibility in the era of new breeding technologies. *Agronomy*, 8(7):114.

Engelhardt, S., Trutzenberg, A., and Hückelhoven, R. (2020). Regulation and functions of rop gtpases in plant-microbe interactions. *Cells*, 9(2016).

Engler, C., Kandzia, R., and Marillonnet, S. (2008). A one pot, one step, precision cloning method with high throughput capability. *PLOS One*, 3(11):e3647.

Eva, A. and Aaronson, S. A. (1985). Isolation of a new human oncogene from a diffuse b-cell lymphoma. *Nature*, 316(18):273–275.

Feiguelman, G., Fu, Y., and Yalovsky, S. (2018). Rop gtpases structure-function and signaling pathways. *Plant Physiology*, 176(1):57–79.

Feng, Q.-N., Kang, H., Song, S.-J., Ge, F.-R., Zhang, Y.-L., Li, E., Li, S., and Zhang, Y. (2016). Arabidopsis rhogdis are critical for cellular homeostasis of pollen tubes. *Plant Physiology*, 170(2):841–56.

Feuerstein, J., Kalbitzer, H. R., John, J., RogerS., G., and Wittinghofer, A. (1987). Characterisation of the metal-ion - gdp complex at the active sites of transforming and nontransforming p21 proteins by observation of the 17o-mn superhyperfine coupling and by kinetic methods. *European Journal of Biochemistry*, 162:49–55.

Fields, S. and Song, O.-K. (1989). A novel genetic system to detect protein-protein interactions. *Nature*, 340:245–246.

Fodor-Dunai, C., Fricke, I., Potocký, M., Dorjgotov, D., Domoki, M., Jurca, M. E., Otvös, K., Zárský, V., Berken, A., and Fehér, A. (2011). The phosphomimetic mutation of an evolutionarily conserved serine residue affects the signaling properties of rho of plants (rops). *The Plant Journal*, 66(4):669–679.

Frantzeskakis, L., Kracher, B., Kusch, S., Yoshikawa-Maekawa, M., Bauer, S., Pedersen, C., Spanu, P. D., Maekawa, T., Schulze-Lefert, P., and Panstruga, R. (2018). Signatures of host specialization and a recent transposable element burst in the dynamic one-speed genome of the fungal barley powdery mildew pathogen. *BMC Genomics*, 19(1):381.

Fricke, I. and Berken, A. (2009). Molecular basis for the substrate specificity of plant guanine nucleotide exchange factors for rop. *FEBS Letters*, 583(1):75–80.

Fu, Y., Gu, Y., Zheng, Z., Wasteneys, G., and Yang, Z. (2005). Arabidopsis interdigitating cell growth requires two antagonistic pathways with opposing action on cell morphogenesis. *Cell*, 120(5):687–700.

Fu, Y., Xu, T., Zhu, L., Wen, M., and Yang, Z. (2009). A rop gtpase signaling pathway controls cortical microtubule ordering and cell expansion in arabidopsis. *Current Biology*, 19(21):1827–32.

Fuchs, V. A. F., Denninger, P., Župunski, M., Jaillais, Y., Engel, U., and Grossmann, G. (2021). Nanodomain-mediated lateral sorting drives polarization of the small gtpase rop2 in the plasma membrane of root hair cells. *BioRxiv*, (459822).

Gao, H., Wang, T., Zhang, Y., Li, L., Wang, C., Guo, S., Zhang, T., and Wang, C. (2021a). Gtpase rop6 negatively modulates phosphate deficiency through inhibition of pht1;1 and pht1;4 in arabidopsis thaliana. *Current Biology*, 63(10):1775–1786.

Gao, J.-P., Xu, P., Wang, M., Zhang, X., Yang, J., Zhou, Y., Murray, J. D., Song, C.-P., and Wang, E. (2021b). Nod factor receptor complex phosphorylates gmgef2 to stimulate rop signaling during nodulation. *Current Biology*, 31:1–13.

Garcia-Mata, R., Boulter, E., and Burridge, K. (2011). The 'invisible hand': regulation of rho gtpases by rhogdis. *Nature Reviews Molecular Cell Biology*, 12(8):493–504.

Garcia-Ruiz, H., Szurek, B., and Van den Ackerveken, G. (2021). Stop helping pathogens: engineering plant susceptibility genes for durable resistance. *Current Opinion in Plant Biotechnology*, 70:187–195.

García-Soto, I., Boussageon, R., Cruz-Farfán, Y. M., Castro-Chilpa, J. D., Hernández-Cerezo, L. X., Bustos-Zagal, V., Leija-Salas, A., Hernández, G., Torres, M., Formey, D., Courty, P.-E., Wipf, D., Serrano, M., and Tromas, A. (2021). The lotus japonicus rop3 is involved in the establishment of the nitrogen-fixing symbiosis but not of the arbuscular mycorrhizal symbiosis. *Frontiers in Plant Science*, 12.

Ge, F.-R., Chai, S., Li, S., and Zhang, Y. (2020). Targeting and signaling of rho of plants guanosine triphosphatases require synergistic interaction between guanine nucleotide inhibitor and vesicular trafficking. *Journal of Integrative Plant Biology*, 62(10):1484–1499.

Glawe, D. A. (2008). The powdery mildews: A review of the world's most familiar (yet poorly known) plant pathogens. *Annual Review of Phytopathology*, 46:27–51.

Grierson, C., Nielsen, E., Ketelaarc, T., and Schiefelbein, J. (2014). Root hairs. *American Society of Plant Biologists*, 12:1–25.

Gu, Y., Fu, Y., Dowd, P., Li, S., Vernoud, V., Gilroy, S., and Yang, Z. (2005). A rho family gtpase controls actin dynamics and tip growth via two counteracting downstream pathways in pollen tubes. *Journal of Cell Biology*, 169(1):127–38.

Gu, Y., Li, S., Lord, E. M., and Yang, Z. (2006). Members of a novel class of arabidopsis rho guanine nucleotide exchange factors control rho gtpase-dependent polar growth. *The Plant Cell*, 18(2):366–381.

Gu, Y., Wang, Z., and Yang, Z. (2004). Rop/rac gtpase: An old new master regulator for plant signaling. *Current Opinion in Plant Biology*, 7(5):527–536.

Gutjahr, C. and Parniske, M. (2013). Cell and developmental biology of arbuscular mycorrhiza symbiosis. *Annu Rev Cell Dev Biol*, 29:593–617.

Hamers, D., van Voorst Vader, L., Borst, J. W., and Goedhart, J. (2014). Development of fret biosensors for mammalian and plant systems. *Protoplasma*, 251(2):333–47.

Hart, M. J., Eva, A., Zangrilli, D., Aaronson, S. A., Evans, T., Cerione, R. A., and Zheng, Y. (1994). Cellular transformation and guanine nucleotide exchange activity are catalyzed by a common domain on the dbl oncogene product. *Journal of Biological Chemistry*, 269(1):62–65.

Harwood, W. A. (2019). *An Introduction to Barley: The Crop and the Model*, volume 1900, book section 1, pages 1–5. Springer Science and Business Media, LLC, part of Springer Nature.

He, Q., Naqvi, S., McLellan, H., Boevink, P. C., Champouret, N., Hein, I., and Birch, P. R. J. (2018). Plant pathogen effector utilizes host susceptibility factor nrl1 to degrade the immune regulator swap70. *Proceedings of the National Academy of Science USA*, 115(33):7834–7843.

Hiwatashi, T., Goh, H., Yasui, Y., Koh, L. Q., Takami, H., Kajikawa, M., Kirita, H., Kanazawa, T., Minamino, N., Togawa, T., Sato, M., Wakazaki, M., Yamaguchi, K., Shigenobu, S., Fukaki, H., Mimura, T., Toyooka, K., Sawa, S., Yamato, K. T., Ueda, T., Urano, D., Kohchi, T., and Ishizaki, K. (2019). The ropgef karappo is essential for the initiation of vegetative reproduction in marchantia polymorpha. *Current Biology*, 29(20):1–7.

Hoefle, C., Huesmann, C., Schultheiss, H., Börnke, F., Hensel, G., Kumlehn, J., and Hückelhoven, R. (2011). A barley rop gtpase activating protein associates with microtubules and regulates entry of the barley powdery mildew fungus into leaf epidermal cells. *The Plant Cell*, 23(6):2422–2439.

Hoefle, C. and Hückelhoven, R. (2014). A barley engulfment and motility domain containing protein modulates rho gtpase activating protein hvmagap1 function in the barley powdery mildew interaction. *Plant Molecular Biology*, 84(4-5):469–478.

Hoefle, C., McCollum, C., and Hückelhoven, R. (2020). Barley rop-interactive partner-a organizes into rac1- and microtubule-associated rop-gtpase activating protein 1-dependent membrane domains. *BMC Plant Biology*, 20(94):1–12.

Hope, H., Bogliolo, S., Arkowitz, R. A., and Bassilana, M. (2008). Activation of rac1 by the guanine nucleotide exchange factor dck1 is required for invasive filamentous growth in the pathogen candida albicans. *Molecular Biology of the Cell*, 19(9):3638–51.

Horstman, A., Tonaco, I. A., Boutilier, K., and Immink, R. G. (2014). A cautionary note on the use of split-yfp/bifc in plant protein-protein interaction studies. *International Journal of Molecular Science*, 15(6):9628–43.

Huang, C., jiao, X., Yang, L., Zhang, M., Dai, M., Wang, L., Wang, K., Bai, L., and Song, C. (2018a). Rop-gef signal transduction is involved in atcap1-regulated root hair growth. *Plant Growth Regulation*, 87(1):1–8.

Huang, J., Liu, H., Berberich, T., Liu, Y., Tao, L.-Z., and Liu, T. (2018b). Guanine nucleotide exchange factor 7b (ropgef7b) is involved in floral organ development in *Oryza sativa*. *Rice*, 11(42):1–13.

Huesmann, C., Hoefle, C., and Huckelhoven, R. (2011). Ropgaps of *Arabidopsis* limit susceptibility to powdery mildew. *Plant Signaling and Behavior*, 6(11):1691–4.

Hunt, M., Banerjee, S., Surana, P., Liu, M., Fuerst, G., Mathioni, S., Meyers, B. C., Nettleton, D., and Wise, R. P. (2019). Small rna discovery in the interaction between barley and the powdery mildew pathogen. *BMC Genomics*, 20(1):610.

Hwang, J.-U., Gu, Y., Lee, Y.-J., and Yang, Z. (2005). Oscillatory rop gtpase activation leads the oscillatory polarized growth of pollen tubes. *Molecular Biology of the Cell*, 16:5385–5399.

Hückelhoven, R. (2005). Powdery mildew susceptibility and biotrophic infection strategies. *FEMS Microbiology Letters*, 245(1):9–17.

Hückelhoven, R., Dechert, C., and Kogel, K. H. (2003). Overexpression of barley bax inhibitor 1 induces breakdown of mlo-mediated penetration resistance to blumeria graminis. *Proceedings of National Academy of Science USA*, 100(9):5555–60.

Hückelhoven, R., Dechert, C., Trujillo, M., and Kogel, K. H. (2001). Differential expression of putative cell death regulator genes in near-isogenic, resistant and susceptible barley lines during interaction with the powdery mildew fungus. *Plant Molecular Biology*, 47(6):739–748.

Hückelhoven, R. and Panstruga, R. (2011). Cell biology of the plant-powdery mildew interaction. *Current Opinion in Plant Biology*, 14(6):738–746.

International Barley Genome Sequencing Consortium, T. (2012). A physical, genetic and functional sequence assembly of the barley genome. *Nature*, 491:711–715.

Jones, J. D. and Dangl, J. L. (2006). The plant immune system. *Nature*, 444(7117):323–9.

Jones, J. D., Vance, R. E., and Dangl, J. L. (2016). Intracellular innate immune surveillance devices in plants and animals. *Science*, 354(6316).

Jones, M. A., Raymond, M. J., Yang, Z., and Smirnoff, N. (2007). Nadph oxidase-dependent reactive oxygen species formation required for root hair growth depends on rop gtpase. *Journal of Experimental Botany*, 58(6):1261–70.

Kaothien, P., Ok, S. H., Shuai, B., Wengier, D., Cotter, R., Kelley, D., Kiriakopolos, S., Muschietti, J., and McCormick, S. (2005). Kinase partner protein interacts with the leprk1 and leprk2 receptor kinases and plays a role in polarized pollen tube growth. *The Plant Journal*, 42(4):492–503.

Katzen, F. (2007). Gateway® recombinational cloning: a biological operating system. *Expert Opinion on Drug Discovery*, 2(4):571–589.

Kawano, Y., Akamatsu, A., Hayashi, K., Housen, Y., Okuda, J., Yao, A., Nakashima, A., Takahashi, H., Yoshida, H., Wong, H. L., Kawasaki, T., and Shimamoto, K. (2010). Activation of a rac gtpase by the nlr family disease resistance protein pit plays a critical role in rice innate immunity. *Cell Host Microbe*, 7(5):362–75.

Kawano, Y., Fujiwara, T., Yao, A., Housen, Y., Hayashi, K., and Shimamoto, K. (2014a). Palmitoylation-dependent membrane localization of the rice resistance protein pit is critical for the activation of the small gtpase osrac1. *The Journal of Biological Chemistry*, 289(27):19079–19088.

Kawano, Y., Kaneko-Kawano, T., and Shimamoto, K. (2014b). Rho family gtpase-dependent immunity in plants and animals. *Frontiers in Plant Science*, 5:522.

Kawasaki, T., Henmi, K., Ono, E., Hatakeyama, S., Iwano, M., Satoh, H., and Shimamoto, K. (1999). The small gtp-binding protein rac is a regulator of cell death in plants. *Proceedings of the National Academy of Science USA*, 96:10922–10926.

Kawasaki, T., Imai, K., Wong, H. L., Kawano, Y., Nishide, K., Okuda, J., and Shimamoto, K. (2009). Rice guanine nucleotide exchange factors for small gtpase osrac1 involved in innate immunity of rice. *Advances in Genetics, Genomics and Control of Rice Blast Disease*, 0:179–184.

Kessler, S. A., Shimosato-Asano, H., Keinath, N. F., Wuest, S. E., Ingram, G., Panstruga, R., and Grossniklaus, U. (2010). Conserved molecular components for pollen tube reception and fungal invasion. *Science*, 330(6006):968–971.

Kiirika, L. M., Bergmann, H. F., Schikowsky, C., Wimmer, D., Korte, J., Schmitz, U., Niehaus, K., and Colditz, F. (2012). Silencing of the rac1 gtpase mtrop9 in medicago truncatula stimulates early mycorrhizal and oomycete root colonizations but negatively affects rhizobial infection. *Plant Physiology*, 159(1):501–16.

Kim, E. J., Hong, W. J., Tun, W., An, G., Kim, S. T., Kim, Y. J., and Jung, K. H. (2021). Interaction of osropgef3 protein with osrac3 to regulate root hair elongation and reactive oxygen species formation in rice (oryza sativa). *Frontiers in Plant Science*, 12:661352.

Kim, E.-J., Park, S.-W., Hong, W.-J., Silva, J., Liang, W., Zhang, D., Jung, K.-H., and Kim, Y.-J. (2020). Genome-wide analysis of ropgef gene family to identify genes contributing to pollen tube growth in rice (oryza sativa). *BMC Plant Biology*, 20(1):1.

Klahre, U., Becker, C., Schmitt, A. C., and Kost, B. (2006). Nt-rhogdi2 regulates rac/rop signaling and polar cell growth in tobacco pollen tubes. *The Plant Journal*, 46(6):1018–31.

Klahre, U. and Kost, B. (2006). Tobacco rhogtpase activating protein1 spatially restricts signaling of rac/rop to the apex of pollen tubes. *The Plant Cell*, 18(11):3033–46.

Koh, S., Andre, A., Edwards, H., Ehrhardt, D., and Somerville, S. (2005). Arabidopsis thaliana subcellular responses to compatible erysiphe cichoracearum infections. *The Plant Journal*, 44(3):516–29.

Kumar, N., Galli, M., Dempsey, D., Imani, J., Moebus, A., and Kogel, K. H. (2021). Npr1 is required for root colonization and the establishment of a mutualistic symbiosis between the beneficial bacterium rhizobium radiobacter and barley. *Environmental Microbiology*, 23(4):2102–2115.

Kunimura, K., Uruno, T., and Fukui, Y. (2020). Dock family proteins: key players in immune surveillance mechanisms. *International Immunology*, 32(1):5–15.

Kusch, S., Frantzeskakis, L., Thieron, H., and Panstruga, R. (2018). Small rnas from cereal powdery mildew pathogens may target host plant genes. *Fungal Biology*, 122(11):1050–1063.

Kusch, S. and Panstruga, R. (2017). mlo-based resistance: An apparently universal "weapon" to defeat powdery mildew disease. *Molecular Plant- Microbe Interactions*, 30(3):179–189.

Laemmli, U. K. (1970). Cleavage of structural proteins during the assembly of the head of bacteriophage t4. *Nature*, 227:680–685.

Lampugnani, E. R., Wink, R. H., Persson, S., and Somssich, M. (2018). The toolbox to study protein–protein interactions in plants. *Critical Reviews in Plant Sciences*, 37(4):308–334.

Lavy, M., Bloch, D., Hazak, O., Gutman, I., Poraty, L., Sorek, N., Sternberg, H., and Yalovsky, S. (2007). A novel rop/rac effector links cell polarity, root-meristem maintenance, and vesicle trafficking. *Current Biology*, 17(11):947–52.

Le Bail, A., Schulmeister, S., Perroud, P.-F., Ntefidou, M., Rensing, S. A., and Kost, B. (2019). Analysis of the localization of fluorescent pprop1 and pprop-gef4 fusion proteins in moss protonemata based on genomic “knock-in” and estradiol-titratable expression. *Frontiers in Plant Science*, 10:1–17.

Lei, M. J., Wang, Q., Li, X., Chen, A., Luo, L., Xie, Y., Li, G., Luo, D., Mysore, K. S., Wen, J., Xie, Z. P., Staehelin, C., and Wang, Y. Z. (2015). The small gtpase rop10 of medicago truncatula is required for both tip growth of root hairs and nod factor-induced root hair deformation. *The Plant Cell*, 27(3):806–22.

Li, E., Cui, Y., Ge, F.-R., Chai, S., Zhang, W.-T., Feng, Q.-N., Jiang, L., Li, S., and Zhang, Y. (2018a). Agc1.5 kinase phosphorylates ropgefs to control pollen tube growth. *Molecular Plant*, 11:1198–1209.

Li, E., Zhang, Y.-L., Shi, X., Li, H., Yuan, X., Li, S., and Zhang, Y. (2020). A positive feedback circuit for rop-mediated polar growth. *Molecular Plant*, 14(3):395–410.

Li, S., Gu, Y., Yan, A., Lord, E., and Yang, Z. (2008). Rip1 (rop interactive partner 1)/icr1 marks pollen germination sites and may act in the rop1 pathway in the control of polarized pollen growth. *Molecular Plant*, 1(6):1021–35.

Li, Z., Takahashi, Y., Scavo, A., Brandt, B., Nguyen, D., Rieu, P., and Schroeder, J. I. (2018b). Abscisic acid-induced degradation of arabidopsis guanine nucleotide exchange factor requires calcium-dependent protein kinases. *Proceedings of National Academy of Science USA*, 115(19):4522–4531.

Lin, W., Tang, W., Pan, X., Huang, A., Gao, X., Anderson, C. T., and Yang, Z. (2021). Arabidopsis pavement cell morphogenesis requires feronia binding to pectin for activation of rop gtpase signaling. *Current Biology*, 32:1–11.

Liu, J., Liu, M. X., Qiu, L. P., and Xie, F. (2020). Spike1 activates the gtpase rop6 to guide the polarized growth of infection threads in lotus japonicus. *The Plant Cell*, 32(12):3774–3791.

Livak, K. J. and Schmittgen, T. D. (2001). Analysis of relative gene expression data using real-time quantitative pcr and the 2(-delta delta c(t)) method. *Methods*, 25(4):402–408.

Lotze, M. T., Zeh, H. J., Rubartelli, A., Sparvero, L. J., Amoscato, A. A., Washburn, N. R., DeVera, M. E., Liang, X., Toer, M., and Billiar, T. (2007). The grateful dead: damage-associated molecular pattern molecules and reduction/oxidation regulate immunity. *Immunological Reviews*, 220:60–81.

Lupwayi, N. Z., Clayton, G. W., Hanson, K. G., Rice, W. A., and Biederbeck, V. O. (2004). Endophytic rhizobia in barley, wheat and canola roots. *Canadian Journal of Plant Science*, 84:37–45.

Mascher, M., Wicker, T., Jenkins, J., Plott, C., Lux, T., Koh, C. S., Ens, J., Gundlach, H., Boston, L. B., Tulpova, Z., Holden, S., Hernandez-Pinzon, I., Scholz, U., Mayer, K. F. X., Spannagl, M., Pozniak, C. J., Sharpe, A. G., Simkova, H., Moscou, M. J., Grimwood, J., Schmutz, J., and Stein, N. (2021). Long-read sequence assembly: a technical evaluation in barley. *The Plant Cell*, 0:1–19.

Mathur, J. and Huelskamp, M. (2002). Microtubules and microfilaments in cell morphogenesis in hicher plants. *Current Biology*, 12:R669–R676.

Mayer, K. F. X., Waugh, R., Brown, J. W. S., Schulman, A., Langridge, P., Platzer, M., Fincher, G. B., Muehlbauer, G. J., Sato, K., Close, T. J., Wise, R. P., and Stein, N. (2012). A physical, genetic and functional sequence assembly of the barley genome. *Nature*, 491(7426):711–716.

McCollum, C., Engelhardt, S., Weiss, L., and Hückelhoven, R. (2020). Rop interactive partner b interacts with racb and supports fungal penetration into barley epidermal cells. *Plant Physiology*, 184(2):823–836.

Mergner, J., Frejno, M., List, M., Papacek, M., Chen, X., Chaudhary, A., Samaras, P., Richter, S., Shikata, H., Messerer, M., Lang, D., Altmann, S., Cyprys, P., Zolg, D. P., Mathieson, T., Bantscheff, M., Hazarika, R. R., Schmidt, T., Dawid, C., Dunkel, A., Hofmann, T., Sprunck, S., Falter-Braun, P., Johannes, F., Mayer, K. F. X., Jurgens, G., Wilhelm, M., Baumbach, J., Grill, E., Schneitz, K., Schwechheimer, C., and Kuster, B. (2020). Mass-spectrometry-based draft of the arabidopsis proteome. *Nature*, 579(7799):409–414.

Miyawaki, K. N. and Yang, Z. (2014). Extracellular signals and receptor-like kinases regulating rop gtpases in plants. *Frontiers in Plant Science*, 5:449.

Molendijk, A. J., Ruperti, B., and Palme, K. (2004). Small gtpases in vesicle trafficking. *Current Opinion in Plant Biology*, 7(6):694–700.

Monat, C., Padmarasu, S., Lux, T., Wicker, T., Gundlach, H., Himmelbach, A., Ens, J., Li, C., Muehlbauer, G. J., Schulman, A. H., Waugh, R., Braumann, I., Pozniak, C., Scholz, U., Mayer, K. F. X., Spannagl, M., Stein, N., and Mascher, M. (2019). Tritex: chromosome-scale sequence assembly of triticeae genomes with open-source tools. *Genome Biology*, 20(1):284.

Muecke, S., Reschke, M., Erkes, A., Schwietzer, C. A., Becker, S., Streubel, J., Morgan, R. D., Wilson, G. G., Grau, J., and Boch, J. (2019). Transcriptional reprogramming of rice cells by xanthomonas oryzae tales. *Frontiers in Plant Science*, 10:162.

Nagawa, S., Xu, T., and Yang, Z. (2010). Rho gtpase in plants: Conservation and invention of regulators and effectors. *Small GTPases*, 1(2):78–88.

Nakamura, T., Aoki, K., and Matsuda, M. (2005). Monitoring spatio-temporal regulation of ras and rho gtpase with gfp-based fret probes. *Methods*, 37(2):146–153.

Ngou, B. P. M., Ahn, H. K., Ding, P., and Jones, J. D. G. (2021). Mutual potentiation of plant immunity by cell-surface and intracellular receptors. *Nature*, 592(7852):110–115.

Noir, S., Colby, T., Harzen, A., Schmidt, J., and Panstruga, R. (2009). A proteomic analysis of powdery mildew (blumeria graminis f.sp. hordei) conidiospores. *Molecular Plant Pathology*, 10(2):223–36.

Nottensteiner, M., Zechmann, B., McCollum, C., and Huckelhoven, R. (2018). A barley powdery mildew fungus non-autonomous retrotransposon encodes a peptide that supports penetration success on barley. *Journal of Experimental Botany*, 69(15):293745–3758.

Nowara, D., Gay, A., Lacomme, C., Shaw, J., Ridout, C., Douchkov, D., Hensel, G., Kumlehn, J., and Schweizer, P. (2010). Higs: host-induced gene silencing in the obligate biotrophic fungal pathogen blumeria graminis. *The Plant Cell*, 22(9):3130–41.

Ono, E., Wong, H. L., Kawasaki, T., Hasegawa, M., Kodama, O., and Shimamoto, K. (2001). Essential role of the small gtpase rac in disease resistance of rice. *Proceedings of National Academy of Science USA*, 98(2):759–764.

Opalski, K. S., Schultheiss, H., Kogel, K.-H., and Hückelhoven, R. (2005). The receptor-like mlo protein and the rac/rop family g-protein racb modulate actin reorganization in barley attacked by the biotrophic powdery mildew fungus blumeria graminis f.sp. hordei. *The Plant Journal*, 41(2):291–303.

Paduch, M., Jelen, F., and Otlewski, J. (2001). Structure of small g proteins and their regulators. *Acta Biochimica Polonica*, 48:829–850.

Patel, J. C. and Galán, J. E. (2006). Differential activation and function of rho gtpases during salmonella-host cell interactions. *The Journal of Cell Biology*, 175(3):453–463.

Pathuri, I. P., Zellerhoff, N., Schaffrath, U., Hensel, G., Kumlehn, J., Kogel, K.-H., Eichmann, R., and Hückelhoven, R. (2008). Constitutively activated barley rops modulate epidermal cell size, defense reactions and interactions with fungal leaf pathogens. *Plant Cellular Reports*, 27(12):1877–1887.

Pavlopoulou, A., Karaca, E., Balestrazzi, A., and Georgakilas, A. G. (2019). In silico phylogenetic and structural analyses of plant endogenous danger signaling molecules upon stress. *Oxidative Medicine and Cellular Longevity*, 2019:1–14.

Pennington, H. G., Jones, R., Kwon, S., Bonciani, G., Thieron, H., Chandler, T., Luong, P., Morgan, S. N., Przydacz, M., Bozkurt, T., Bowden, S., Craze, M., Wallington, E. J., Garnett, J., Kwaaitaal, M., Panstruga, R., Cota, E., and Spanu, P. D. (2019). The fungal ribonuclease-like effector protein csep0064/bec1054 represses plant immunity and interferes with degradation of host ribosomal rna. *PLOS Pathogens*, 15(3):1–33.

Pham, T. A. T., Schwerdt, J. G., Shirley, N. J., Xing, X., Hsieh, Y. S. Y., Srivastava, V., Bulone, V., and Little, A. (2019). Analysis of cell wall synthesis and metabolism during early germination of blumeria graminis f. sp. hordei conidial cells induced in vitro. *The Cell Surface*, 5:1–13.

Platre, M. P., Bayle, V., Armengot, L., Bareille, Joseph, Marques-Bueno, M. M., Creff, A., Maneta-Peyret, L., Fiche, J.-B., Nolmann, M., Miege, C., Moreau, P., Martiniere, A., and Jaillais, Y. (2019). Developmental control of plant rho gtpase nano-organization by the lipid phos- phatidylserine. *Science*, 364(6435):57–62.

Pliego, C., Nowara, D., Bonciani, G., Gheorghe, D. M., Xu, R., Surana, P., Whigham, E., Nettleton, D., Bogdanove, A. J., Wise, R. P., Schweizer, P., Bindschedler, L. V., and Spanu, P. D. (2013). Host-induced gene silencing in barley powdery mildew reveals a class of ribonuclease-like effectors. *Molecular Plant- Microbe Interactions*, 26(6):633–642.

Poraty-Gavra, L., Zimmermann, P., Haigis, S., Bednarek, P., Hazak, O., Stelmakh, O. R., Sadot, E., Schulze-Lefert, P., Gruissem, W., and Yalovsky, S. (2013). The arabidopsis rho of plants gtpase atrop6 functions in developmental and pathogen response pathways. *Plant Physiology*, 161(3):1172–1188.

Pruitt, R. N., Locci, F., Wanke, F., Zhang, L., Saile, S. C., Joe, A., Karelina, D., Hua, C., Frohlich, K., Wan, W. L., Hu, M., Rao, S., Stolze, S. C., Harzen, A., Gust, A. A., Harter, K., Joosten, M., Thomma, B., Zhou, J. M., Dangl, J. L., Weigel, D., Nakagami, H., Oecking, C., Kasmi, F. E., Parker, J. E., and Nurnberger, T. (2021). The eds1-pad4-adr1 node mediates arabidopsis pattern-triggered immunity. *Nature*, 598(7881):495–499.

Qiu, J. L., Jilk, R., Marks, M. D., and Szymanski, D. B. (2002). The arabidopsis spike1 gene is required for normal cell shape control and tissue development. *The Plant Cell*, 14(1):101–18.

Qu, S., Zhang, X., Song, Y., Lin, J., and Shan, X. (2017). Theseus1 positively modulates plant defense responses against botrytis cinerea through guanine exchange factor4 signaling. *Journal of Integrative Plant Biology*, 59(11):797–804.

Reiner, T., Hoefle, C., and Hückelhoven, R. (2016). A barley skp1-like protein controls abundance of the susceptibility factor racb and influences the interaction of barley with the barley powdery mildew fungus. *Molecular Plant Pathology*, 17(2):184–195.

Ridley, A. J. (2006). Rho gtpases and actin dynamics in membrane protrusions and vesicle trafficking. *Trends in Cell Biology*, 16(10):522–529.

Ried, M. K., Banhara, A., Hwu, F. Y., Binder, A., Gust, A. A., Hofle, C., Huckelhoven, R., Nurnberger, T., and Parniske, M. (2019). A set of arabidopsis genes involved in the accommodation of the downy mildew pathogen hyaloperonospora arabidopsidis. *PLoS Pathogens*, 15(7):e1007747.

Saisho, D. and Takeda, K. (2011). Barley: Emergence as a new research material of crop science. *Plant and Cell Physiology*, 52(5):724–727.

Sander, E. E., van Delft, S., ten Klooster, J. P., Reid, T., van der Kammen, R. A., Michiels, F., and Collard, J. G. (1998). Matrix-dependent tiam1/rac signaling in epithelial cells promotes either cell–cell adhesion or cell migration and is regulated by phosphatidylinositol 3-kinase. *The Journal of Cell Biology*, 143(5):1385–1398.

Schaefer, A., Höhner, K., Berken, A., and Wittinghofer, A. (2011). The unique plant rhogaps are dimeric and contain a crib motif required for affinity and specificity towards cognate small g proteins. *Biopolymers*, 95(6):420–433.

Scheler, B., Schnepf, V., Galgenmüller, C., Ranf, S., and Hückelhoven, R. (2016). Barley disease susceptibility factor racb acts in epidermal cell polarity and positioning of the nucleus. *Journal of Experimental Botany*, 67(11):3263–3275.

Schmidt, A. and Hall, A. (2002). Guanine nucleotide exchange factors for rho gtpases: turning on the switch. *Genes and Development*, 16:1587–1609.

Schnepf, V., Vlot, A. C., Kugler, K., and Hueckelhoven, R. (2018). Barley susceptibility factor racb modulates transcript levels of signalling protein genes in compatible interaction with blumeria graminis f.sp. hordei. *Molecular Plant Pathology*, 19(2):393–404.

Schultheiss, H., Dechert, C., Kogel, K.-H., and Hückelhoven, R. (2002). A small gtp-binding host protein is required for entry of powdery mildew fungus into epidermal cells of barley. *Plant Physiology*, 128(4):1447–1454.

Schultheiss, H., Dechert, C., Kogel, K.-H., and Hückelhoven, R. (2003). Functional analysis of barley rac/rop g-protein family members in susceptibility to the powdery mildew fungus. *The Plant Journal*, 36(5):589–601.

Schultheiss, H., Hensel, G., Imani, J., Broeders, S., Sonnewald, U., Kogel, K.-H., Kumlehn, J., and Hückelhoven, R. (2005). Ectopic expression of constitutively activated racb in barley enhances susceptibility to powdery mildew and abiotic stress. *Plant Physiology*, 139(1):353–362.

Schultheiss, H., Preuss, J., Pircher, T., Eichmann, R., and Hückelhoven, R. (2008). Barley ric171 interacts with racb in planta and supports entry of the powdery mildew fungus. *Cellular Microbiology*, 10(9):1815–1826.

Schulze-Lefert, P. and Vogel, J. (2000). Closing the ranks to attack by powdery mildew. *Trends in Plant Science*, 5(8):343–348.

Schweizer, P., Pokorny, J., Abderhalden, O., and Dudler, R. (1999). A transient assay system for the functional assessment of defense-related genes in wheat. *Molecular Plant-Microbe Interactions*, 12(8):647–654.

Shin, D. H., Cho, M. H., Kim, T. L., Yoo, J., Kim, J. I., Han, Y. J., Song, P. S., Jeon, J. S., Bhoo, S. H., and Hahn, T. R. (2010). A small gtpase activator protein interacts with cytoplasmic phytochromes in regulating root development. *Journal of Biological Chemistry*, 285(42):32151–32159.

Shin, D. H., Kim, T.-L., Kwon, Y.-K., Cho, M.-H., Yoo, J., Jeon, J.-S., Hahn, T.-R., and Bhoo, S. H. (2009). Characterization of arabidopsis ropgef family genes in response to abiotic stresses. *Plant Biotechnology Reports*, 3(3):183–190.

Shirasu, K., Nielsen, K., Piffanelli, P., Oliver, R., and Schulze-Lefert, P. (1999). Cell-autonomous complementation of mlo resistance using a biolistic transient expression system. *The Plant Journal*, 17(3):293–299.

Singh, B., Mehta, S., Aggarwal, S. K., Tiwari, M., Islam Bhuyan, S., Bhatia, S., and Islam, M. A. (2019). *Barley, Disease Resistance, and Molecular Breeding Approaches*. Disease Resistance in Crop Plants. Springer Nature Switzerland AG.

Smokvarska, M., Jaillais, Y., and Martiniere, A. (2021). Function of membrane domains in rho-of-plant signaling. *Plant Physiology*, 185(3):663–681.

Sorek, N., Poraty, L., Sternberg, H., Bar, E., Lewinsohn, E., and Yalovsky, S. (2017). Corrected and republished from: Activation status-coupled transient s acylation determines membrane partitioning of a plant rho-related gtpase. *Molecular Cell Biology*, 27(6):2144–54.

Sorek, N. and Yalovsky, S. (2010). *Protein–Lipid Modifications and Targeting of ROP/RAC and Heterotrimeric G Proteins*, book section Chapter 4, pages 71–90. Signaling and Communication in Plants. Springer-Verlag Berlin Heidelberg.

Spanu, P. D. (2014). Messages from powdery mildew dna: How the interplay with a host moulds pathogen genomes. *Journal of Integrative Agriculture*, 13(2):233–236.

Spanu, P. D. (2017). Cereal immunity against powdery mildews targets rnase-like proteins associated with haustoria (ralph) effectors evolved from a commonancestral gene. *The New Phytologist*, 213(3):969– 971.

Sternberg, H., Buriakovsky, E., Bloch, D., Gutman, O., Henis, Y. I., and Yalovsky, S. (2021). Formation of self-organizing functionally distinct rho of plants domains involves a reduced mobile population. *Plant Physiology*, 187(4):1–24.

Studer, G., Rempfer, C., Waterhouse, A. M., Gumienny, R., Haas, J., and Schwede, T. (2019). Qmeandisco-distance constraints applied on model quality estimation. *Bioinformatics*, 36(6):1765–1771.

Takamatsu, S. (2018). Studies on the evolution and systematics of powdery mildew fungi. *Journal of General Plant Pathology*, 84(6):422–426.

Takeuchi, H. and Higashiyama, T. (2016). Tip-localized receptors control pollen tube growth and lure sensing in arabidopsis. *Nature*, 531(7593):245–8.

Tang, W. (2022). Mechano-transduction via the pectin-feronia complex activates rop6 gtpase signaling in arabidopsis pavement cell morphogenesis. *Current Biology*, 32(3):1–10.

Thomas, C., Fricke, I., Scrima, A., Berken, A., and Wittinghofer, A. (2007). Structural evidence for a common intermediate in small g protein-gef reactions. *Molecular Cell*, 25(1):141–149.

Thomas, C., Fricke, I., Weyand, M., and Berken, A. (2009). 3d structure of a binary rop-prone complex: The final intermediate for a complete set of molecular snapshots of the ropgef reaction. *Biological Chemistry*, 390(5-6):427–435.

Thomas, W. T. B., Powell, W., and Wood, W. (1984). The chromosomal location of the dwarfting gene present in the spring barley variety golden promise. *Heredity*, 53(1):177–183.

Trutzenberg, A., Engelhardt, S., Weiss, L., and Huckelhoven, R. (2022). Barley guanine nucleotide exchange factor *Hv*GEF14 is an activator of the susceptibility factor *Hv*RACB and supports host cell entry by blumeria graminis f. sp. hordei. *Mol Plant Pathol*, 23(10):1524–1537.

Vetter, I. R. and Wittinghofer, A. (2001). The guanine nucleotide-binding switch in three dimensions. *Science*, 294(5545):1299–1304.

Wang, M., Feng, H., Xu, P., Xie, Q., Gao, J., Wang, Y., Zhang, X., Yang, J., Murray, J. D., Sun, F., Wang, C., Wang, E., and Yu, N. (2021). Phosphorylation of mtropgef2 by lyk3 mediates mtrop activity to regulate rhizobial infection in medicago truncatula. *Journal of Integrative Plant Biology*, 63(10):1787–1800.

Wang, Q., Li, Y., Ishikawa, K., Kosami, K.-I., Uno, K., Nagawa, S., Tan, L., Du, J., Shimamoto, K., and Kawano, Y. (2018). Resistance protein pit interacts with the gef osspk1 to activate osrac1 and trigger rice immunity. *Proceedings of the National Academy of Science USA*, 115(49):1–10.

Wang, W., Liu, Z., Bao, L.-J., Zhang, S.-S., Zhang, C.-G., Li, X., Li, H.-X., Zhang, X.-L., Bones, A. M., Yang, Z.-B., and Chen, Y.-L. (2017). The ropgef2-rop7/rop2 pathway activated by phyb suppresses red light-induced stomatal opening. *Plant Physiology*, 174(2):717–731.

Weiss, L., Gaelings, L., Reiner, T., Mergner, J., Kuster, B., Feher, A., Hensel, G., Gahrtz, M., Kumlehn, J., Engelhardt, S., and Huckelhoven, R. (2022). Posttranslational modification of the rho of plants protein racb by phosphorylation and cross-kingdom conserved ubiquitination. *PLoS One*, 17(3):e0258924.

Winge, P., Brembu, T., Kristensen, R., and Bones, A. M. (2000). Genetic structure and evolution of rac-gtpases in arabidopsis thaliana. *Genetics*, 156(4):1959–1971.

Worthylake, D. K., Rossman, K. L., and Sondek, J. (2000). Crystal structure of rac1 in complex with the guanine nucleotide exchange region of tiam1. *Nature*, 408(6813):682–688.

Wu, C.-F. and Lew, D. J. (2013). Beyond symmetry-breaking: Competition and negative feedback in gtpase regulation. *Trends in Cell Biology*, 23(10):476–483.

Wu, G., Gu, Y., Li, S., and Yang, Z. (2001). A genome-wide analysis of arabidopsis rop-interactive crib motif-containing proteins that act as rop gtpase targets. *The Plant Cell*, 13(12):2841–56.

Wu, G., Li, H., and Yang, Z. (2000). Arabidopsis ropgaps are a novel family of rho gtpase-activating proteins that require the cdc42/rac- interactive binding motif for rop-specific gtpase stimulation. *Plant Physiology*, 124(4):1625–1636.

Xu, Y., Cai, W., Chen, X., Chen, M., and Liang, W. (2021). A small rho gtpase osracb is required for pollen germination in rice. *Dev Growth Differ*, 64(2):88–97.

Yalovsky, S. (2015). Protein lipid modifications and the regulation of rop gtpase function. *Journal of Experimental Botany*, 66(6):1617–24.

Yamaguchi, K., Imai, K., Akamatsu, A., Mihashi, M., Hayashi, N., Shimamoto, K., and Kawasaki, T. (2012). Swap70 functions as a rac/rop guanine nucleotide-exchange factor in rice. *The Plant Journal*, 70(3):389–397.

Yamaguchi, K. and Kawasaki, T. (2012). Function of arabidopsis swap70 gef in immune response. *Plant Signaling and Behavior*, 7(4):465–468.

Yamaoka, N., Matsumoto, I., and Nishiguchi, M. (2007). The role of primary germ tubes (pgt) in the life cycle of blumeria graminis: The stopping of pgt elongation is necessary for the triggering of appressorial germ tube (agt) emergence. *Physiological and Molecular Plant Pathology*, 69(4-6):153–159.

Yang, B., Sugio, A., and White, F. F. (2006). Os8n3 is a host disease-susceptibility gene for bacterial blight of rice. *Proceedings of National Academy of Science USA*, 103(27):10503–10508.

Yang, Y., Li, R., and Qi, M. (2000). In vivo analysis of plant promoters and transcription factors by agroinfiltration of tobacco leaves. *The Plant Journal*, 22(6):543–551.

Yang, Z. and Watson, J. (1993). Molecular cloning and characterization of rho, a ras-related small gtp-binding protein from the garden pea. *Proceedings of the National Academy of Science USA*, 90(18):8732–8736.

Ye, R. D. (2020). The rho guanine nucleotide exchange factor p-rex1 as a potential drug target for cancer metastasis and inflammatory diseases. *Pharmacological Research*, 153:1–7.

Yoo, J. H., Park, J.-H., Cho, S.-H., Yoo, S.-C., Li, J., Zhang, H., Kim, K.-S., Koh, H.-J., and Paek, N.-C. (2011). The rice bright green leaf (bgl) locus encodes osropgef10, which activates the development of small cuticular papillae on leaf surfaces. *Plant Molecular Biology*, 77(6):631–641.

Yuan, H., Jin, C., Pei, H., Zhao, L., Li, X., Li, J., Huang, W., Fan, R., Liu, W., and Shen, Q. H. (2021). The powdery mildew effector csep0027 interacts with barley catalase to regulate host immunity. *Frontiers in Plant Science*, 12:1–13.

Zhang, Y. and McCormick, S. (2007). A distinct mechanism regulating a pollen-specific guanine nucleotide exchange factor for the small gtpase rop in arabidopsis thaliana. *Proceedings of the National Academy of Science USA*, 104(47):18830–18835.

Zhang, Z., Henderson, C., Perfect, E., Carver, T. L. W., Thomas, B. J., Skamnioti, P., and Gurr, S. J. (2005). Of genes and genomes, needles and haystacks: Blumeria graminis and functionality. *Molecular Plant Pathology*, 6(5):561–575.

Zheng, Z.-L. and Yang, Z. (2000). The rop gtpase: an emerging switch in plants. *Plant Molecular Biology*, 44(1):1–9.

Zhou, X., Lu, J., Zhang, Y., Guo, J., Lin, W., Van Norman, J. M., Qin, Y., Zhu, X., and Yang, Z. (2021). Membrane receptor-mediated mechano-transduction maintains cell integrity during pollen tube growth within the pistil. *Developmental Cell*, 56(7):1–13.

Zhu, K., Debreceni, B., Bi, F., and Zheng, Y. (2001). Oligomerization of dh domain is essential for dbl-induced transformation. *Molecular Cell Biology*, 21(2):425–37.

Zhu, M., Riederer, M., and Hildebrandt, U. (2018). Uv-c irradiation compromises conidial germination, formation of appressoria, and induces transcription of three putative photolyase genes in the barley powdery mildew fungus, blumeria graminis f. sp. hordei. *Fungal Biology*, 123(3):218–230.

Acknowledgements

I am thankful for the support I have been given along the way, an endeavour like a doctoral thesis can not be performed by a single person alone. First of all, I would like to thank Prof. Ralph Hückelhoven for entrusting me with this project. I am grateful for your support during my time at the Chair of Phytopathology. I am also thankful for having Prof. Caroline Gutjahr as my mentor, thank you for always taking time out of your busy schedule for me. In addition, I would like to thank Prof. Ralph Hückelhoven and Prof. Caroline Gutjahr for taking the time as examiners of my dissertation. I would also like to thank the chairman of the examination committee, Prof. Erwin Grill.

I am convinced that a friendly and collaborative work environment produces the best results. Therefore I would like to thank my colleagues in the RACer lab: Stefan Engelhardt, Johanna Hofer, Lukas Weiss, Christopher McCollum and Michaela Stegmann (Kopischke). You welcomed me with open arms and patiently introduced me to new methods. I always enjoyed our scientific discussions and I am grateful for Stefan's guidance, Johanna's methodological expertise and friendship, Lukas' help with the establishment of FRET-FLIM in *N. benthamiana* and Christopher's help with identifying fungal structures. A special thanks goes to my friend and mentor Michaela Stegmann (Kopischke) for establishing FRET-FLIM in our lab and the moral support throughout my doctoral work. I would also like to thank Alexander Völkl for performing the BiFC measurements and analysis during his internship.

At the chair of Phytopathology, I felt welcomed by my colleagues and would like to thank the whole staff for that. Thanks to all phyto doctoral students for the fun times from snow shoe hike to scientific discussions in the corridor between the labs. I would like to highlight my gratitude to Lina Muñoz, for your friendship, dancing lessons and life advice. Sabine Eschrig, thank you for always asking the right scientific questions and your engagement for others. My friend Alex Kutschera for introducing me to the makers world and encouraging out of the box thinking. Parvinderdeep Kahlon, my partner in crime! Thank you for the unconditional support, inspiring discussions and realisation that in nature, greatness is seldomly achieved alone.

I would like to also thank Daria for a wonderful exchange and your help in cover page design.

I will be forever grateful to my always supportive family. The past year has brought us closer together. You always believed in me and lifted up my spirits when it got tough.
Especially, Konstanze Trutzenberg for being my rock and Michael Trutzenberg for saving my life, several times. Manja Trutzenberg for being my best friend, Noah Trutzenberg for teaching me integrity and awareness.

At last, I thank my partner Michael for your tireless support and love.
I would not want to have done this without you.